

MARTIN
MARIETTA



N66-15 364

(ACCESSION NUMBER)

(THRU)

197

(CODE)

(PAGES)

(CATEGORY)

(NASA CR OR TMX OR AD NUMBER)

FACILITY FORM 802

MARTIN COMPANY

UNCLASSIFIED

FINAL REPORT FOR
LUNAR ROCK CORING DEVICE DESIGN STUDY

By Donald S. Crouch

October 1965

Prepared Under Contract No. NAS9-3542 by

MARTIN COMPANY

Baltimore, Maryland 21203

Martin Report No. ER 13952

FOR

NATIONAL AERONAUTICS AND SPACE ADMINISTRATION

Manned Spacecraft Center

Houston, Texas

UNCLASSIFIED

ER 13952

ABSTRACT

A study of rock coring techniques applicable for lunar surface operation within the constraints of early LEM missions resulted in the selection of a rotary-percussion system employing tungsten-carbide core bits. Fabrication of a breadboard model, and subsequent evaluation tests demonstrated that twelve feet of consolidated rock core can be obtained without gaseous or liquid lubrication and hole flushing agents which are always employed with commercial drilling equipment. Parallel analytical studies were conducted to the degree required for specifying the design and specifications for a coring device which can be operated in the lunar environment.

TABLE OF CONTENTS

	<u>Page No.</u>
ABSTRACT	1
SUMMARY	1
INTRODUCTION	3
POTENTIAL DESIGN APPROACHES	5
Basic Data Evaluation	5
Rotary Diamond Coring Technique	6
Diamond Coring Feasibility Tests	7
Preliminary Design Approaches for Rotary Coring Device	12
Prime Mover Systems	13
Self-Contained Power Sources	15
BREADBOARD MODEL CORING DEVICE	16
Basic Design	16
Control System	19
Rotary Drive	20
Vertical Traverse Drive	20
Percussion Mechanism	20
Drill String - Core Bit, Core Barrel and Extension Tubes	26
Coring Dust Transport System	27
Electric Motor Prime Mover	27
Environmental Control System	27
Power Cable	29
Anchoring Technique	30
Core Orientation	31

	<u>Page No.</u>
CORING DEVICE TEST PROGRAM	35
Rock Penetration Tests	35
Ten-Foot Coring Tests	42
Extended Depth Coring Tests	46
Spacesuit Interface Tests	47
High Vacuum Motor Operation	48
CORING DEVICE OPERATING PROCEDURES	52
Site Selection	52
Transport to Coring Site	52
Emplacement of Coring Device	52
Core Orientation	53
Coring Procedure	54
LUNAR DRILL LOAD SIMULATOR	56
CONCLUSIONS AND RECOMMENDATIONS	56
Study Results	56
Additional Study Requirements	57
Prototype Coring Device Design Specifications	59
Suggested Future Program Plans	60
BIBLIOGRAPHY	61
APPENDIX A: Basic Data Evaluation	A-1
APPENDIX B: Rotary Coring Preliminary Analytical Model.	B-1
APPENDIX C: Rotary Diamond Coring Feasibility Tests	C-1
APPENDIX D: Preliminary Design Approaches for Rotary Coring Device	D-1
APPENDIX E: Prime Mover Systems	E-1

ER 13952

	<u>Page No.</u>
APPENDIX F: Self-Contained Power Sources	F-1
APPENDIX G: Motor Environmental Control System	G-1
APPENDIX H: Coring Device Cable Temperature	H-1
APPENDIX I: Lunar Drill Load Simulator	I-1
APPENDIX J: Drawings and Specifications (Separate Cover)	J-1

LIST OF ILLUSTRATIONS

<u>Figure No.</u>		<u>Page No.</u>
1.	Diamond Coring Feasibility Test Equipment	8
2.	Feasibility Test Set-Up Schematic	9
3.	Feasibility Test Coring Bits	10
4.	Rotary Lunar Coring Device	14
5.	Rotary-Percussion Coring Device	17
6.	Rotary-Percussion Coring Device With Control Box	18
7.	Coring Device Control Box	21
8.	Control Box With Cover Removed	21
9.	Gear Box - Left Profile	22
10.	Gear Box - Right Profile	22
11.	Gear Box - Top View	23
12.	Rotary and Vertical Traverse Drives	23
13.	Percussor Unit	24
14.	Percussor Housing Retainer Top and Bottom Plates	24
15.	Assembled Drill String	25
16.	Drill String Components	25
17.	Coring Device Control Circuitry	28
18.	Rock Anchor, Anchor Drill and Core Bit	32
18A.	Conceptual Hard Rock Anchor	33
18B.	Conceptual Overburden Anchor	34
19.	Feasibility Test Rock Samples	37
20.	Solid Basalt Photomicrograph	38
21.	Vesicular Basalt No. 1 Photomicrograph	38
22.	Vesicular Basalt No. 2 Photomicrograph	39

LIST OF ILLUSTRATIONS (Cont.)

<u>Figure No.</u>		<u>Page No.</u>
23.	California Pumice Photomicrograph	39
24.	Obsidian Photomicrograph	40
25.	Granite Biotite Gneiss Photomicrograph.	40
26.	Biotite Schist Photomicrograph	41
27.	Marble Photomicrograph	41
28.	Field Evaluation Tests	44
29.	Coring Device and Accessories	45
30.	Drilling Rock Anchor Holes	45
31.	Spacesuit Interface Tests.	49
32.	Vacuum Test of Motor	50

LIST OF TABLES

<u>Table No.</u>		<u>Page No.</u>
1.	Motor Temperature Rises at Low Ambient Pressures	51

ER 13952

SUMMARY

A preliminary basic data evaluation revealed that the rotary diamond coring technique utilizing thin-wall core bits should be initially investigated for the ten-foot lunar rock coring device. This selection was based on the following criteria:

- . Requirement for obtaining consolidated cores to depths of ten feet
- . Inherent simplicity, reliability, and light weight
- . Payload and power limitations of the Lunar Excursion Module
- . Astronaut capability and dexterity limitations
- . Possibility that residual LEM descent stage pressurizing helium may be available as a coring dust removal and bit cooling agent
- . Previous related investigations by other contractors did not include an extensive evaluation of special design, thin-wall bits

Subsequent coring feasibility tests were conducted using "set" and "impregnated matrix" diamond thin-wall core bits employing both natural and synthetic diamonds. Although satisfactory coring penetration rates were attainable, rapid diamond dulling occurred in medium-hard and hard rock materials unless excessive quantities of cooling and core dust removal gas were employed. Interface meetings with NASA and Grumman Aircraft Company revealed that the availability of LEM pressurizing helium could not be guaranteed. As a result, the diamond rotary coring technique was eliminated for the coring of hard rock materials. Other feasibility tests using the rotary-percussion coring technique revealed that this approach will best meet the lunar operating requirements.

A breadboard model rotary percussion coring device was designed and fabricated. Evaluation tests revealed that the device is capable of coring medium-hard rock from a depth of at least twelve feet without the use of a gaseous or liquid dust removal and bit coolant agent. Dust removal and transport to the surface is accomplished by the use of helices machined into the core bit, core barrel, and core barrel extension tubes. Additional analytical studies were conducted to define the environmental control system requirements. Detailed specifications and drawings were developed for the lunar rock coring device.

Evaluation of various prime mover systems for the lunar rock coring device revealed that the electric motor is preferred over the gas and pneumatic turbines. Further, an analysis of AC and DC electric motor systems using the LEM power source indicated that the DC system would be more efficient (delivered power per unit weight) for operating radii up to approximately 350 feet. For operating radii greater than 350 feet, the lighter weight of the AC power transmission cable compensates for the weight and voltage conversion efficiency of an inverter, and the AC system becomes more efficient. However, the total delivered power by either system at a distance of 350 feet is unacceptable unless a large percentage of the payload weight is devoted to the power cable. Therefore, it is recommended that the DC drill system be employed at distances not exceeding 100 to 150 feet from the LEM vehicle.

Various portable electric power sources were studied with respect to their applicability for increasing the operating range of the lunar coring device. These power systems included:

- . Silver-zinc batteries
- . Fuel cells
- . Solar concentrators
- . Solar cells
- . Radioisotope generators
- . Nuclear reactors
- . Chemical dynamic alternator systems

It was determined that a significant portion of the 250-pound payload capability of the LEM spacecraft would be required for transporting a portable power supply to the lunar surface. If a portable power source is desired, a 70-pound, 2000 watt-hour, rechargeable, silver-zinc battery would best meet the requirements. The complexity and weight of the other power sources studied would not be recommended for powering the lunar coring device.

Hardware delivered under this contract included the following major items:

- . Breadboard Model Lunar Coring Device

Specifications

Coring Mode	-	Rotary-Percussion
Prime Mover	-	28 VDC Permanent Magnet Motor
Power Requirement	-	20 to 25 Amperes @ 28 VDC
Coring Capability	-	12 Feet (tested)
Core Diameter	-	1 Inch
Penetration Rate	-	0.5 to 1.0 Inch Per Minute (Vesicular Basalt)
Rotational Speed	-	270 Revolutions Per Minute
Impact Energy	-	16 Inch-Pounds (Fixed)
Impact Frequency	-	6 Blows Per Revolution (1620 bpm nominal)
Control	-	Semiautomatic
Envelope Dimensions	-	14" x 14" x 30"
Weight	-	63 Pounds (Including All Accessories)
Projected Flight Model Weight	-	40 Pounds

- . Lunar Drill Load Simulator (Motor)
- . Electrodynamic Brake
- . Electrodynamic Brake Control Box
- . Power Cables (12 & 100 Feet)

The last four items were supplied for LEM Power System Tests for simulating the electrical loading characteristics of the lunar coring device.

INTRODUCTION

During the past several hundred years, many techniques have been developed for drilling and coring in the terrestrial subsurface. Techniques developed by the Chinese in the 1500's are still in use today, with the exception that the crude materials and muscle power have been replaced with steel and powerful engines.

The majority of present-day subsurface drilling and coring is accomplished by employing rotary, percussion, or rotary-percussion techniques. There have been many technological advances in the drilling industry which have resulted in significant improvements in the drilling techniques using the commercial efficiency scale, cost per foot of drilled hole, as a criterion. However, there has been a minimum of effort (or requirements) directed toward the power optimization of drilling techniques, reduction of equipment weight, and conservation of bit cooling and chip removal gases. Early feasibility studies performed by Hughes, Texaco, and Armour represent the first attempts to optimize terrestrial drilling techniques for use on the lunar surface. These studies were oriented toward the development of a device capable of drilling a complete hole to a depth of five feet on the lunar surface. The purpose of this five-foot hole was to measure the bearing strength and hardness of the lunar surface as determined by penetration rate, and to produce core dust for subsequent instrument analysis. The extraction of consolidated cores was not required of these early drilling devices.

The Lunar Rock Coring Device Design Study was oriented toward the development of a drill capable of extracting consolidated subsurface cores from depths of ten feet. The general design objectives included:

- . An appraisal of possible methods of rock coring on the lunar surface taking into consideration the local vacuum, temperature, and gravity conditions
- . The recommended method and coring device design must be compatible with the limited dexterity and mobility of the spacesuited astronaut
- . Operation of the coring device must be automatic, or semi-automatic requiring minimum astronaut attention
- . The study shall include the design of a coring device capable of cutting ten (10) feet of core one (1) inch in diameter from consolidated rock
- . Portable power supplies as well as direct operation from the LEM fuel cell shall be considered

Although the development of hardware was not specifically required by the Request for Proposal, Martin believed that a breadboard model coring device was desirable to thoroughly evaluate the selected coring technique. A hardware requirement was subsequently added as a contractual item for the Study.

EA 13952

The initial phase of the study consisted of an evaluation of basic data influencing the design of the coring device. This included lunar geological and environmental factors, material selection considerations, human factors, Apollo LEM interfaces, and drilling methods. As a result of the basic data evaluation and feasibility tests, a design approach was selected for the coring device. Detail design and fabrication of the machine was completed, and various evaluation tests performed.

This report includes the work performed from September 21, 1964 through July 27, 1965, and was conducted under the auspices of Mr. W. Benckert, Program Manager, and Mr. M. B. Goldman, Manager of Logistic Support, Baltimore Division, Martin Company. Other individuals, and their specialty areas, who contributed to this program included:

The Martin Company

Fritz Albrecht, Electrical Systems
Paul W. Boone, Materials Specialist
Donald S. Crouch, Program Technical
Director
Albert H. Haron, Environmental Control System
Donald F. Malzahn, Testing Evaluation
Gus A. Rouvellat, Thermal Analysis
and Design
Bernard A. Thill, Human Factors
Rowland M. Younger, Engineering
Supervisor

The Black and Decker Mfg. Co.

Richard Koen, Engineering Supervisor
Melvin H. Neuhardt, Engineering
Supervisor
Robert A. Riley, Engineering Manager
Allen C. Stanley, Project Engineer

Dr. Elbert King, Geology and Geochemistry Section of the Lunar Technology Branch, NASA-Houston, provided program direction and monitoring.

POTENTIAL DESIGN APPROACHES

Basic Data Evaluation

The initial phase of this study was devoted to the evaluation of existing data which could influence the design of the lunar rock coring device. Predominant subjects for study included: 1) Apollo-LEM Interfaces, 2) Lunar Surface Geological and Environmental Factors, 3) Coring Techniques, 4) Man/Machine Interfaces, and 5) Materials Selection Criteria. The results of this basic data evaluation are presented in Appendix A.

The primary restrictions imposed upon the coring device design are required by the Lunar Excursion Module. Factors such as minimum size, weight, and power consumption greatly influenced the design approach for the basic machine and its prime mover. Structural elements such as the core barrel, extensions, and traversing column were limited to thirty (30) inches in length in order to facilitate storage within the LEM scientific equipment bay. Subassemblies such as the ten feet of drill bit extension rods required the design of mechanical couplers to enable disassembly and stowage. A power system analysis was conducted to determine that the most efficient means for utilizing the 28 V dc, 2400 watt-hours allotted for the coring device mission is a simple dc-motor driven directly by the LEM power source which may consist of a fuel cell or silver zinc batteries.

The foregoing represents the general LEM interface areas considered during this study. These interfaces must be defined and coordinated in greater detail as the design of the LEM, lunar coring device, and other scientific payloads approach finalization.

Study of current interpretations of lunar surface geology established the guidelines for the hardness range of materials for which the machine was designed to core. The test program for the breadboard models included the coring of materials such as basalt, obsidian and pumice. Other locally available materials were tested including granite biotite gneiss, biotite schist, sandstone, and marble.

The primary lunar surface environmental factors which influenced the design of the coring device were temperature and ambient pressure. An analysis was conducted to determine the effects of operating the electric motor under these environmental conditions. The analysis revealed that an active thermal control system will be required, and a conceptual design for a workable system was completed.

A study of coring techniques which may be applicable for the lunar coring device was conducted as summarized in Appendix A. Coring techniques which were considered, and subsequently rejected included: 1) Flame and electric arc drills, 2) Chemical softeners, 3) Pellet impact and abrasive laden jets, and 4) Explosive shape charges. The study revealed that only two techniques warranted further evaluation - rotary and rotary-percussion coring. The rotary technique was previously studied⁽¹⁾⁽²⁹⁾⁽³⁰⁾ and rejected for use on the unmanned Surveyor lunar lander for complete-hole drilling to a five-foot depth. However, most of these early tests were conducted with standard, off-the-shelf wide kerf diamond bits which are not particularly desirable for the lunar application because of excessive axial pressures and power requirements. The

inherent mechanization simplicity, reliability, and light weight of the rotary systems warranted further investigation with narrow kerf core bits specifically designed for the lunar application. Therefore, the initial feasibility tests conducted under this contract were oriented toward development of a pure rotary coring system.

A brief study of man/machine interface factors was also conducted prior to the design of the coring device. Primary man/machine design considerations for the lunar coring device included: 1) A maximum of automatic operation features commensurate with the previously discussed payload restrictions, and 2) A minimum of astronaut effort required for initial emplacement and operation of the device. The final breadboard model design resulted in a semi-automatic operation which requires periodic attention by the astronaut for core removal and coupling of additional drill rod extensions as greater coring depths are attained. The device was also designed to facilitate performance of most astronaut tasks from a standing position. This included major tasks such as coupling and uncoupling drill rod extensions, and "feeding" of these extensions to the coring device driving mechanism from the standing position. These features, which are required by the state-of-the-art Apollo spacesuit, require some tradeoff with weight and reliability. Subsequent coring device models may not require standup position operation if significant dexterity improvements are developed for later versions of the Apollo spacesuits.

A brief review was conducted of state-of-the-art materials and lubrication systems which may be applicable for the final model space-qualified lunar coring device. The results of this review are presented in Appendix A.

Rapid improvements are being made with solid film lubricants and materials with "built-in" lubricants such as the sulfurized steels which are designed for near-vacuum environments. Utilization of these lubrication techniques may eliminate the requirement for a pressurized gear box (normally required for lubricant retention in low pressure environments) since the total operating time will be relatively short. Lubricant retention is mandatory for preventing galling and cold welding of sliding or rolling surfaces such as gears and ball bearings.

Specific recommendations for materials and lubricants for the space qualified lunar coring devices are presented in the Conclusions and Recommendations Section.

Rotary Diamond Coring Technique

As a result of the basic data evaluation (Appendix A), the rotary diamond coring technique initially appeared to best meet the requirements for the lunar coring device. The desirable features of simplicity of operation and mechanization, inherent light weight compared to other systems, and predicted reliability warranted further investigation of this technique during the early feasibility tests.

In order to further evaluate the capabilities and requirements for the rotary coring technique, a preliminary analytical model was developed using an assumed electric motor as a prime mover. Estimated parameters were assigned to the system which approximated those anticipated for a final model coring device. The detailed analysis of the preliminary analytical model coring device is presented in Appendix B.

The early feasibility tests revealed that heating of the core bit and removal of the core cuttings were major problems inherent with the rotary diamond coring technique. Therefore, the analytical model consisted of an open loop helium coolant system which served the triple purpose of cooling the electric motor and coring bit, and flushing the core cuttings from the bottom of the drill hole. A power level of 600 watts was assumed as the input to the coring device electric motor. Estimated motor and drilling efficiencies were assigned to the system, along with core bit hold-down pressures and rotational speeds.

A primary purpose of the preliminary analytical model was to determine the helium requirements for effective operation of the system. Helium was chosen for the analytical model because of its relatively high heat capacity. The analysis revealed that steady state coring would require 1.85 pounds of helium per hour and full load operation would require 4.5 pounds per hour. The initial estimated drilling task included 6 hours of steady state operation and 1 hour of full load operation. The analysis revealed that a 7-hour drilling task would require 15.6 pounds of helium, with a container weight of 10 pounds per pound of gas. Therefore, the total calculated payload penalty for the helium coolant system was 171.6 pounds, exclusive of the weight of the basic coring device.

In view of the excessive payload penalty for transporting a helium coolant system, the possibility of utilizing residual helium from the LEM descent stage propellant pressurization system was considered. Preliminary estimates indicated that 16 to 18 pounds of residual helium may be available from the LEM pressurization system. This helium could be transported to the lunar coring work site by means of a connecting hose from the LEM or by intermittent filling of a portable container. Since utilization of residual helium from the LEM initially appeared feasible, the rotary diamond coring technique was further evaluated. (Subsequent information revealed that the availability of LEM descent stage helium could not be guaranteed.)

Diamond Coring Feasibility Tests

A series of rotary diamond coring feasibility tests was conducted to evaluate the drilling efficiency and durability of various special-design bits for operation within the restrictions of the lunar surface application. Equipment was provided to measure drilling parameters including motor voltage, current, power and rpm; coolant air pressure, flow rate, inlet and outlet temperatures; bit pressure and penetration rate. Figure 1 pictorially illustrates some of the equipment utilized during the early test program, Figure 2 schematically depicts the functional location of the drilling instrumentation, and Figure 3 is a representative sampling of the diamond core bits which were evaluated.

The feasibility test program resulted in the evaluation of the following general categories of diamond core bits:

1. Standard Wide Kerf (5/16-inch) Set Diamond
2. Standard Wide Kerf (5/16-inch) Diamond Impregnated Matrix
3. Special Design Thin-Wall Set Diamond

ER 13952



Figure 1. Diamond Coring Feasibility Test Equipment

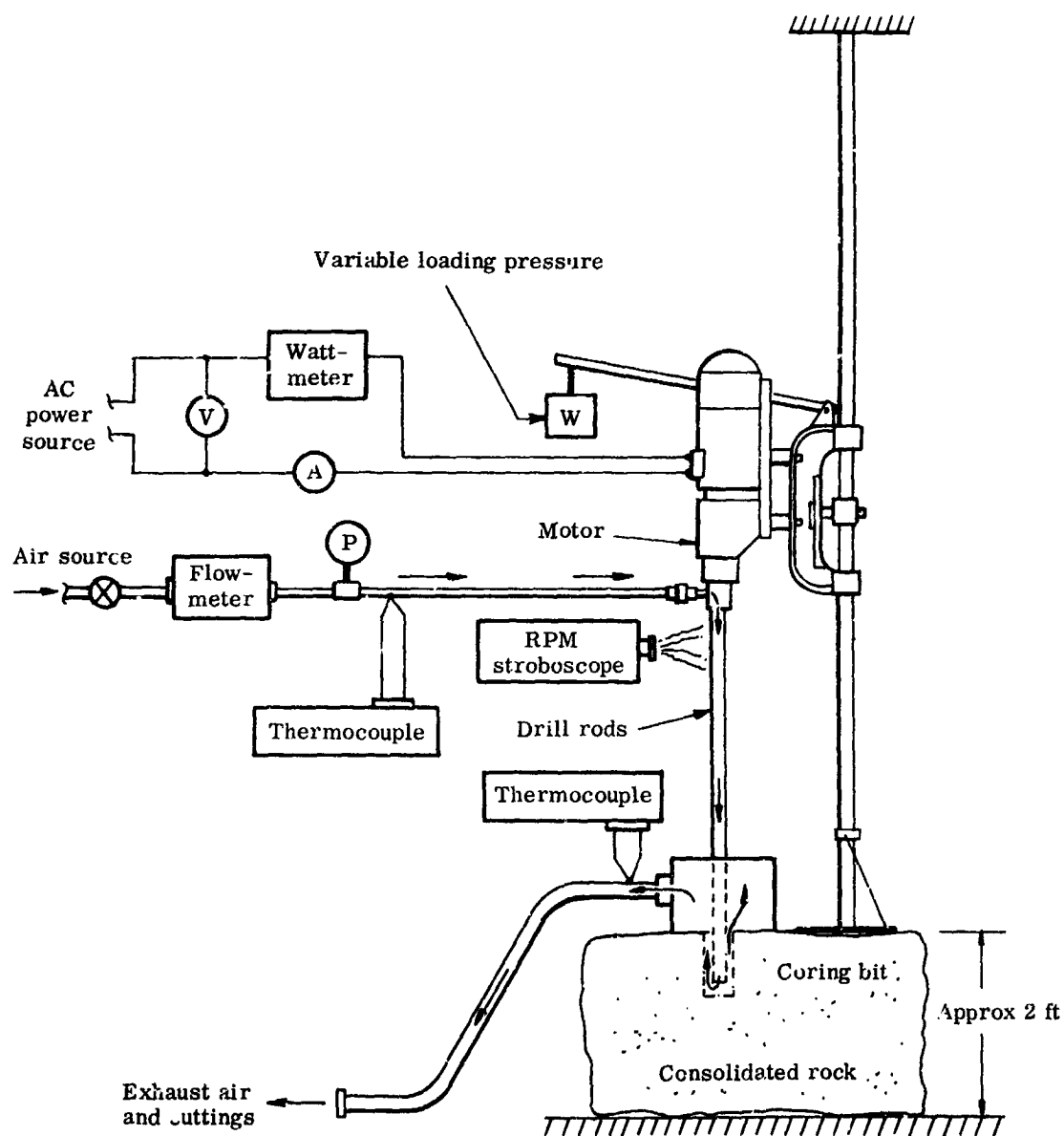


Figure 2. Feasibility Test Set-Up

ER 13952

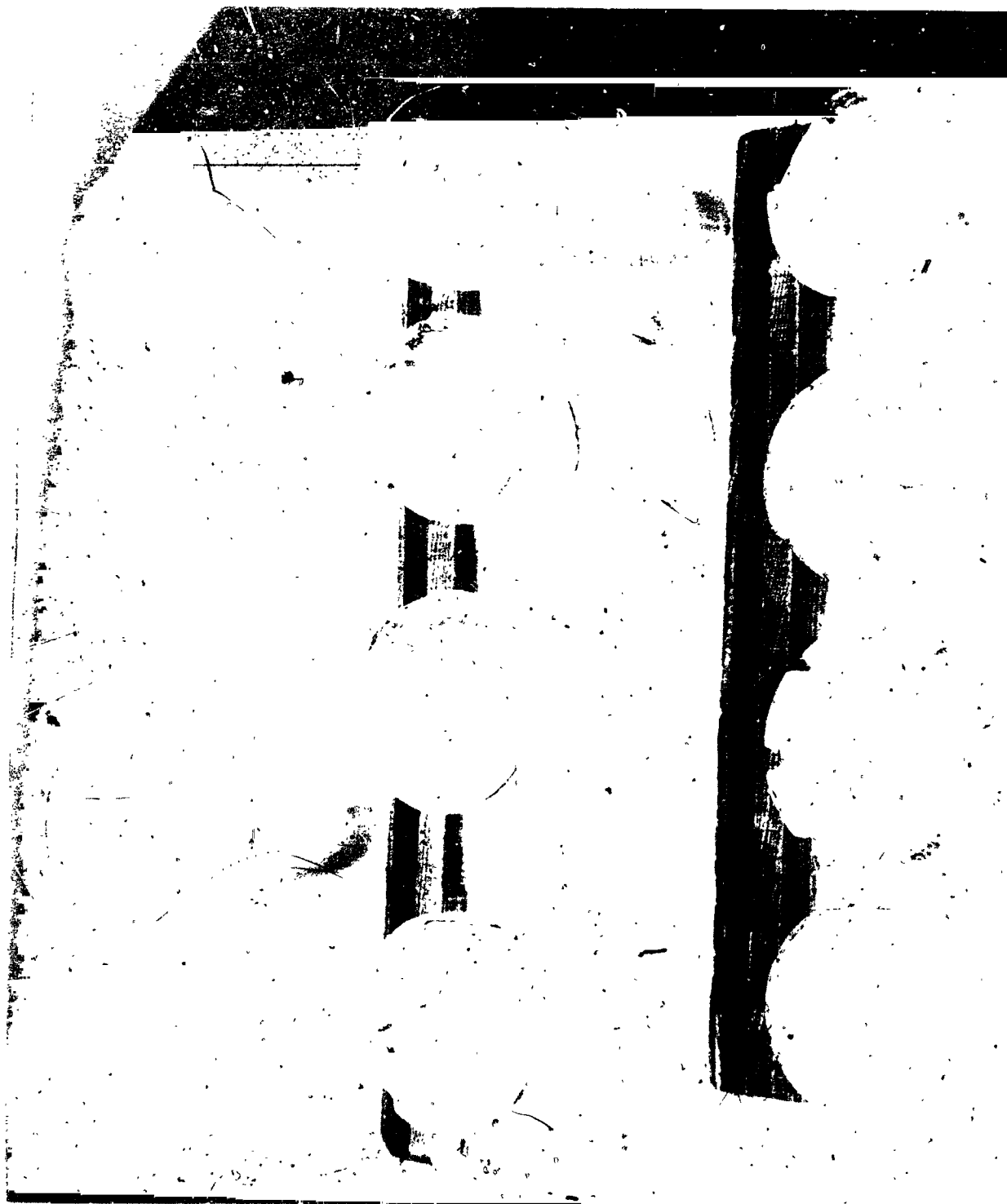


Figure 3. Feasibility Test Coring Bits

4. Special Design Thin-Wall Diamond Impregnated Matrix
5. Special Design Thin-Wall Set (Synthetic) Diamond
6. Special Design Rotary Carbide

Representative test results are presented in Appendix C.

The early feasibility tests were conducted using a small dc motor capable of operating in the 500-600 watt power range. Coolant flow rates were purposely maintained at relatively low levels commensurate with the total residual helium anticipated to be available in the LEM descent stage propulsion system. A special gear box was designed for the test motor which permitted rotational speed variations ranging from 300 to 2400 rpm. Variations in both axial bit pressures and rotational speeds were used for the penetration rate optimization tests.

The possibility of utilizing the wide kerf bits for the lunar coring device was immediately eliminated during the feasibility tests. Excessive power consumption (1500-2200 watts) and axial bit pressures (300 to 800 pounds) were required to attain a significant penetration rate with these types of bits. Elimination of the wide kerf bits for possible use on the lunar coring device also eliminated the use of a double core barrel for the prevention of core fracturing. The clearances obtainable with the narrow kerf bits are not sufficient to accommodate an inner, non-rotating core housing.

Feasibility coring tests of the thin wall set diamond bits resulted in significantly improved penetration rates as compared to the wide-kerf, standard diamond bits. Maximum penetration rates of 30 inches per hour were obtained in the extremely hard granite biotite gneiss at reasonable power levels of 600-700 watts as indicated in Appendix C. Softer materials such as marble could be penetrated at rates up to 135 inches per hour. However, these relatively high penetration rates rapidly decreased after a few inches of drilling due to diamond dulling. The rapid diamond dulling was attributed to two factors:

1. The relatively low coolant flow rates (5 to 20 scfm) maintained during the tests were not sufficient to remove the excessive heat generated by the diamond coring technique. Diamond discoloration and rapid polishing suggested the possibility of phase change due to high point contact temperatures.
2. The low gas flow rates were not sufficient to maintain a clean drill hole completely free of coring dust. Therefore, the dust tended to accumulate at the hole bottom which prevented the small diamonds from cutting effectively. As a result, the coring dust impacted at the hole bottom, and aggravated the heat generation problem. The employment of mechanical dust transport spirals did not significantly improve the problem of maintaining a dust-free hole at the cutting bit.

Approximately ten (10) set-diamond, thin-wall bit configurations were designed by various manufacturers including Wheel Trueing Tool Company, Anton Smit, and Hoffman Brothers. Variations in diamond type (natural and synthetic), size, shape, orientation and matrix composition were tested. The test results were similar with all bit configurations - rapid diamond dulling after two (2) to twelve (12) inches of coring in the hard to medium-hard rock materials including basalt, granite biotite gneiss, biotite schist, and marble. The only material tested which could be satis-

factorily cored without diamond dulling was pumice. The relatively low cutting energy required for this material, aided by the "natural" dust storage reservoirs provided by the vesicles resulted in penetration rates of approximately 11 inches per minute.

Due to the limited success of the thin-wall set diamond bits for coring of hard to medium-hard rock materials, subsequent testing was conducted with impregnated diamond matrix core bits. Since dulling of individual diamonds was found to be unavoidable, the use of a diamond impregnated matrix which would abrade and expose new diamonds appeared feasible for the lunar application. Approximately six (6) core bit configurations were designed and tested in an effort to develop a matrix which would abrade properly under the light loading conditions. Very limited success was attained with this type of bit because the matrix was either too hard for sufficient abrasion, or too soft resulting in loss of complete diamonds during the coring process. As a result, the impregnated matrix bits performed similarly to the set diamond bits, with penetration rates decreasing rapidly after dulling of the outer layer of diamonds.

An experimental rotary tungsten-carbide bit was designed by the Pratt and Whitney Tool Company. The tungsten-carbides are generally employed for rotary-percussion drilling in the low power drilling machines. The experimental bit, as shown in Figure 3, consisted of eighteen (18) small carbide cutters brazed on the core barrel. This bit also did not perform satisfactorily in the pure rotary mode due to rapid drilling of the carbide cutters. This type of bit possesses inherent characteristics such as extreme impact resistance which make it adaptable to the rotary-percussion drilling mode.

In summary, none of the previously listed diamond and carbide core bits are suitable for rotary coring of hard to medium-hard rock materials under lunar operating restrictions for the ten-foot lunar rock coring device. Only soft materials such as pumice, and possibly unwelded tuff and small grain size rubble can be cored successfully with the diamond bits.

Preliminary Design Approaches for Rotary Coring Device

A study was undertaken to determine the most efficient design for the pure rotary coring device. This study was conducted concurrently with the performance of the early diamond coring feasibility tests, when it appeared that the pure rotary technique would best meet the lunar coring requirements. The pure rotary technique was the least complicated to mechanize, requiring only a rotational and axial loading of the cutting head for coring. The optimized rotational and axial thrust requirements were obtained from the feasibility tests. Since the axial thrust requirement for the bit exceeds the restraining capability of the light-weight coring device under a 1/6-G environment, the use of rock anchors is mandatory.

Three basic techniques were considered for the rotary coring device as illustrated in Appendix D. These included: 1) Direct Drive Device, 2) Continuous Feed, and 3) Intermittent Feed. The intermittent feed technique was selected as a logical compromise based on mechanization simplicity, and ease of handling by a spacesuited astronaut.

The first model coring device employing the pure rotary, intermittent feed technique is illustrated in Figure 4. The driving motor is mounted on a vertical, geared column thirty (30) inches in length. A low rpm, high torque gear and slip clutch assembly is employed to drive the motor vertically on the geared column. A one-way clutch and drive device supplies the rotation to the thin-wall drilling tubes.

Operation of the machine is relatively simple. With the motor and gear box assembly in the extreme upward position, the drive device locking wheel is loosened, and the thin-wall diamond core bit and tube is hand-fed through the drive assembly until the bit contacts the lunar surface. The drive device locking wheel is tightened, and the machine is turned on. The motor and gear box assembly rotate and drive the core bit and tube downward until the lower limit is reached. A new drill tube extension is then coupled to the original tube, the drive device locking wheel is loosened, and the motor and gear box assembly is traversed vertically to the extreme upward position. This sequence is repeated several times until a total of ten feet of drill tubes are driven into the lunar surface.

Before the pure rotary coring device reached the testing phase of the program, it became evident from the diamond coring feasibility tests that a rotary-impact mechanism would be required for coring hard rock materials. As a result, an impacting mechanism was designed and incorporated on the basic rotary machine shown in Figure 4. Details of this final breadboard model rotary-percussion coring device are presented in a later section of this report.

Prime Mover Systems

A brief study was conducted of possible prime mover systems which could be utilized for powering the lunar coring device. The results of this study are summarized in Appendix E. Since electrical power will be available in the LEM for possible powering of an electric motor, other potential prime mover systems would probably have to operate from readily available energy sources which would not be charged to the scientific equipment payload weight limitation in order to remain competitive with the electrical system.

The possible use of residual fuel from the LEM descent stage would provide a "free" energy source with no charge to the scientific equipment payload. The study indicated that the residual aerazine 50 (50 percent hydrazine and unsymmetrical dimethyl hydrazine) and nitrogen tetroxide could possibly be utilized to drive a small turbine for powering the lunar coring device. The turbine would consume approximately 6.7 pounds of fuel per 0.5 HP-hour, which is considered to be an adequate power operating level for the coring device. However, if residual fuel is not available in the LEM descent stage, the 47 to 50 pounds of scientific equipment payload weight which would be allocated for sufficient fuel for a 7-hour drilling mission would not be recommended. Other factors such as high temperature and toxic exhaust gases would also reduce the desirability of this type of system.

The possibility of using pneumatic power generated by solar heating of cryogenic gas for driving a small turbine was also considered. However, a detailed analysis assuming helium as a system gas revealed that the solar heat energy would be insufficient for this particular application.

ER 13952

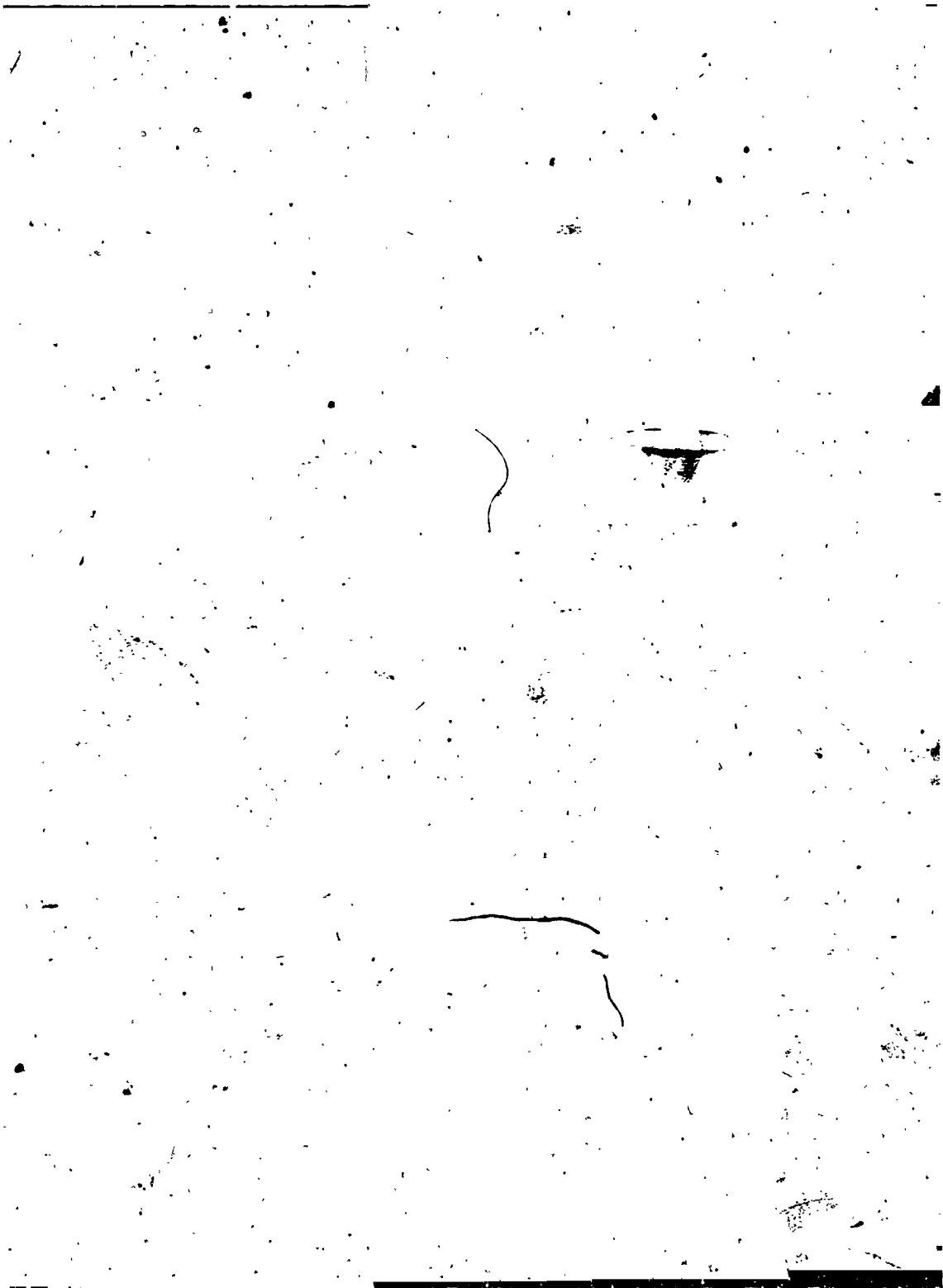


Figure 4. Rotary Lunar Coring Device

The prime mover systems study also included dc vs. ac electrical system efficiencies and weight. Low speed and high speed dc motor systems driven directly from the LEM power source were compared with low and high speed, 400 cps, 3-phase systems obtained through power conversion equipment. The study showed that the power delivered to the lunar coring device per unit weight was more efficient with the low speed dc system for power cable operating radii up to 350 feet. However, both the dc and ac delivered power were relatively low at this distance. The study revealed that the operating radius of the coring device should not exceed 100 to 150 feet unless a relatively large percentage of the drill system weight is devoted to the power cable. A 100-foot cable using the recommended 6 AWG aluminum conductor would weigh approximately 7 pounds.

Self-Contained Power Sources

A study was conducted to determine potential power supplies which may be utilized for portable operation of the lunar coring device. Utilization of a power cable connected to the LEM power source presents obvious restrictions on the operating radius and available drilling time for the coring device. The results of this study are presented in Appendix F.

The study considered several potential power sources including: 1) batteries, 2) fuel cells, 3) chemical dynamic systems, 4) photovoltaic devices, 5) solar concentrators, and 6) nuclear powered devices. Power operating level, total operating time, and system weight and complexity were considered as tradeoff parameters.

The study revealed that only the silver-zinc battery system should be considered as a possible portable power supply for the lunar coring device. It was estimated that a 2160 watt-hour, high discharge rate battery will weigh approximately 70 pounds. This is a relatively high scientific equipment payload weight penalty if the basic LEM power system were a fuel cell. However, if the basic LEM power system is also supplied by silver zinc batteries, it should be possible to package the batteries in such a manner that the 2400 watt-hour capacity allotted to the drill could be supplied in a separate unit and transported to the drilling site by the astronaut. Several distinct advantages would be gained by this recommendation:

1. The lunar surface astronaut would have complete freedom for drill site selection without being restricted by the length of the power cord.
2. The scientific payload would not be penalized by the weight of the battery or long power cable. (It is assumed that the 2400 watt-hour battery would be considered as a portion of the LEM power system weight.)
3. Emplacement of the lunar drill could be accomplished more rapidly without the burden of unwinding and laying a long power cable.
4. Conducted noise from the lunar drill to the LEM (via a power cable) would be eliminated.
5. Radiated noise from the lunar drill would be reduced since the power cable tends to exhibit the characteristics of an antenna.
6. It is possible that the weight of internal LEM electrical harness, circuit breaker, and connectors may be reduced if use of the heavy duty power cable for the drill is eliminated.

BREADBOARD MODEL CORING DEVICE

Basic Design

As a result of the preliminary coring feasibility tests, it became evident that a rotary-percussion device driving a tungsten-carbide core bit would be required for coring medium-hard to hard rock materials within the operating restrictions dictated by the LEM payload vehicle and lunar environment. The major operating restrictions for the lunar coring device include: 1) weight and size limitation, 2) limited available power, and 3) lack of sufficient gas for core bit coolant and rapid dust removal as required for the diamond rotary coring technique unless specifically transported to the lunar surface for this purpose.

A spring and ratchet-type cam mechanism was designed for adaptation to the previously developed rotary-coring device (Figure 4) to provide the required percussive blows to the core bit. Figure 5 shows the basic coring device with the percussion assembly incorporated. Figure 6 shows the final breadboard model lunar coring device with control box incorporated.

The lunar rock coring device provides three (3) distinct forces to the tungsten-carbide core bit: 1) rotation at approximately 270 rpm, 2) controlled axial pressure of approximately 40 pounds, and 3) percussive blows at a rate of approximately 1,620 bpm.

The machine consists of four (4) major assemblies:

- 1) **Basic Mounting Structure** - Consists of base plate for anchoring and leveling on a rock outcrop, 30-inch vertical stabilizing column, and auxiliary stabilization leg.
- 2) **Integrated Motor and Gear Box** - Consists of 24 V dc motor, gear reduction box, rotary drive, percussion assembly and vertical traversing drive assembly.
- 3) **Drill String** - Consists of replaceable tungsten-carbide core bit, core barrel, and six (6) core barrel extension tubes.
- 4) **Control Box** - Consists of switches, relays and ammeter required for semi-automatic operation of the coring device.

The integrated motor and gearbox assembly provides the rotation and percussive blows to the core bit through the core barrel and core barrel extension tubes. Axial pressure is provided to the core bit by the clutch-controlled vertical traversing drive system. This system is capable of power driving the integrated motor and gearbox assembly in either direction at a maximum rate of 1. inches per minute. When the machine is coring (downward direction) the magnitude of axial pressure is controlled by tightening or loosening the slip clutch.

The rotary-percussion machine (Figure 6) maintains the same drill string "feed through" characteristic of the original rotary coring machine of Figure 4. However, since the percussive blows must be applied to the top of the drill string (to minimize energy losses), a percussor assembly must be coupled to the top of the drill string

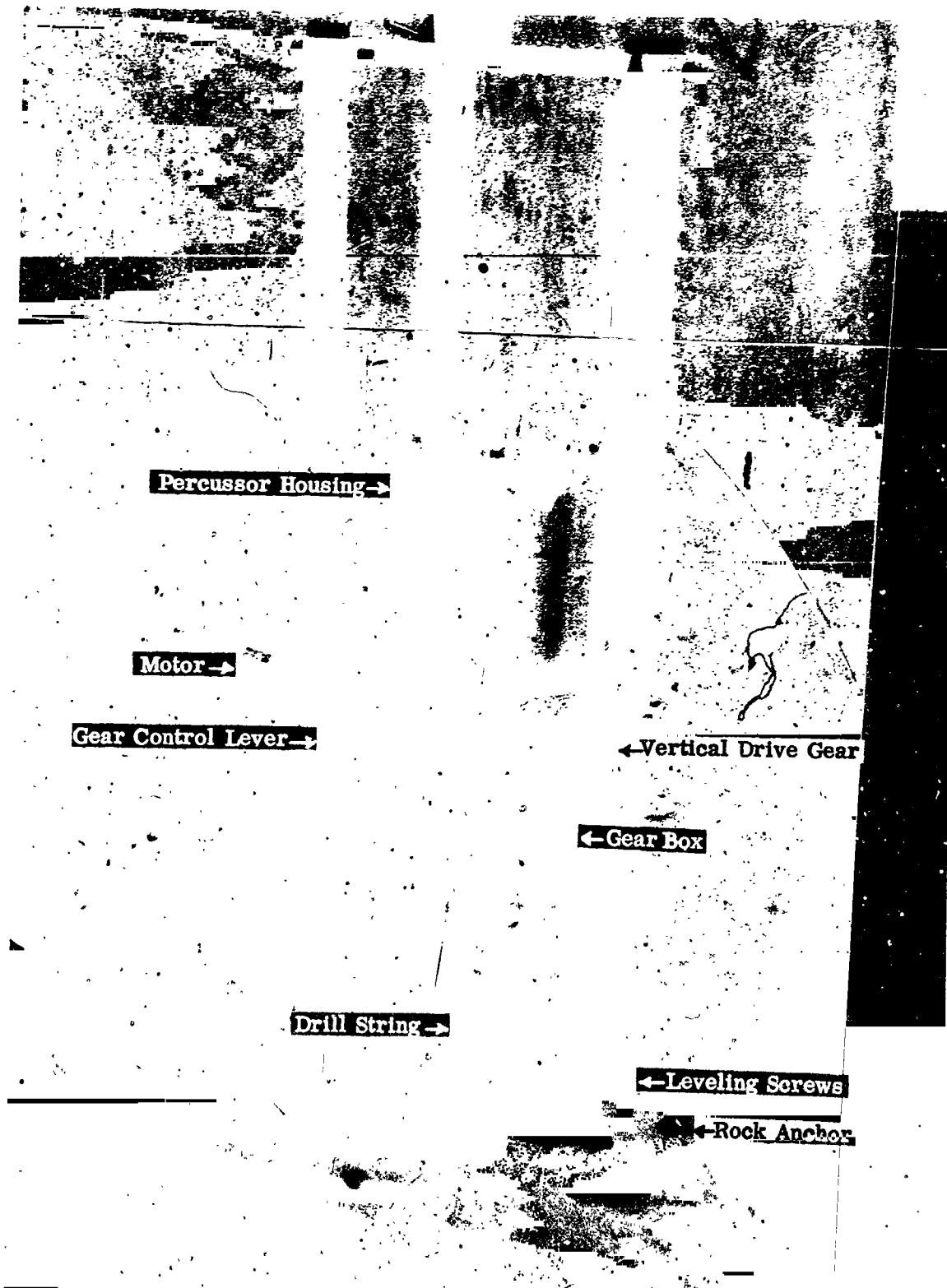


Figure 5. Rotary-Percussion Coring Device

ER 13952

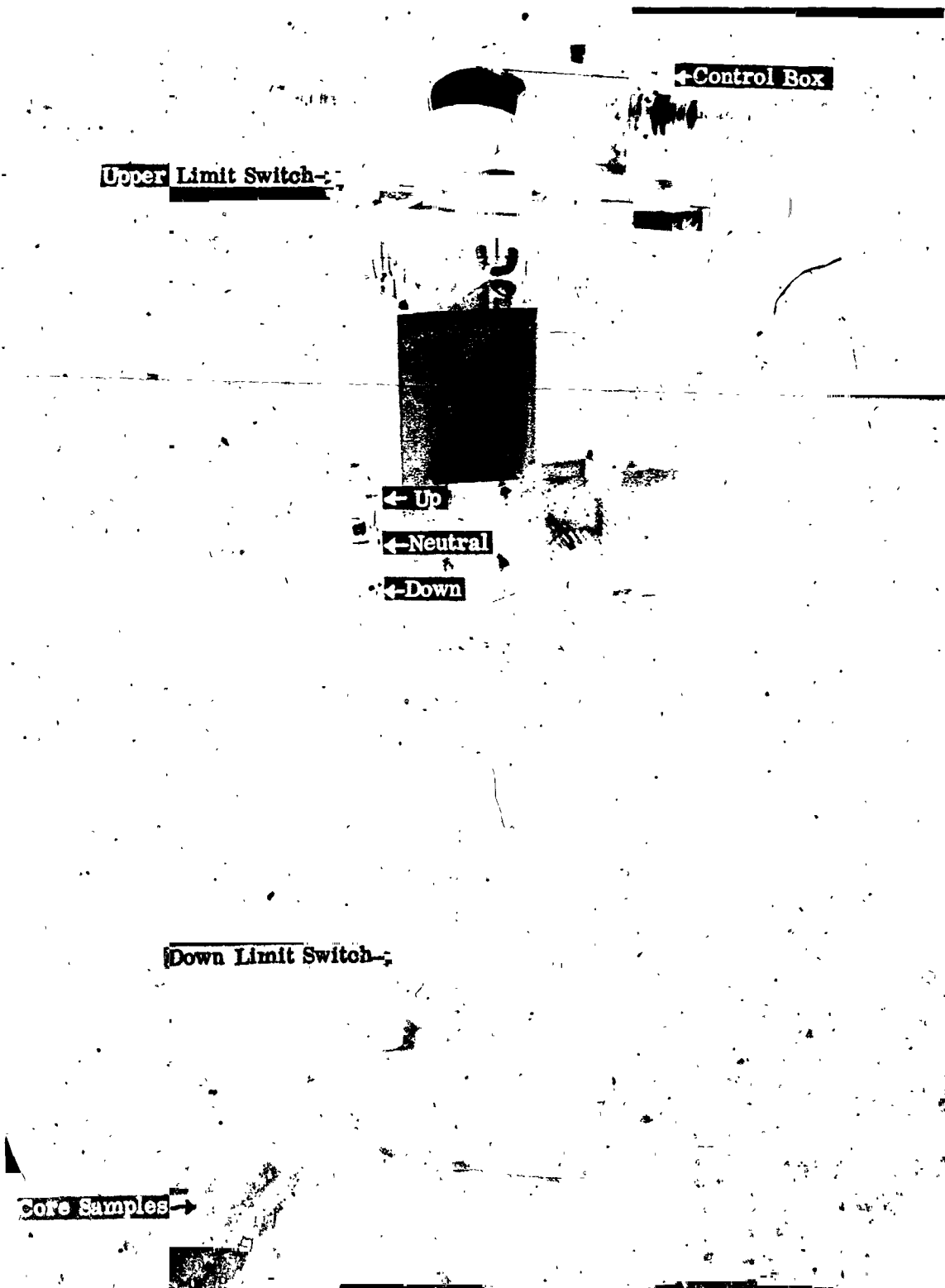


Figure 6. Rotary-Percussion Coring Device With Control Box

which is restrained by the removable top of the percussor housing. In order to add extension tubes, the percussor housing top must be removed, and the entire drill string pulled upward through the percussion housing assembly. After the extension tube has been added to the drill string, the drill string assembly is "fed" down through the percussion assembly housing, seated in place, and the percussor housing top is re-installed. This technique was initially selected to maintain the highest possible working level for the astronaut. An alternative technique would involve coupling and uncoupling of the drill tubes on the under side of the gear box assembly, with a means provided for rotating the entire integrated motor and gear box assembly around the traversing column to facilitate removal of the drill string from the core hole when required. This technique would require the spacesuited astronaut to perform operational tasks at a lower working level.

Detail design descriptions of the breadboard model coring device are presented in the following paragraphs. The design drawings and specifications are presented in Appendix J under separate cover.

Control System

Control of the lunar coring device can be accomplished with a minimum of accessories if visual monitoring by an astronaut is practical. Figure 5 represents the simplest possible controls configuration. The gearshift lever is operated manually in order to set the machine in either a "neutral" or "running" position. However, the direction of vertical traverse must be controlled by the polarity of the dc power source. The polarity switching can be accomplished at the power source (LEM) or by the incorporation of a double pole-double throw switch (not shown) mounted on the coring device. The sequence of operations with the minimum control system is as follows:

- 1) With the machine and core barrel in place, the astronaut would engage the gear control lever, and apply power of correct polarity (by a local or LEM DPDT switch) to begin the coring operation.
- 2) When the machine reached the lower limit of traverse, an astronaut would be required to manually turn the power off. If this function were not immediately accomplished, the machine would continue to run with slippage of the drive clutch. Although this would not necessarily damage the machine, wasteful power consumption would continue until the power was turned off.
- 3) Reverse traversing would be accomplished by manually placing the gear lever in the "neutral" position, and reapplying the power (locally or from the LEM) with reverse polarity.

A higher degree of automation can be accomplished by incorporation of the control box shown in Figures 6, 7, and 8. The control box contains "OFF," "ON," "UP," and "DOWN" pushbuttons. Microswitches are located on the machine structure near the upper and lower terminations of the vertical stabilizing column as shown in Figure 6. These microswitches are electrically connected to relays located within the control box. When the machine is placed in motion in either an upward or downward direction, the microswitch and relay circuitry will automatically remove power from the motor when the maximum allowable travel is attained. Therefore, when the machine is placed in a coring mode, it can continue to operate without attention, and

automatic shutdown will occur at the completion of the traverse. When the astronaut is available for attending the machine, he will disengage the gear lever, depress the "UP" button, and the machine will return to its starting position, and automatically shut down in preparation for core removal.

The ammeter was employed in the breadboard coring device control box to aid in proper adjustment of the vertical drive clutch which controls axial bit pressure. When the coring operation is initiated, the correct axial pressure can easily be set by simultaneous adjustment of the slip clutch and monitoring of the ammeter for an optimum current reading.

The complexity and weight of the control system can be reduced on the final model coring device. The breadboard model control box weighs approximately five (5) pounds, which is considered to be excessive in view of its limited function.

A detailed schematic for the electrical control system is shown in Figure 17.

Rotary Drive

The rotary drive power for the drill string is supplied by the basic 8650 rpm dc motor. The motor rpm is reduced by a ratio of 32:1 through several gear reductions as shown in Figures 9, 10, and 11. The final output horizontal gear rotates at approximately 270 rpm, and transmits power to the vertical drill string drive (percussor unit) through a 1:1 bevel gear and spline as shown in Figures 12 and 13.

Vertical Traverse Drive

The vertical traverse drive power is also supplied by the basic 8650 rpm dc motor. The motor rpm is reduced by a ratio of 5519:1 through a system of standard gears and worm gears as shown in Figures 9, 10, and 11. The final output shaft (Figure 12) rotates at approximately 1.6 rpm. Power is transmitted from the output shaft to the output gear through an adjustable friction clutch which is "pinned" to the outer gear. An Allen-type screw adjustment tightens the clutch and allows it to "grip" the rotating output shaft. The output gear engages the geared vertical traversing column which allows the integrated motor and gear box assembly to travel up or down with a controllable pressure. The clutch can be adjusted to provide a range of axial drill string pressures varying from 0 to approximately 100 pounds.

Percussion Mechanism

Percussive impact energy is supplied to the drill string by a ratchet-type cam and spring mechanism. The percussion mechanism consists of a rotating percussor unit (Figure 13) which is spline driven by the bevel output gear (Figure 12). The percussor unit consists of a 6-lobe, 1/4-inch rise ratchet cam and spring ($K = 100 \text{ lb/in}$) which is preloaded to approximately 50 pounds. When the percussor unit is properly emplaced in the percussor housing (Figure 7), the "fixed" ratchet cam (Figure 8) engages the rotating ratchet cam (Figure 13). With the percussion housing restrainer top (Figure 14) emplaced, rotation of the percussor unit causes the 6-lobe cams to rise, compress the spring, and fall six times for each revolution of the drill string. For a 270 rpm

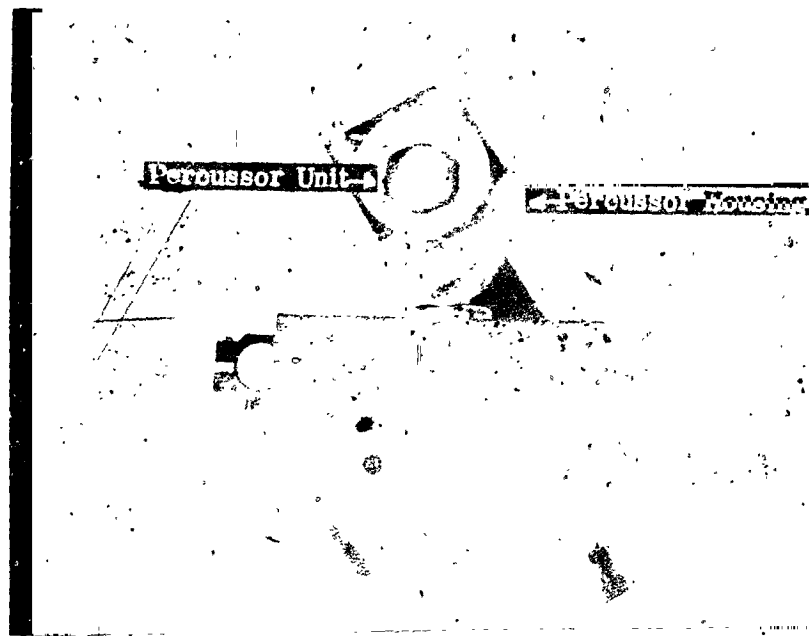


Figure 7. Coring Device Control Box



Figure 8. Control Box With Cover Removed

ER 13952

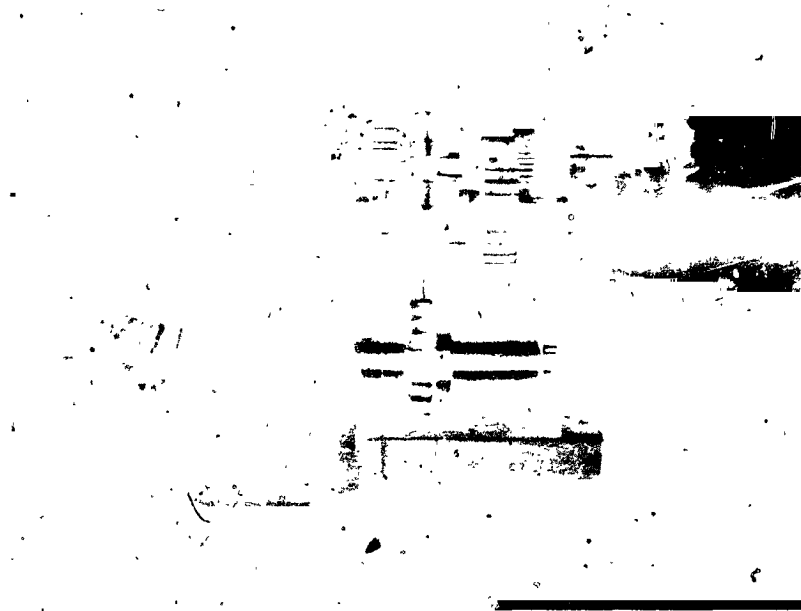


Figure 9. Gear Box - Left Profile

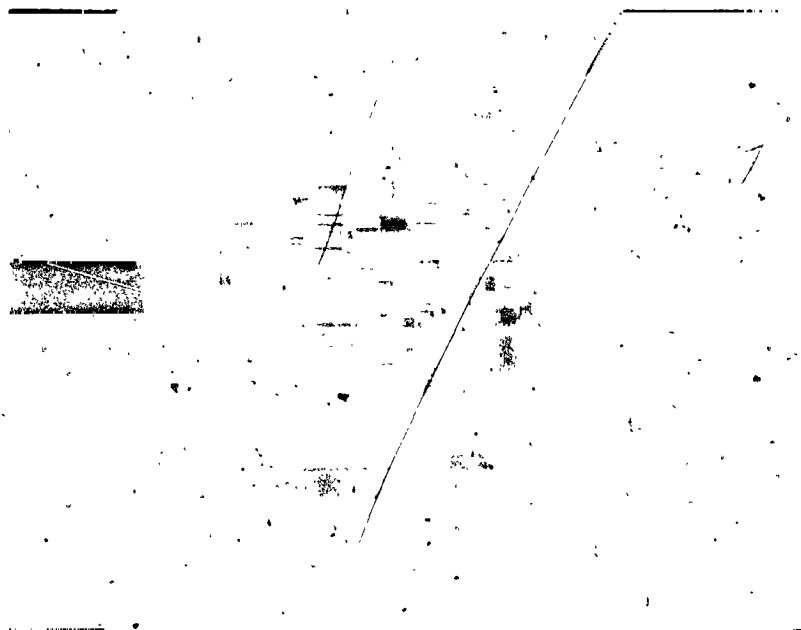


Figure 10. Gear Box - Right Profile

ER 13952

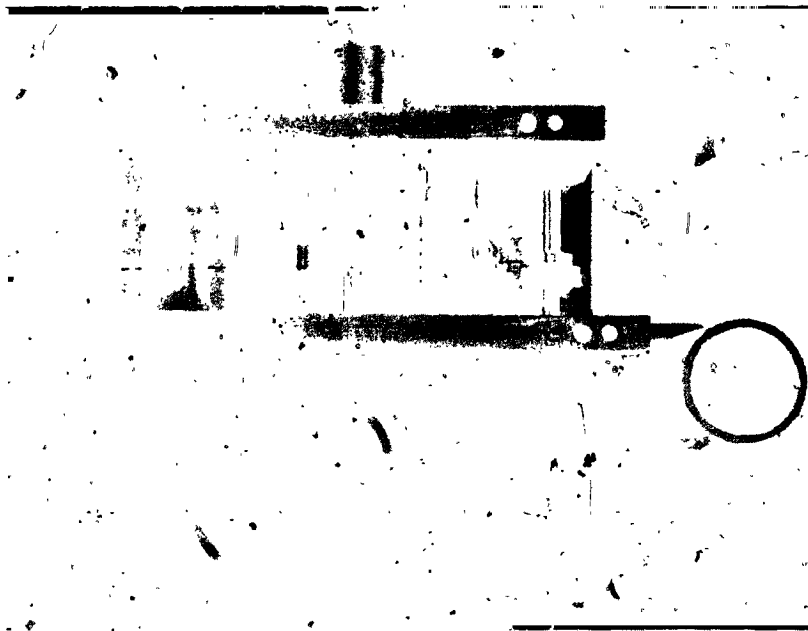


Figure 11. Gear Box - Top View

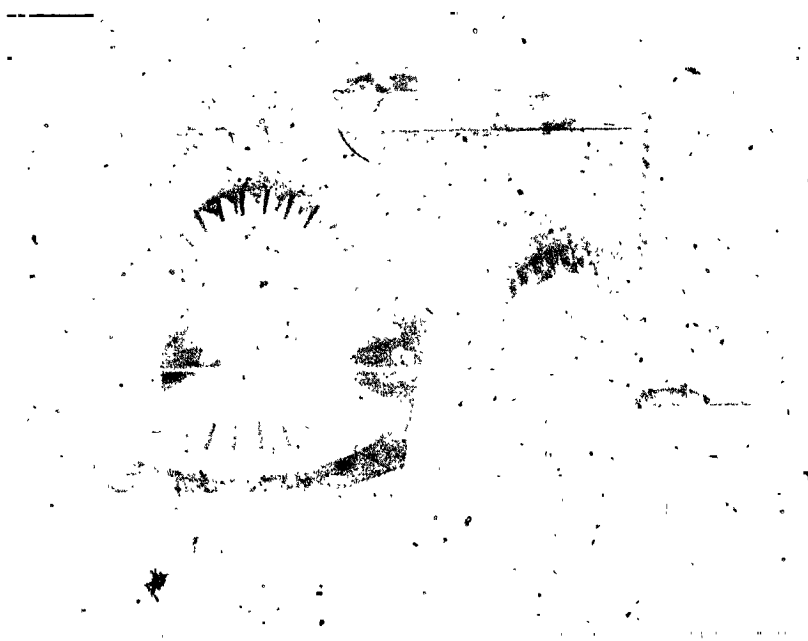


Figure 12. Rotary and Vertical Traverse Drives

ER 13952

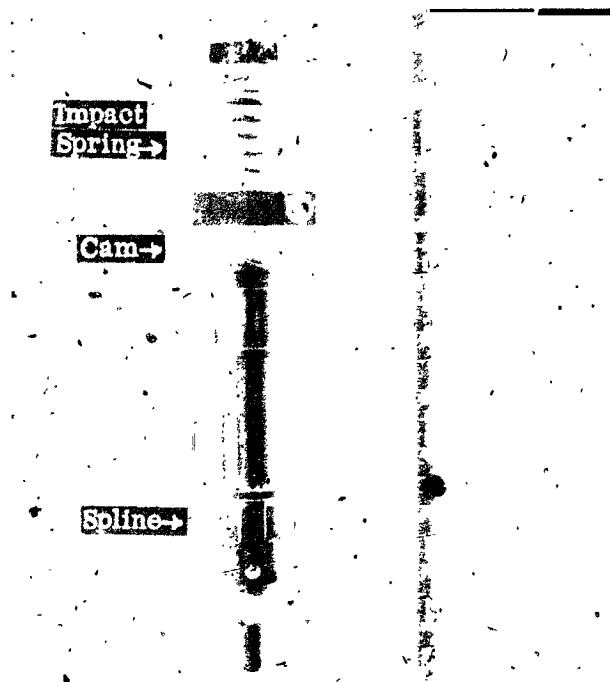


Figure 13. Percussor Unit



Figure 14. Percussor Housing Retainer Top & Bottom Plates

ER 13952



Figure 15. Assembled Drill String



Figure 16. Drill String Components

drill string rotational speed, the percussive impact frequency is 1620 bpm. The percussive energy per blow is approximately 16 inch-pounds. This energy level was found to be optimum for medium-hard materials such as vesicular basalt and marble with the standard core bits employed with the breadboard coring device.

Drill String - Core Bit, Core Barrel, and Extension Tubes

The drill string assembly for the breadboard model lunar coring device (Figures 15 and 16) consists of the rotary-percussion tungsten-carbide core bit, core barrel and six core barrel extension tubes. The core barrel, (or upper extension tube) is coupled to the lower portion of the percussor unit, which, in turn, is driven by the basic machine.

Most of the tungsten-carbide, rotary percussion core bits used during this program were modifications of a standard (6" length x 1.5" diameter) commercial bit manufactured by Pratt and Whitney Tool Company. The scope of the program was not sufficient to justify a percussion bit optimization study, which would be desirable during the next phase of the program. The Pratt and Whitney bits were modified by: 1) Reducing the overall length to two inches, 2) cutting an inside taper for the core catcher bushing, and 3) cutting a thread to facilitate coupling to the core barrel. The core bits, with an I.D. of one inch and O.D. of 1.5 inches (0.25-inch cutting kerf) consist of seven carbide cutters brazed to the steel case. A dust transport spiral rising behind each carbide cutter is machined into the steel case. These seven spirals align properly with the corresponding spirals on the core barrel when the two components are properly coupled.

The core extractor consists of a split, tapered bushing which is emplaced into the mating, tapered portion of the core bit. As the drill string is retracted, the core extractor is forced down into the narrow portion of the core bit taper, thus forcing the extractor to "clamp" the rock core. Further retraction of the drill string causes the rock core to fracture at the drill face, and the entrapped core within the core barrel can be brought to the surface.

The core barrel is constructed from a 18 1/4-inch steel tube with threads at each end to facilitate coupling to the core bit and extension tube. Accumulation of rock core within the barrel is currently limited to approximately 17.5 inches due to the threaded coupling inserts.

The core barrel was initially constructed from steel, although subsequent coring tests have indicated that percussive energy losses in an aluminum core barrel are not excessive. Subsequent coring device models should incorporate an aluminum core barrel.

The six core barrel extension tubes are constructed from 16 1/2-inch aluminum tubing with threaded steel inserts mounted in each end to facilitate coupling. The tubes are finished with the Martin hardcoat (aluminum oxide) process, which reduces surface abrasion, "down-the-hole" side wall friction, and coring dust adhesion.

An early version of the coring device incorporated six inner steel percussion rods to transmit the percussion energy directly from the percussor hammer to the top of the steel core barrel. Subsequent field testing of the machine revealed that the aluminum extension tubes were sufficient to transmit the percussion energy, and the inner steel percussion rods were eliminated from the system.

Coring Dust Transport System

Coring dust removal from the bottom of the drill hole to the surface is accomplished by means of mechanical spirals machined into the periphery of the core bit, core barrel, and core barrel extension tubes. When the elements of the drill string are properly coupled, the seven spirals, originating behind the seven carbide cutters on the face of the core bit, provide continuous transport of the dust from the bottom to the top of the drill string. Each spiral has a lead of 2 5/8 inches, a groove depth of 1/32-inch, and width of 3/16-inch. A combination of drill string rotation, and vibration (from percussor) aids in causing the finely-ground coring dust to move upward along the spirals until deposited at the surface. Further optimization of the extension tube spiral geometry may be desirable in order to increase cutting removal efficiency and reduce weight.

The breadboard model test program revealed that the mechanical spiral was sufficient to transport the dry coring dust from the bit face to the surface without the use of gaseous or liquid flushing agents which are employed in most commercial drilling rigs. However, subsequent drilling tests in an extremely high vacuum (10^{-10} mm Hg) may reveal the need for gaseous lubrication to reduce friction and dust adhesion to the core barrel and tube extensions.

Electric Motor Prime Mover

The electric motor, which was designed specifically for the lunar rock coring device, is a direct current, permanent-magnet, mechanically commutated machine. A permanent-magnet motor was chosen in lieu of a shunt or series field in order to increase power operating efficiency and reduce weight. The motor has a nominal operating output of approximately 373 watts (0.5 horsepower), a no-load rotational speed of 8500 rpm, and a maximum operating efficiency of 74%. Optimum voltage operation was set at 24 V dc in order to conform with the LEM power source voltage variations within the range of 20-32 V dc. Motor performance characteristics (Torque vs. Output Power, Input Current, RPM, and Efficiency) are illustrated in Appendix I.

A cylindrical, non-hermetically sealed housing was designed for the basic motor as shown in Figures 5, 7, 8, and 9. The permanent field magnets are composed of two segments diametrically opposed, having an inside radius of 1.1 inches, an outside radius of 1.5 inches, and an axial length of 1.5 inches. Stackpole Carbon Company ceramagnet A-9 is used as a magnet material. Armature laminations consist of M-19 transformer grade steel which possess very low electrical and magnetic losses. The 32-bar commutator is constructed from zirconium copper capable of operation at extremely high temperatures. The armature is wound with 17-gage copper wire, with 4 turns per coil, and two coils per slot. High temperature glass cloth insulation is used throughout the motor armature.

Environmental Control System

A thermal analysis was conducted (Appendix G) to determine the effects of operating the lunar coring device motor at rated load in a vacuum. A nominal operating current of 20 amperes, and a total heat dissipation (bearing friction, copper losses, etc.) of 135 watts was used for the analysis. Maximum allowable operating tempera-

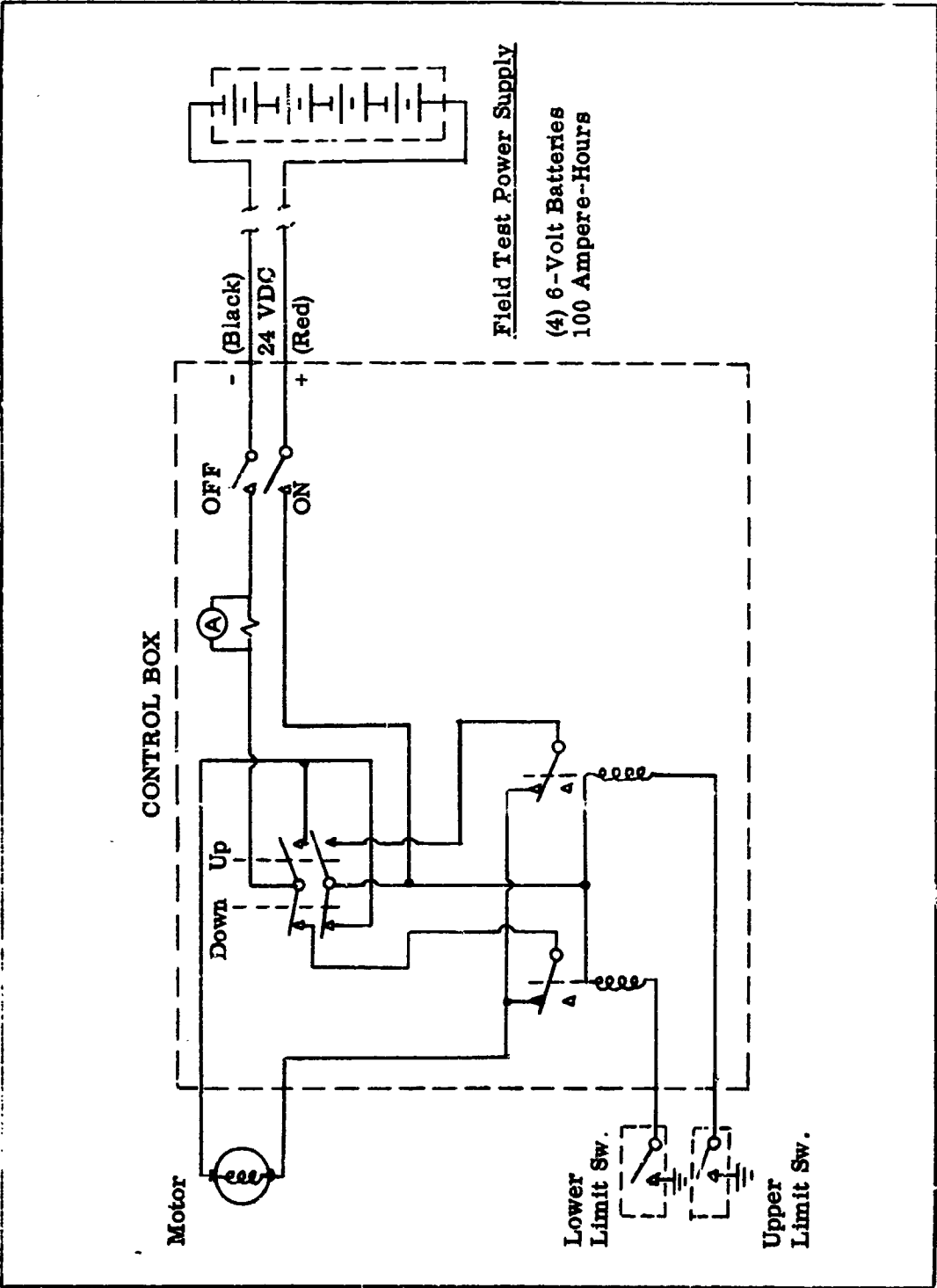


Figure 17. Coring Device Control Circuitry

ture of the motor armature using state-of-the-art insulation and brushes is approximately 205° C. Preliminary conclusions obtained from the thermal analysis are as follows:

- 1) The heat storage capacity of the motor is insufficient to maintain the assumed maximum allowable operating temperature. The 205° C temperature would be attained within 0.33 hours of continuous 20-ampere operation.
- 2) If a reasonable case temperature (105° C) is assumed for the preliminary analysis which can easily be maintained by an evaporative cooling system, the motor armature temperature would still exceed the maximum assumed allowable temperature of 205° C in a vacuum. In order to maintain an armature temperature of 205° C while depending on radiation only for armature-to-case heat transfer, the case temperature must theoretically be maintained below absolute zero. This, of course, is impossible.
- 3) The only practical technique for obtaining adequate armature-to-case heat transfer is by convection through a nitrogen pressurized case. The analysis indicated that the 205° C armature temperature could be maintained if the motor housing is nitrogen pressurized, and the motor case is maintained at approximately 39° C by water boil-off at 0.46 psia.

A preliminary environmental control system was analytically designed using the nitrogen pressurized motor and evaporative cooling technique as shown in Appendix G. Nitrogen leakage rates through the rotating motor shaft seal were included in the analysis, and corresponding allowances were made for nitrogen replenishment. The analysis revealed that 3.52 pounds of water or ethylene glycol would be required for the 2400 watt-hour drilling mission. The environmental control system consists of the following major items:

- 1) N₂ Pressurization System - Tank, pressure transducer, pressure regulator, and plumbing
- 2) Cooling System - Water jacket, wicking, pressure relief valve, plumbing, and insulation
- 3) Expendables - Water (or ethylene glycol) and nitrogen.

The total weight of the environmental control system, including expendables, was estimated at 8.86 pounds.

Power Cable

The 100-foot power cable recommended for the lunar coring device consists of a double AWG No. 6 aluminum conductor with lightweight insulation. Total weight of the cable, including conductor, insulation, and connectors is estimated to be 7.0 pounds. The aluminum was selected for a conductor material because its resistance per pound is significantly less than copper.

A thermal analysis was performed to determine the cable operating temperature in the lunar environment. A typical current profile (Appendix H) was selected for the analysis which was based on penetration rate-power consumption data obtained during the field tests of the lunar coring device.

Two possible cable insulation models were considered for the analysis: a) A white insulation ($\alpha = 0.4$, $\epsilon = 0.8$) and b) an aluminized tape wrapped cable ($\alpha = 0.147$, $\epsilon = 0.58$). The theoretical maximum temperatures which these cable models would experience are 92°C and 84.5°C respectively. These temperatures are well within the maximum allowable for aluminum.

Anchoring Technique

As previously described, the lunar rock coring device was designed to operate at a nominal axial bit pressure of approximately 30 to 40 pounds. A minimum weight of 240 earth pounds would be required to restrain this pressure in the 1/6-G lunar environment. Therefore, unless lunar surface materials could be used as ballast, the weight of the basic coring device is insufficient to provide the necessary restraint for the coring operation.

The technique selected for securing the breadboard model lunar coring device to a rock outcrop is the employment of an expansion-type rock anchor. A Phillips Drill Company commercial (Type JS-14M) 1/4-inch diameter, 2 1/4-inch long expansion anchor was successfully employed during the evaluation tests of the breadboard model coring device. This type of anchor is threaded on one end (Figures 5 and 18) and split-hollowed on the opposite end. A tapered stud is inserted into the hollow end of the anchor, and the entire anchor and stud assembly emplaced in a predrilled hole 1/4-inch in diameter and 1 3/8-inch deep in the rock face. The anchor is expanded by applying several light blows with a hammer which causes the tapered stud to "spread" the split-hollow end (below rock surface) of the anchor. Pull-out tests of this type anchor in solid basalt revealed that 400 pounds of restraining force can be attained with a properly emplaced anchor.

Pre-drilling of the anchor holes in the rock outcrop is accomplished by use of the coring device drilling adapter shown in Figure 16. The lunar coring device is hand-restrained during this process. Three anchors are currently employed for restraining the device. After emplacement of the three anchors, the coring device is manually placed on the anchor bolts, and restraining nuts employed to lock the machine to the rock outcrop. Three leveling bolts are also incorporated on the base of the machine to compensate for roughness of the rock face, and any tendencies for the machine to be unstable.

Although the previously described anchoring technique proved to be satisfactory for the breadboard model coring device, the additional weight, and operator time required for use of the drill chuck attachment is not particularly desirable for the flight model. In addition, the lunar surface model may consist of an unconsolidated overburden which would preclude use of the standard rock-type anchor. Therefore, in order to provide an anchoring capability for a variety of drilling conditions, a minimum of two distinct types of anchors will be required.

Figure 18.A illustrates a hard rock anchor similar in principle to the 1/4-inch diameter Phillips anchor employed with the breadboard coring device. The recommended tubular anchor would be emplaced in holes (approximately 1 1/2-inches diameter) which were predrilled with the core bit, thus eliminating the requirement for a special chuck and drill. Expansion of the anchors could be accomplished with the geological hammer or with the percussion capability of the coring device. The latter technique would require that the basic coring device be removed from the vertical traverse column and hand-held while expanding the anchors. Two anchors will be sufficient to restrain the coring device. A slot, rather than a hole, is employed on one side of the base plate in order to provide for minor misalignments during anchor emplacement.

Figure 18.B illustrates an overburden anchor for emplacement in soft pumice, unwelded tuff, or unconsolidated rubble. The anchors are emplaced at an angle of approximately 30 degrees relative to the load axis of the coring device. In this manner, the anchors are restrained by both compressive and frictional forces of the overburden, rather than pure friction of a 0-degree emplacement angle. The anchors are approximately 12 inches in length, with provisions for locking to the coring device base plate at any interval along the anchor. Either of the two techniques previously recommended for expanding the hard rock anchor would also be used for driving the overburden anchors.

The flight model coring device should also be provided with the necessary hardware for anchoring and drilling from one of the LEM landing pads in the event that the immediate lunar surface is not suitable for emplacement of either the hard rock or overburden anchors.

Core Orientation

Lateral (North-South) core orientation can be more easily attained with large commercial drilling rigs because 1) the larger diameter core samples will not easily shear (and rotate) prior to core pulling, and 2) the employment of a double core barrel (with inner barrel non-rotating with respect to core) reduces the shear forces applied by the drill to the core sample. Therefore, if the core has not rotated prior to pulling, the lateral orientation can be maintained by "straight-up" pulling of the core and marking with respect to north-south orientation.

The power limitations of the lunar rock coring device will not permit the use of wide diameter core bits, or core bits with wide kerfs sufficient to maintain clearance for a double core barrel system. Therefore, it is very probable that the core samples obtained by the lunar coring device will shear and rotate within the core barrel prior to retrieval, thus losing a lateral orientation reference. One possible solution to this problem would be to scribe an orientation reference mark with an aluminum pencil or diamond on the rock face to be cored prior to coring, and reconstructing the entire core sample relative to the scribe mark after return to earth. A second alternative would be to scribe the rock using "down-the-hole" tools prior to coring at various depth intervals of interest. This technique will be described in greater detail in a later section of this report.

ER 13952

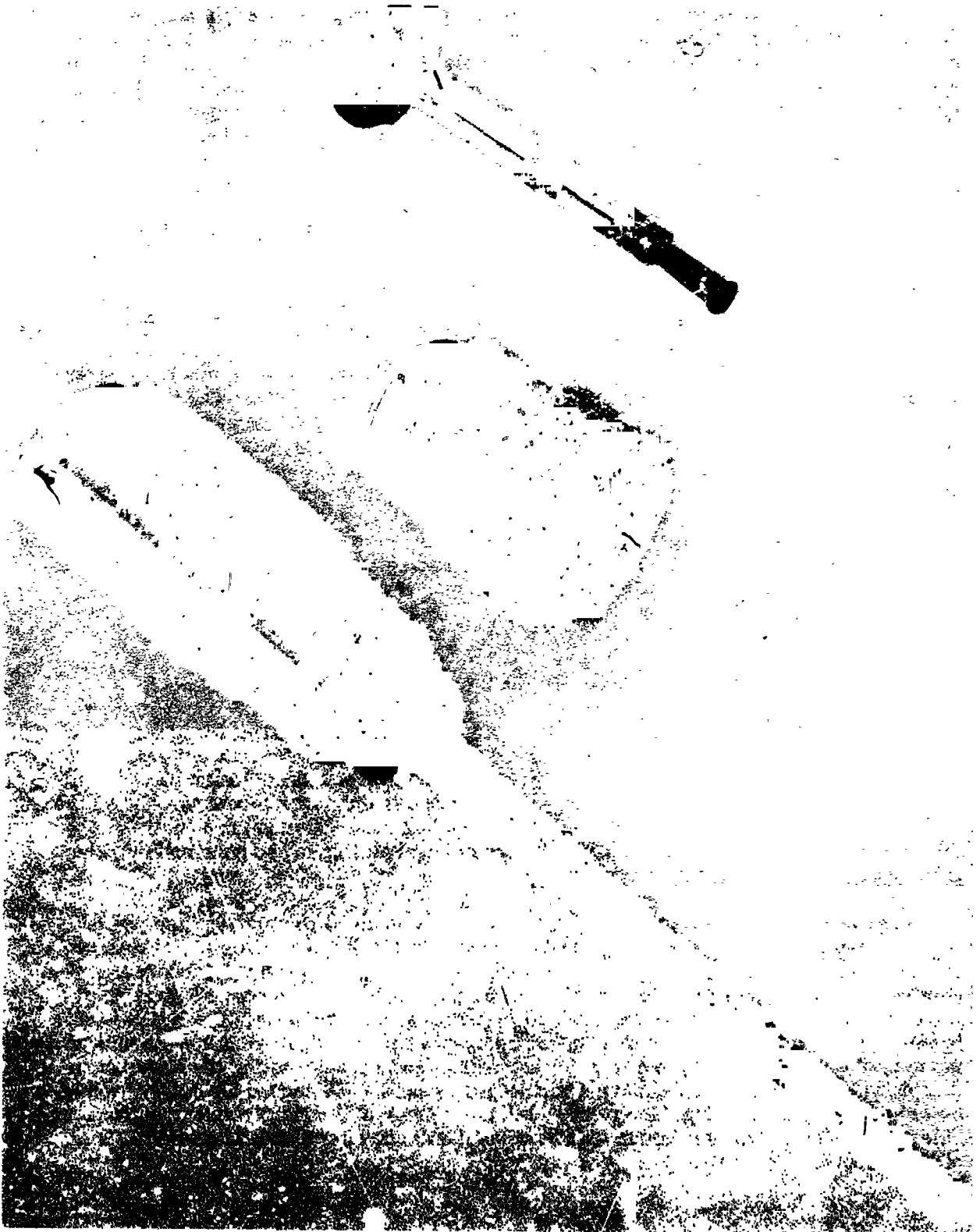


Figure 18. Rock Anchor, Anchor Drill and Core Bit

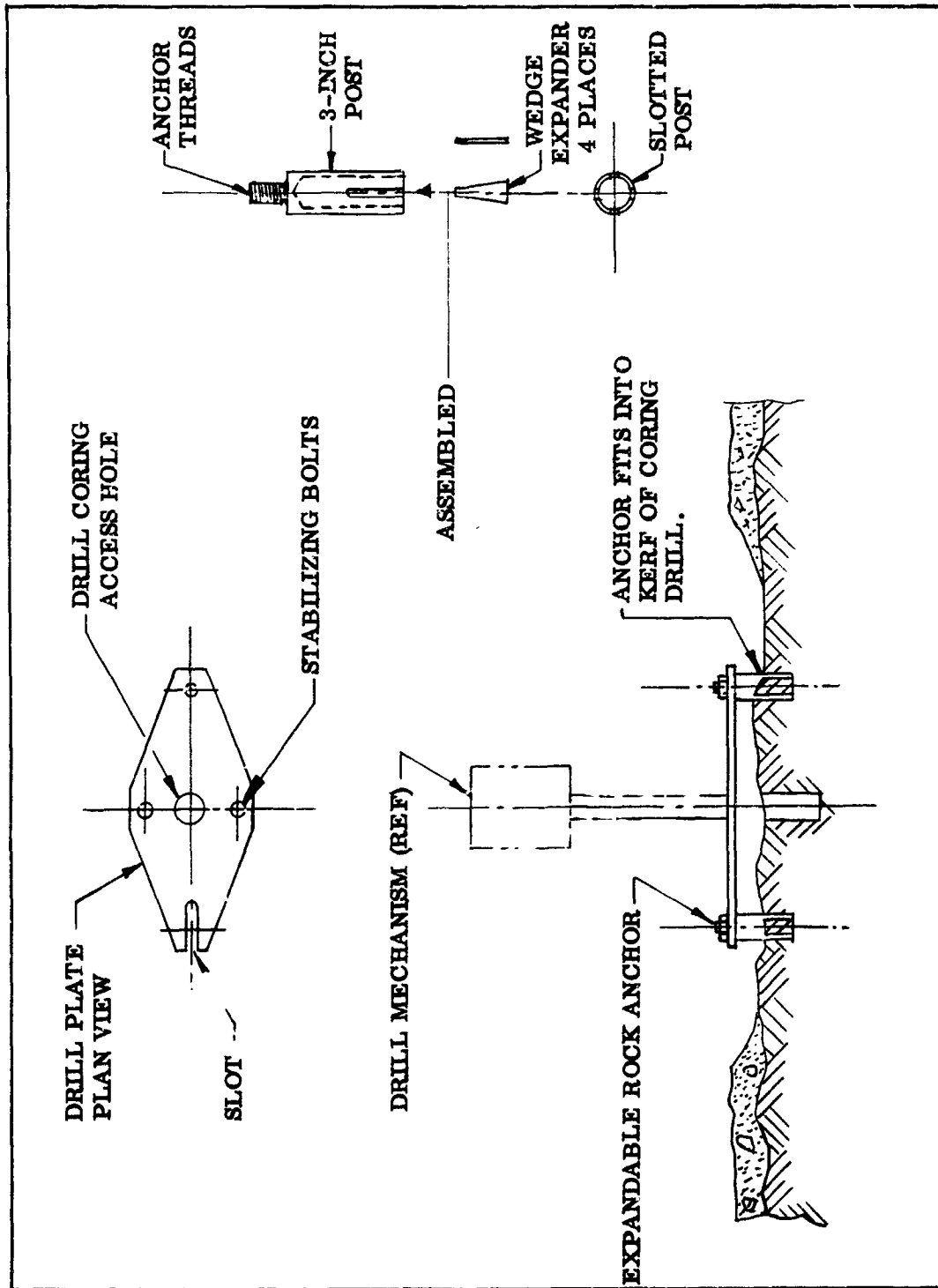


Figure 18A. Conceptual Hard Rock Anchor

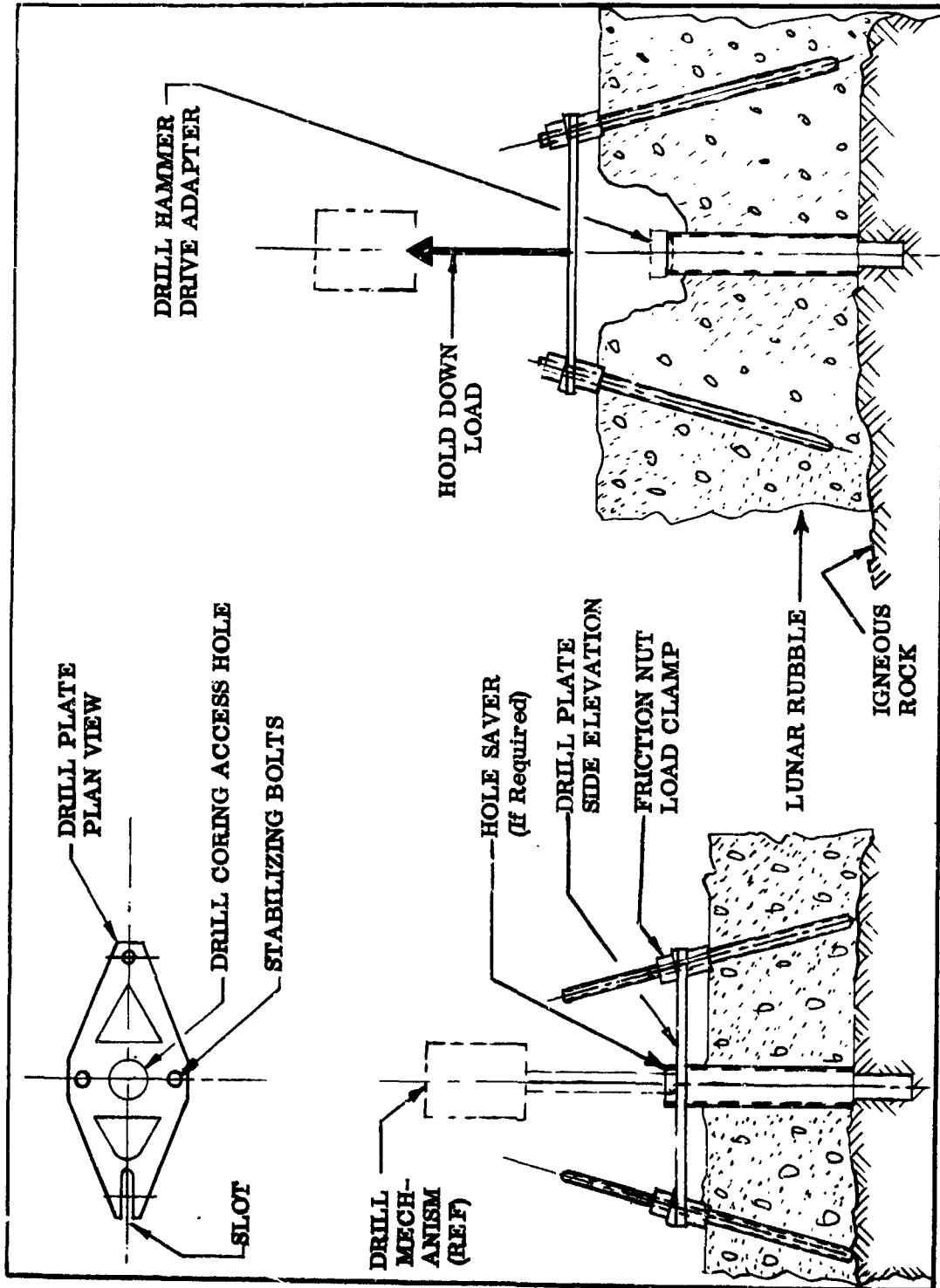


Figure 18.B. Conceptual Overburden Anchor

Vertical orientation of the core sample can be obtained by means of a clinometer to measure the inclination angle of the drill string. An azimuth measuring device would be required to determine the direction of the clinometer-measured core inclination. A vertical history of the core sections can be attained by packaging the core segments in pre-numbered sample bags while describing the operation for permanent recording by the communication system.

CORING DEVICE TEST PROGRAM

Rock Penetration Rate Tests

Rock penetration rate tests of both the early diamond rotary bits and final rotary percussion breadboard coring device were conducted in a variety of rock samples. Figure 19 illustrates the rock samples which were used for the limited depth penetration rate tests. Field evaluation tests of the coring device to greater depths were conducted in local marble quarries.

Brief geological descriptions of the rock samples, with accompanying photomicrographs taken from thin section samples are presented below.

Basalt (Figure 20) - Dark gray, dense, fine grained, sub-conchoidal fracture. Holocrystalline, intergranular, laths of labradorite (88%), augite (9%), magnetite (3%), some slight tendency toward parallel orientation of the labradorite crystals, no vesicles. Bend, Oregon.

Vesicular Basalt No. 1 (Figure 21) - Medium gray, medium grained, uneven fracture, equidimensional vesicles up to 2 mm (10-15%). Holocrystalline, intergranular, plagioclase (65-70%), augite and pigeonite (15%), magnetite (2%). Bend, Oregon.

Vesicular Basalt No. 2 (Figure 22) - Medium gray, medium grained (coarser than vesicular basalt no. 1), uneven fracture, equidimensional to highly elongate vesicles up to 20 mm (10-15%). Intergranular, labradorite (50%), augite and pigeonite (35%), magnetite (1%), interstitial glass and glass lining vesicles (2%). Bend, Oregon.

Pumice (Figure 23) - Light to dark gray, pumaceous and scoriaceous volcanic glass. Vesicles (60%), elongate to highly elongate up to 15 mm, but mostly 4 to 8 mm. SiO₂ (75%). Tiny microlites of feldspar and magnetite. Mono Craters, California.

Obsidian (Figure 24) - Volcanic glass, dense, conchoidal fracture, flow banded, containing numerous microlites of feldspar and magnetite. Newberry flow, Bend, Oregon.

Granite Biotite Gneiss (Figure 25) - Light gray to pinkish, dense, medium to coarse grained, poorly developed gneissic texture. Biotite (5%), muscovite (2%), pink K-feldspar (30%), white plagioclase (30%), quartz (30%), magnetite (1%). Baltimore County, Maryland.

Biotite Schist (Figure 26) - Medium gray, hard, good schistose texture. Biotite (35%), quartz (35%), pink K-feldspar (15%), plagioclase (10%), apatite (1%), magnetite (1%). Biotite contains particle emitters surrounded by pleochroic halos, zircon. Baltimore County, Maryland.

Marble (Figure 27) - White to cream colored, 100% calcite, grain size 1/4 to 1/2 mm, granoblastic. Many of the calcite grains are polysynthetically twinned which may have resulted from the drilling or blasting in the quarry.

Numerous rock penetration rate tests were performed during the final two months of the program. Most of these tests were necessarily oriented toward identification of problem areas with the basic coring device, rather than optimization of coring penetration rates. Several design changes were performed during this period as a result of the problems encountered during final testing of the breadboard model coring device. These problems and modifications included:

- 1) Motor - Partial demagnetization of the permanent magnets occurred during one of the penetration rate tests as a result of excessive current flow during a stall condition. The motor was redesigned with larger permanent magnets. No further de-magnetization problems were encountered.
- 2) Tungsten-Carbide Rotary Percussion Bits - The initial carbide bits were fabricated as an integral part of the core barrel. Complete replacement of the core barrel was required after the carbide cutters dulled sufficiently to prevent satisfactory rock penetration. This problem was corrected by redesign of the core barrel and bits so that the core bit can be unscrewed from the core barrel when replacement is required.

Although the wear characteristics of the carbide bits for "dry" coring are much better than the rotary diamonds, occasional replacements will probably be required during a lunar mission if hard rock materials similar to the solid basalt are encountered. Significant dulling of the present-type carbide bits occurred after drilling 20 inches in the solid basalt or granite biotite gneiss. However, the core bit would probably drill the complete ten feet in a material similar to the vesicular basalts without replacement of the core bit.

Optimization of the tungsten-carbide bits may improve the wear-out characteristics. With the low levels of power and percussive energy available for the lunar coring device, it is highly desirable that a sharp edge be maintained on the carbide cutters in order to assure maximum penetration rates. If further improvements are not possible, replacement of the bit after each 20-inch section of drilling would be recommended for the lunar mission in order to insure maximum penetration rates with the limited available power.

- 3) Core Retainer - An improved core retainer (breaker) was designed as a result of deficiencies in the early model. This was accomplished by increasing the taper in the core bit to facilitate a tighter grip on the core by the retainer bushing during retraction.
- 4) Traversing Drive Output Shaft - A heavier duty shaft was incorporated due to shearing of the original shaft during a coring test.

ER 18952

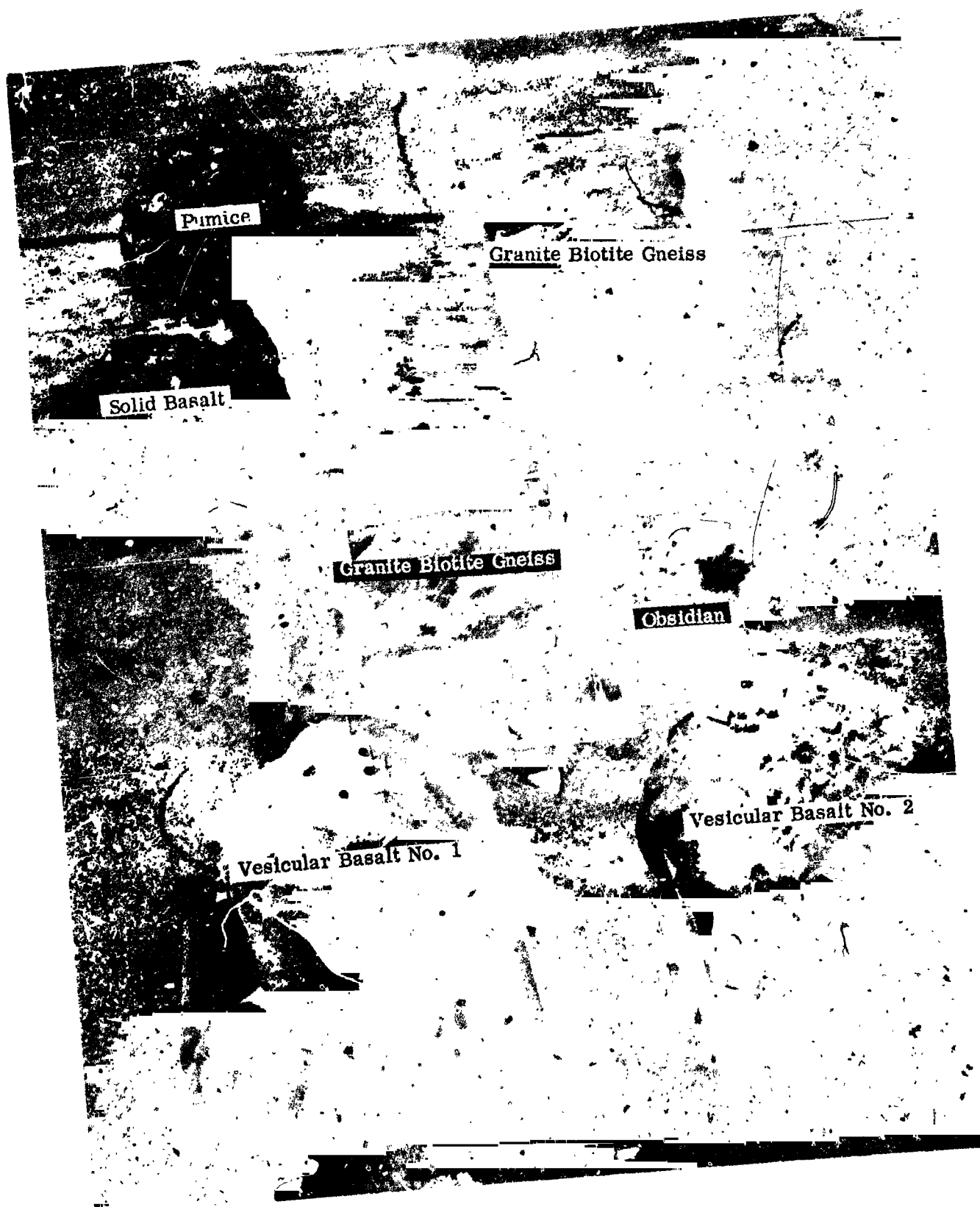


Figure 19. Feasibility Test Rock Samples

ER 13952

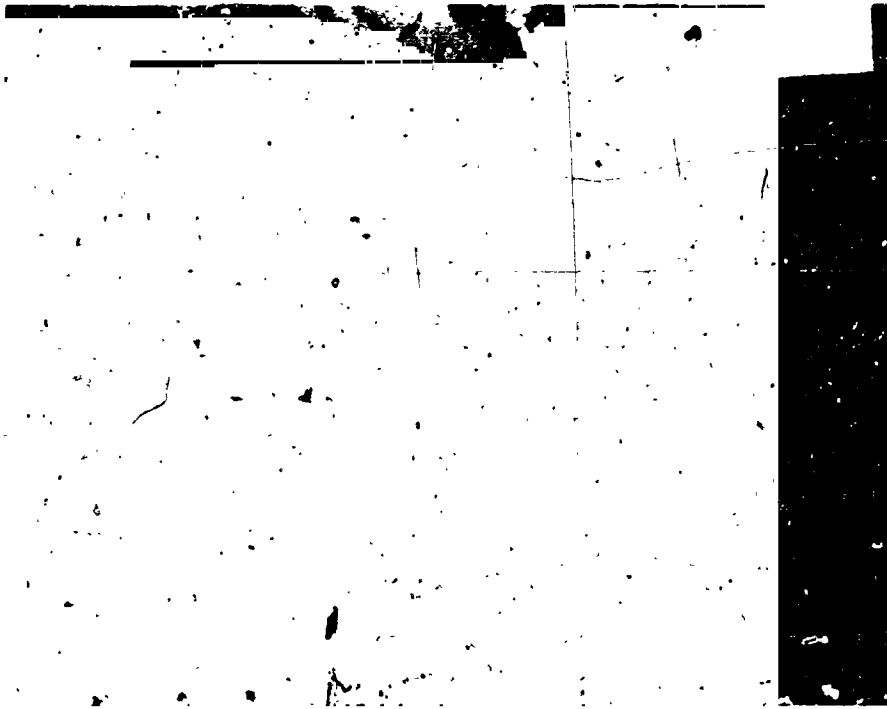


Figure 21. Vesicular Basalt Photomicrograph

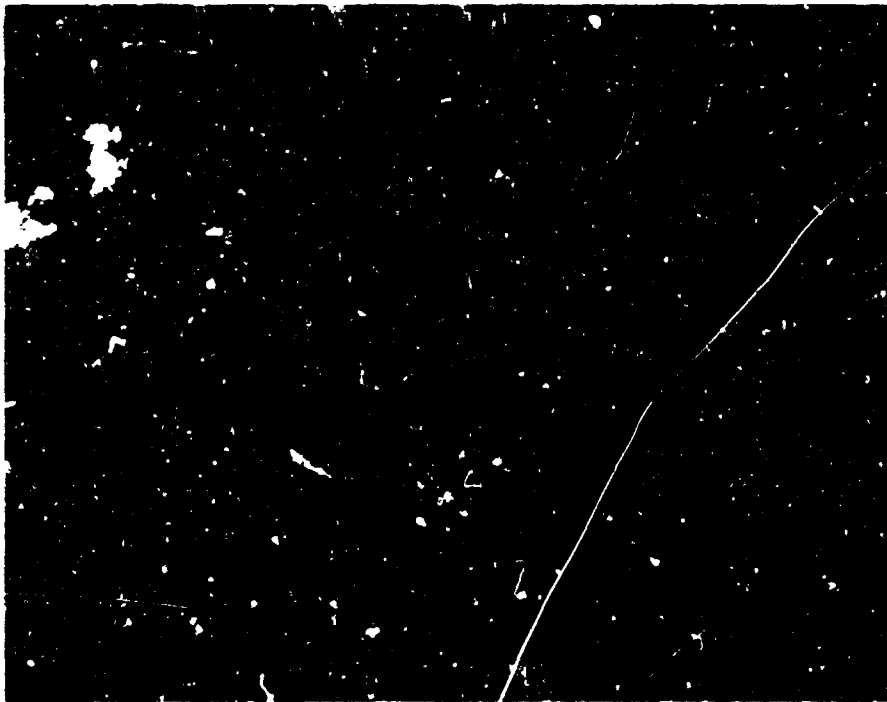


Figure 20. Solid Basalt Photomicrograph

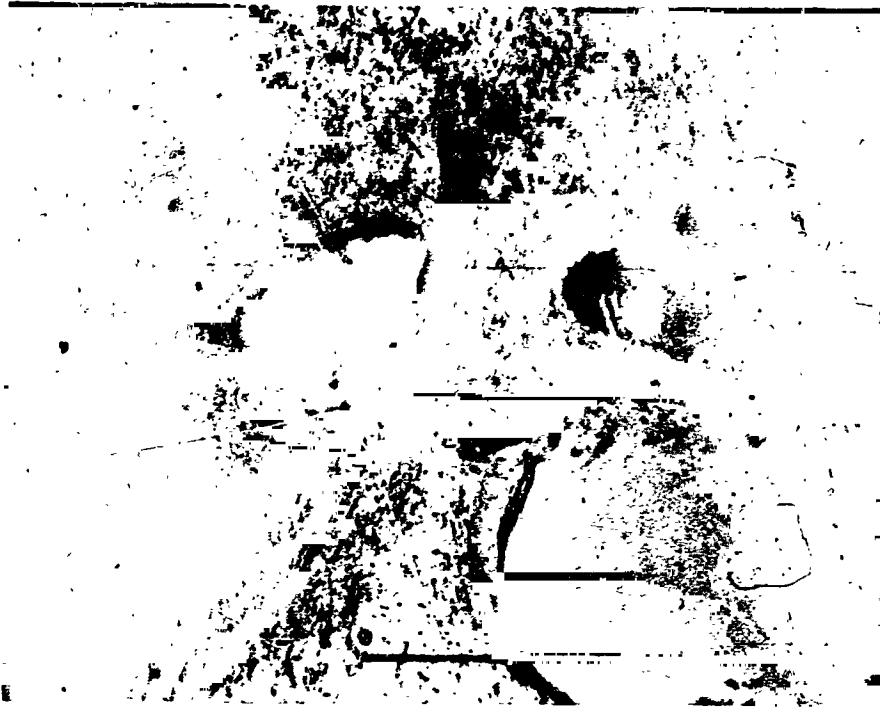


Figure 23. California Pumice Photomicrograph

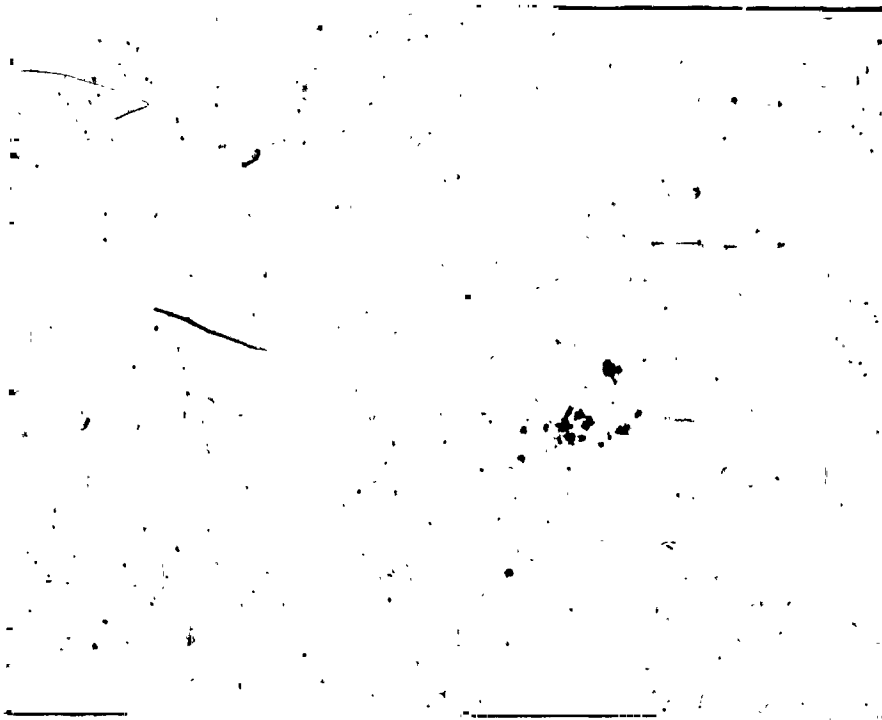


Figure 22. Vesicular Basalt No. 2 Photomicrograph

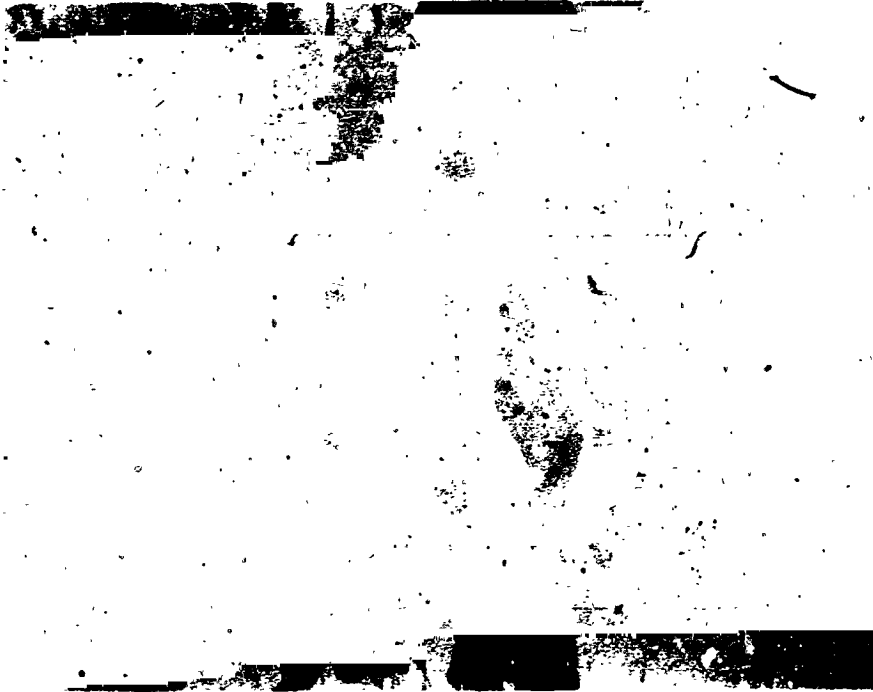


Figure 25. Granite Biotite Gneiss Photomicrograph

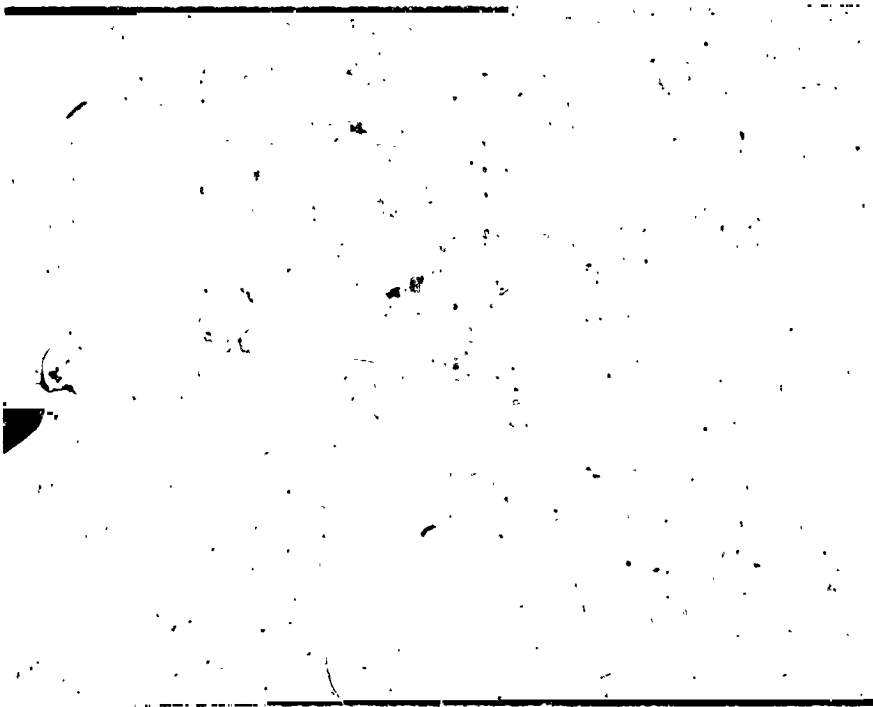


Figure 24. Obsidian Photomicrograph

ER 13952

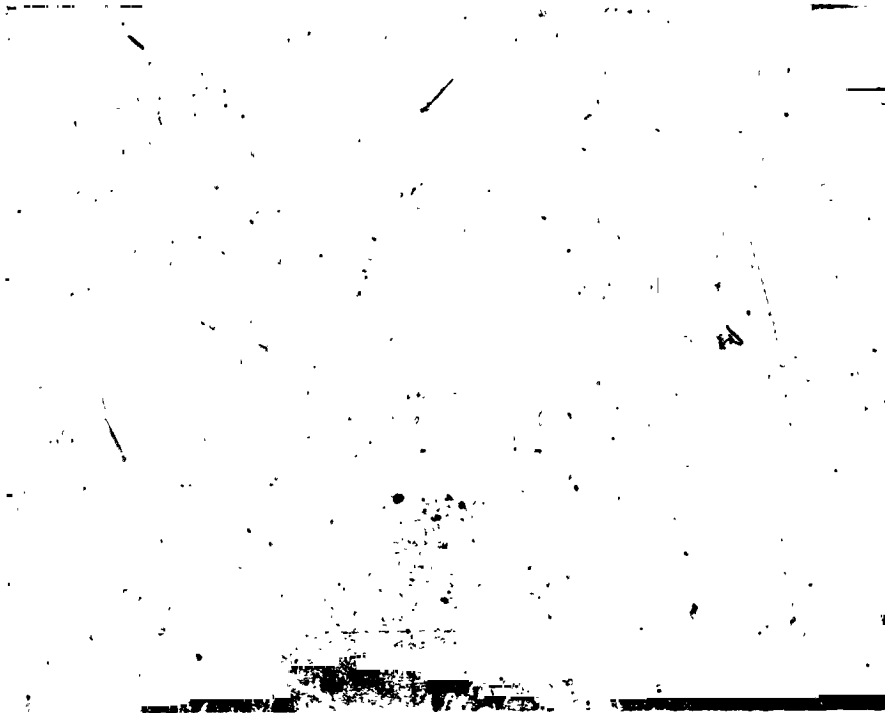


Figure 27. Marble Photomicrograph

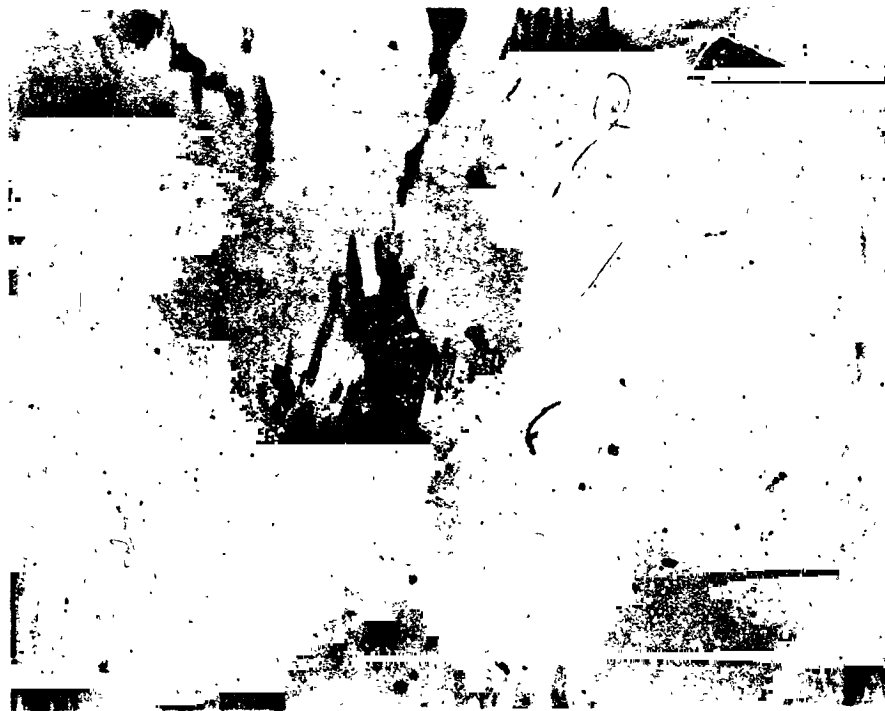


Figure 26. Biotite Schist Photomicrograph

- 5) Gear Box - A gear change was incorporated to facilitate forward (normal) rotation of the drill string simultaneously with reverse traversing (for core retraction) of the motor. The initial design did not possess this capability. The penetration rate tests clearly demonstrated that the drill string would tend to jam in the hole while retracting without rotation.

The final evaluation tests of the breadboard model coring device resulted in the representative penetration rates listed below. These rates were extrapolated from the results of drilling tests conducted to a maximum depth of 18 inches in the test samples shown in Figure 19. Coring tests conducted to a depth of ten feet were performed only in marble as described in the next section of this report.

Solid Basalt	- 1.5 feet per hour
Vesicular Basalt No. 1	- 5 feet per hour
Vesicular Basalt No. 2	- 8 feet per hour
Granite Biotite Gneiss	- 2 feet per hour
Obsidian	- Relatively high rate, but core tends to fracture and rock anchors pulled out.
Pumice	- Core pulverized and hard rock anchors were unsatisfactory

The drilling tests clearly demonstrated that a variable energy percussive blow is required in order to satisfactorily core a wide range of material hardnesses. Pure rotary drilling of the pumice with the rotary percussion bit will sometimes result in a consolidated core. However, a thin-wall diamond bit with pure rotary drilling would probably be optimum for obtaining consolidated cores from the pumice.

The present breadboard coring device is optimized for drilling medium-hard materials such as the vesicular basalt and marble. Although satisfactory penetration rates were attained in the hardest basalt sample, it was evident that excessive heat generation and "bit dragging" was occurring as a result of insufficient percussive energy for satisfactory penetration. When the coring penetration rate and percussive energy blows are optimized, the heat generated by the tungsten-carbide bit is much less than with the rotary diamond bits. Therefore, it is recommended that future models of the lunar coring device incorporate a variable energy percussive blow mechanism in order to satisfactorily core the wide range of materials expected on the lunar surface.

Ten-Foot Coring Tests

The size of available samples of basalt, obsidian, and pumice limited penetration rate testing of the breadboard coring device to depths of 18 inches. Evaluation tests to 10-foot depths were conducted in two local marble quarries. Although the limited time prevented testing to depths of 10 feet in a variety of materials, the marble tests were satisfactory for evaluating two important parameters: 1) the ability of the seven helices machined into the bit, core barrel, and extension tubes to transport coring dust from a depth of ten feet to the surface, and 2) no apparent loss of percussive energy and reduction in penetration rate as a result of percussing through ten feet of aluminum drill string with nine mechanical (threaded) couplings.

The first series of tests were conducted in the Beaver Dam Quarry located in Baltimore County, Maryland. Figures 28, 29, and 30 illustrate various phases of the operation. All of the tests were conducted without the use of a gas for bit cooling and dust removal. Power was supplied by four 6-volt, 120-ampere hour automobile batteries.

A maximum coring depth of 6 feet was attained at the Beaver Dam Quarry. At this depth, moisture was encountered which caused the (wet) coring dust to pack around the core bit and jam the drill string. Until the moisture condition was encountered at the 6-foot level, the mechanical helix proved to be effective for transporting the coring dust to the surface. Penetration rates averaging 4.5 feet per hour were attained at operating current and voltage levels of 23-28 amperes and 24 volts respectively. This penetration rate and power consumption was comparable to that attained in the vesicular basalt. Consolidated core samples six to twelve inches long were obtained from both materials.

The remainder of the 10-foot coring tests were conducted at Campbell's marble quarry in Texas, Maryland. Rock outcrops exceeding ten feet in depth were available for the tests. However, this particular rock did not core as well as the Beaver Dam marble. Average cores varied in length from 1/4 to 4 inches. The equipment and set-up was similar to that shown in Figures 28, 29, and 30.

Successful coring to a depth of ten feet was attained at the Campbell quarry. The dust transport system (helix) was completely effective down to the ten-foot level. Although the penetration rate was somewhat slower (average 2.5 feet per hour @ 23-28 amps) at the Campbell quarry, the penetration rate remained relatively constant throughout the entire ten feet of drilling. However, the penetration rate was found to be very dependent upon the condition (sharpness of carbide cutters) of the coring bit. A very slight dulling of the bit in some instances resulted in a 30-50 percent decrease in penetration rate. Replacement of the bit resulted in a resumption of the 2.5 feet per hour penetration rate.

Another important factor which can affect the penetration rate of the coring device is alignment of the drill string with respect to the core hole. During the coring of the ten-foot hole it was found that slight movements (shift of position) of the coring device on the rock anchors can result in relatively high side-loading of the drill string at the bottom of the hole. This, in turn, results in excessive power consumption with a corresponding decrease in penetration rate.

The basic coring device also possesses a slight misalignment problem which tended to reduce penetration rate at the extreme lower portion of the vertical traverse. When the integrated motor and gear box assembly is at the top of its vertical traverse, the vertical traverse and support columns will flex somewhat as a result of the torque and axial thrust loading during the coring process. As the motor and gear assembly moves to the lower portion of travel where the vertical traverse and support columns are mechanically attached to the base plate, the resultant flexing is substantially reduced. This results in the coring of a slightly oversize (and perhaps slightly misaligned) hole when the motor and gear assembly is at the top of its travel. As the motor and gear assembly moves down the vertical traverse column, the drill string approaches a "true aligned" condition which, in turn, results in some side loading in the upper portion of the hole section. This characteristic of the coring device resulted in faster penetration rates during the first several inches of travel as compared

ER 13952

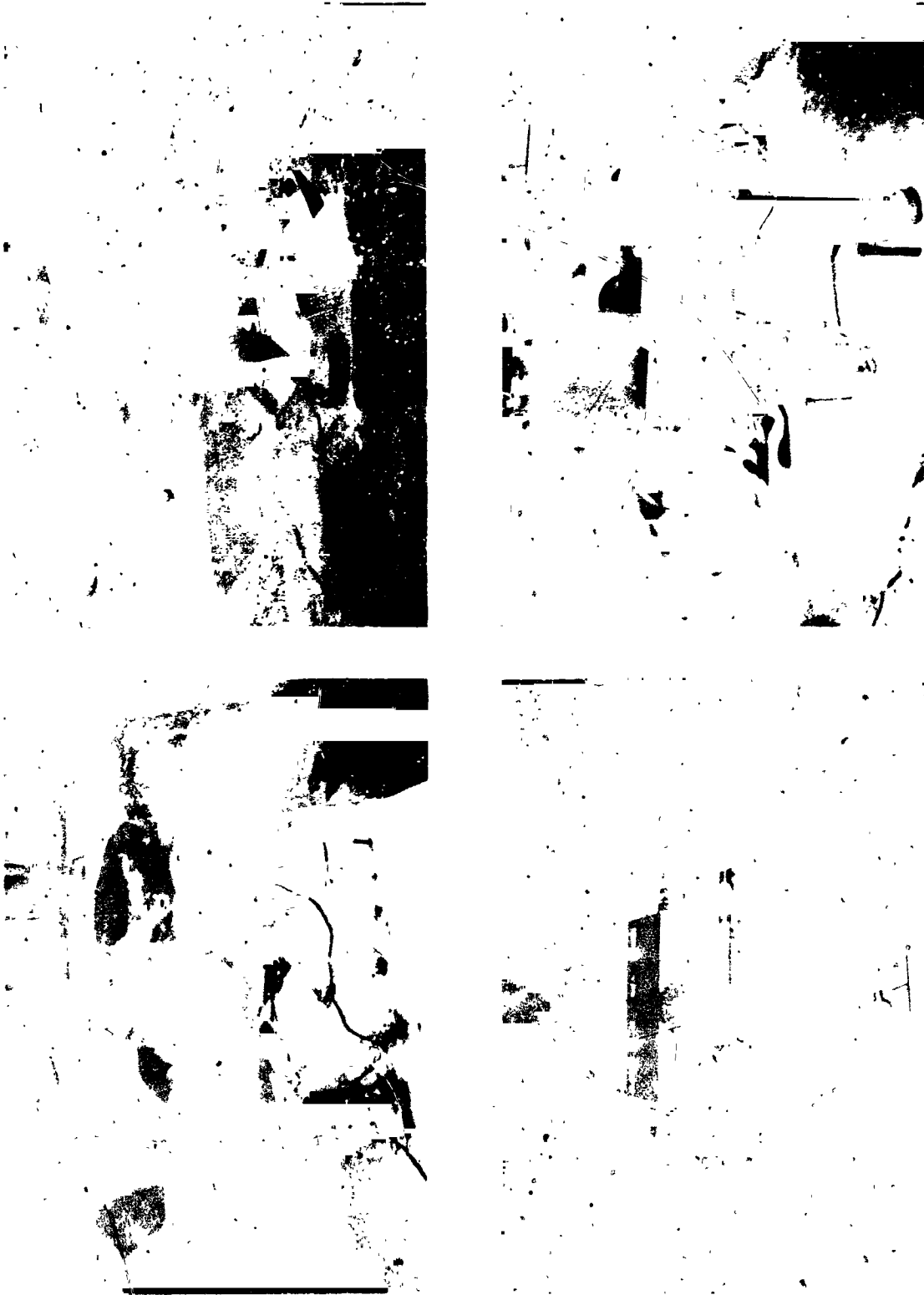


Figure 28. Field Evaluation Tests



Figure 29. Coring Device and Accessories



Figure 30. Drilling Rock Anchor Hole

to the final several inches, and was always apparent regardless of drilling depth. This undesirable characteristic can be eliminated on future models by a slight structural design change, possibly by lightening vertical drive assembly columns so that the drill will be "self-aligning."

Extended Depth Coring Tests

In order to further evaluate the coring depth capability of the lunar coring device, an additional ten feet of core barrel extension tubes were fabricated. The primary purpose of the extended depth coring tests was to determine if a significant decrease in penetration rate would occur as a result of percussive energy losses over a 20-foot drill string.

Several penetration tests were conducted at the Campbell quarry on the same rock outcrop where the successful ten-foot coring test had previously been performed. However, the maximum depth obtained with the additional equipment was twelve feet. At this depth, the coring bit encountered moisture (probably a subsurface joint plane) which resulted in blockage of the dust transport system and subsequent jamming of the entire drill string. The moist drill cuttings would enter the dust transport spirals behind each carbide cutter and completely block the spiral grooves. As coring continued, the moist cuttings accumulated in the bottom of the hole and the maximum torque capability of the motor was rapidly exceeded. Each time the core bit jammed, the drill string was manually removed from the drill holes, and the dust transport spirals cleaned in preparation for a new attempt. The drill system was incapable of coring past the joint plane and the tests were terminated. Other drilling locations, both on the same rock outcrop and at other areas within the quarry were test drilled, but joint planes encountered at varying depths precluded coring to depths greater than twelve feet.

From the extended depth coring tests, it can be concluded that the mechanical coring dust transport system is ineffective for the lunar coring device if moisture is encountered. A gaseous or liquid flushing agent would probably be required to remove the subsurface cuttings and prevent drill string jamming. However, since subsurface moisture is not probable within the upper ten feet of the lunar surface, no further investigation of this problem is warranted.

During the final field tests of the lunar coring device, a new technique for coring dust removal was investigated. Two 1/8-inch diameter holes were drilled in each of the seven grooves of the dust transport spiral in the top of the extension tube located immediately above the core barrel in the drill string. The purpose of this modification was to determine if the coring dust would rise upward on the transport spirals to the level of the collection holes, and drop into the hollow center of the extension tube. A partitioning plug was inserted between the core barrel and extension tube to prevent the coring dust from settling down between the core barrel inner wall and rock core.

The coring tests revealed that the subsurface dust storage technique is feasible. The fourteen dust entry holes (2 holes in each of the 7 spirals) which were drilled in the extension tubes resulted in the collection of approximately 50% of the total generated coring dust. The remaining 50% of the coring dust bypassed the entry holes and was transported to the surface in the usual manner.

Although time limitations prohibited a thorough evaluation of the subsurface dust storage technique, it is apparent that further optimization could result in collection of 100% of the generated cuttings. This technique may prove to be of value for deeper drilling missions where mechanical transport of the bit cuttings to the surface is impractical.

Spacesuit Interface Tests

A series of man/machine interface tests was conducted to evaluate the ability of a spacesuited subject to operate the breadboard model lunar coring device. The tests were conducted using the International Latex Corporation (AX-IL-012) state-of-the-art spacesuit. Tasks such as controls operation, assembly and disassembly of drill string components, and assembly of the percussion mechanism were studied. The major problem encountered was the difficulty in bending or stooping to the level required for handling of the core barrel and extensions. Some design improvements can be incorporated to alleviate these difficulties, but the major problem results from the 30-inch limitation for the height of the coring device.

Specific problem areas which were identified during the interface tests are listed below.

- 1) Percussor Housing - The drill string feed-through technique which requires removal of the percussor housing top each time the drill string is pulled from the core hole is somewhat difficult to accomplish in the spacesuit. In addition, the percussor housing is subject to the entry of dust when its top is removed. An alternative to this technique is to design the vertical traverse and support columns so that the integrated motor and gear housing can be manually rotated (repositioned) away from the axis of the drill string to facilitate manual pulling of the drill string when required. However, this would involve coupling and uncoupling the drill string from the bottom side of the integrated motor and gear housing assembly. This also is difficult to accomplish (Figure 31) because the astronaut cannot see the top of the core barrel when coupling to the percussor.

The human factors problems in this area may be somewhat alleviated with the latest state-of-the-art Apollo spacesuit. Subsequent design decisions in this area should be predicated on the capabilities of the latest spacesuit configuration in order to avoid possible overdesign for the human factors problems.

- 2) Accessories Storage - Provisions should be incorporated for temporarily storing the accessory equipment (extension tubes, core bits, etc.) at a convenient working level to the astronaut on the basic coring device.
- 3) Uncoupling of Drill String Components - The threaded couplings used to mechanically join the core bit, core barrel, and tube extensions are often difficult to separate after a coring operation. The only reliable manual technique for separating the coupled joints requires the use of a spanner-type wrench and small hammer. If this technique is employed, provisions should be incorporated for clamping (vice gripping) one section of the drill string while the other is uncoupled by use of the spanner wrench and small hammer. A small clamping mechanism could probably be incorporated on the top of the coring device

structure for holding the drill string during uncoupling. A low speed power drive could also be incorporated to perform the uncoupling task with a corresponding increase in machine complexity.

- 4) Anchor Emplacement - The emplacement of hard rock-type anchors is difficult if the base of the coring device is located at the standing surface level of the astronaut. A long tubular tool for manipulating and expanding the rock anchors from a stand-up astronaut position could be designed to accomplish this task.
- 5) Control Button Operation - Operation of the coring device with the spacesuit revealed that the "up," "down," "on," and "off" pushbutton control switches should be somewhat larger in order to ensure proper engagement by the astronaut.

High Vacuum Motor Operation

An informal vacuum test of the coring device motor was conducted for the purpose of identifying problem areas which may be encountered on subsequent flight models. The test was conducted at a vacuum level varying from 2.0 to 7.0×10^{-5} mm Hg. Specific areas of interest included brush wear and bearing lubrication at low ambient pressures. The breadboard model coring device motor does not include the environmental control system hardware (Appendix G), and therefore, a full-load operational test could not be conducted.

The equipment set-up for the vacuum test is illustrated in Figure 32. A test fixture was provided for mounting the motor and electrodynamic loading device. Thermocouples were employed to measure the temperature at the following locations: 1) motor case near output shaft, 2) motor case midway between the end caps, 3) vacuum chamber wall, and 4) vacuum chamber ambient. The test was conducted for a period of 165 minutes with the motor operating at a no-load current level of 1.6 amperes. Although the motor does not include the environmental control system, the test was initially planned for full-load motor operation with intermittent duty cycle. However, a mechanical failure of the electrodynamic loading device (test equipment) and lack of time prevented the performance of a full-load motor test in the vacuum.

Table 1 presents a running time history of the test with accompanying motor case temperature rises.

As shown in Table 1, the maximum motor case temperature (near output shaft) increased rapidly during the first two hours of operation, and then began to stabilize at approximately 245° F. This temperature would have exceeded the maximum allowable for the motor components if a continuous duty cycle, full-load operation test had been conducted.

Subsequent examination of the motor revealed that less than 0.010 inches of brush wear had occurred during the vacuum test. Negligible evaporation of the General Electric F-50 bearing lubrication oil occurred as a result of the low pressure operation. Satisfactory operation of the coring device electric motor in the lunar vacuum can be assured if the environmental control system recommended in Appendix G is incorporated, which will include pressurization of the motor case to a level greater than that experienced during the informal test.

ER 13952



Figure 31. Spacesuit Interface Tests

ER 13952

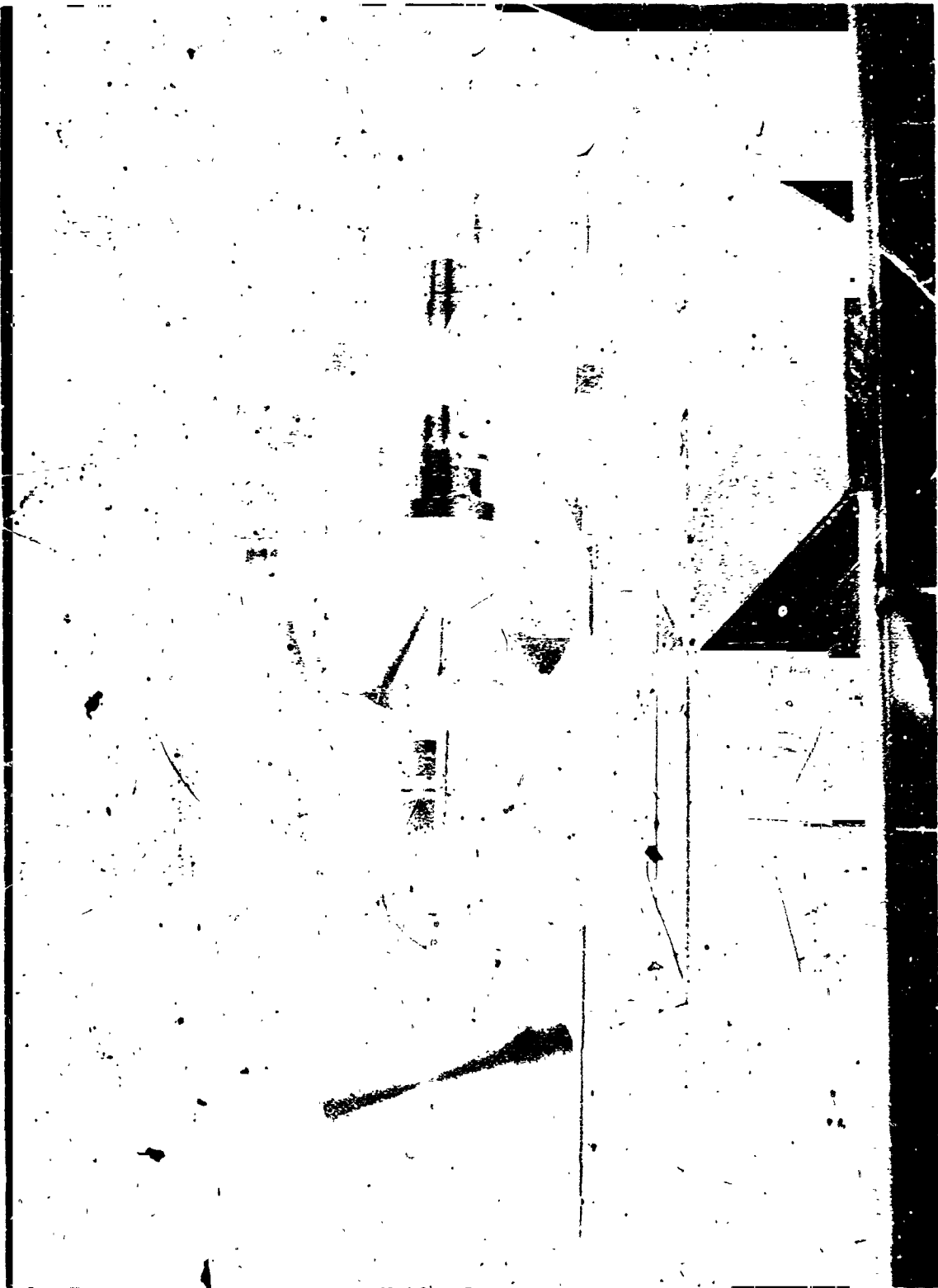


Figure 32. Vacuum Test of Motor

ER 13952

TABLE 1.
MOTOR TEMPERATURE RISES AT LOW AMBIENT PRESSURES

Time (Minutes)	Volts	Current (Amps)	T ₁ °F	T ₂ °F	T ₃ °F	T ₄ °F	Pressure mm Hg x 10 ⁻⁵
0	27.8	1.6	73	120	105	75	7.0
5	27.8	1.6	73	125	105	75	4.0
15	27.8	1.6	75	134	110	75	3.2
25	27.8	1.3	75	145	120	76	3.0
35	27.8	1.6	75	160	130	76	2.8
45	27.8	1.6	75	165	140	77	2.6
55	27.8	1.6	75	175	148	77	2.6
65	27.8	1.6	75	187	157	78	2.5
75	27.8	1.6	75	200	164	79	2.5
85	27.8	1.6	75	208	170	79	2.5
95	27.8	1.5	75	216	176	80	2.4
105	27.8	1.6	75	225	182	80	2.4
115	27.8	1.6	75	230	186	81	2.4
125	27.8	1.6	75	235	190	82	2.3
135	27.8	1.6	75	240	195	82	2.2
145	27.8	1.6	75	242	196	83	2.2
155	27.8	1.6	75	245	198	83	2.1
165	27.8	1.6	76	246	199	83	2.0

NOTES: T₁ = Vacuum Chamber Wall
T₂ = Motor Case Near Output Shaft
T₃ = Motor Case Midway Between End Caps
T₄ = Vacuum Chamber Ambient

CORING DEVICE OPERATING PROCEDURES

The general instructions for operating the coring device, and a proposed technique for obtaining core orientation is presented below. It is to be noted that the instructions pertain to the current breadboard model coring device, and subsequent design improvements may result in significant changes in operating instructions. Also, various assumptions will be made regarding equipment which will be required for complete and accurate orientation of the core, but which was not developed under this contract. References will also be made to design features anticipated for a flight model coring device, but which are not incorporated in the present breadboard model.

Site Selection

The first task required of the astronaut is selection of the drilling site. The criteria established for this study was predicated on the availability of consolidated rock within a reasonable radius of the LEM landing area. If a number of rock outcrops are present, the astronaut will choose the outcrop to be cored with the lunar coring device. However, if a rock outcrop is not present, or if the lunar surface in the immediate vicinity of the LEM landing area is not satisfactory for the emplacement of anchoring devices, the flight model coring device will have mechanical restraints capable of attaching directly to the LEM landing gear. In this mode, the coring device will probably drill through the LEM landing pad into whatever material is available at that location.

Transport to Coring Site

The lunar rock coring device is a completely integrated unit (Figure 31) requiring very little assembly time. However, if stowage space in the LEM scientific equipment bays is a problem, the device can be delivered to the lunar surface partially disassembled. In a flight model configuration, accessory equipment such as tube extensions, spare core bits, anchors, and other miscellaneous equipment will be clamped or restrained to the basic coring device. Therefore, only one trip will be required by the astronaut to transport the coring device and accessories from the LEM scientific equipment bay to the selected drilling site. It is also probable that the power cable, if not greater than 100 feet, can be carried and simultaneously layed along the surface as the astronaut transports the coring device to the work site. The lunar weight of the coring device and power cable should be less than six pounds.

Emplacement of Coring Device

Emplacement of the coring device consists of locating the desired coring location on the selected rock outcrop, and installing the anchoring studs. This is accomplished in the following manner:

- 1) Connect power cable to coring device control box. Screw 1/4-inch drill to 5-inch adapter section. Screw adapter section to coring device output shaft.

(NOTE: For field testing of breadboard model, four 6-volt or two 12-volt batteries connected in series should be utilized for a 24 V power source. Attach red alligator clip of power cable to positive battery terminal and black alligator clip to negative terminal.)

- 2) Select approximate location for rear anchor stud. Align machine until 1/4-inch drill adapter is properly located over the spot where the rear anchor is to be installed.
- 3) Place control lever in neutral position. Depress "down" and "on" buttons. Allow drill to traverse down until 1/4-inch drill bit is approximately 1/2-inch above rock surface. Depress "off" button.
- 4) Place control lever in "down-percussion" position. Manually rotate spindle cw and ccw slightly as engaging pressure is applied to control lever.

CAUTION: Down button must be depressed.

Depress "on" button, and restrain coring device until approximately 1 3/8 inches of rock has been penetrated. Depress "off" button.

- 5) Place control lever in "up-percussion" position. Use engaging procedure as in step 4. Depress "up" and "on" buttons, and allow drill to traverse up until drill bit is clear of rock surface. Depress "off" button.
- 6) Insert anchor stud in hole, and tap several times with a hammer until stud is fully expanded. Lift machine and place rear anchor hole over stud. Screw retaining nut several turns on anchor stud.
- 7) The drilling positions for the second and third anchors are determined by rotating the machine around the rear anchor as a center point, and "bore sighting" the correct drilling spots. These drilling spots can be marked by using the base plate of the coring device as a template, and scratching the drilling location on the rock surface with a small screwdriver.
- 8) Align machine and repeat items 3 through 5 for each of the two holes. Insert two anchor studs through the base plate mounting holes into the two pre-drilled rock holes, and expand each anchor with several taps of a hammer.
- 9) Screw retaining nuts on studs, and tighten all retaining nuts and leveling screws until the coring device is firmly locked to the rock outcrop. Unscrew 1/4-inch drill adapter from output shaft.

Core Orientation

After the coring device has been securely anchored to the rock outcrop, an orientation reference mark must be inscribed on the face of the rock to be cored. This can be accomplished manually by using a diamond-tipped scriber or aluminum pencil. The marker can be properly referenced with respect to the coring device by the incorporation of two diametrically opposed guide slots milled into the base plate drill string guide hole. Two additional alignment points will be required on the percussor housing

which will also be aligned with the milled slots in the base plate. The azimuth established by the alignment points on the percussor housing can then be determined with reference to the azimuth of the sample location from the LEM by use of a simple surveying instrument which will be included in the geological tool kit. This, in turn, establishes the azimuth of the reference mark inscribed on the rock face with the rock chisel. The azimuth of the alignment points and sample location could also be recorded relative to the LEM by use of the lunar surface camera.

Since the coring operation will probably result in shearing of the rock core at various intervals, orientation of the entire core will require collection, and subsequent reconstruction of all core segments upon return to earth.

Inscribing a reference mark with a diamond scribe will probably be limited to hard rock materials such as basalt. Reference marks inscribed on softer materials such as pumice and unwelded tuff would be easily obscured during the coring process. A possible approach to this problem is to permanently embed a small metal reference indicator in the material instead of depending on an inscribed mark.

An alternative down-the-hole approach to the previously described core orientation technique (surface orientation with subsequent core reconstruction) would also provide an oriented core. This approach would require the coupling of a carbide chisel adapter to the drill string (in lieu of core bit) for scribing the rock to be cored at the bottom of the drill hole. Alignment of the drill string from the subsurface chisel to the surveying orientation scribe on the percussor housing must be maintained in order to obtain accurate orientation data of the subsurface rock to be cored. A minor modification to the existing coring device spindle can be incorporated which will permit percussion (without rotation) of the drill string, and orientation marking of the subsurface rock with the chisel. This orientation technique may be more practical than the core reconstruction technique, especially if an oriented core from a relatively deep depth is required.

Vertical orientation of the core can be measured by use of a clinometer. Two separate measurements (parallel and perpendicular to alignment points) will establish the vertical orientation of the core.

Coring Procedure

- 1) Place core retainer bushing in tungsten-carbide core bit. Screw core bit to the core barrel, ensuring that helices on outer peripheries are aligned when hand-tightened. Screw 5-inch adapter section to other end of core barrel.
- 2) Place coring device control lever to neutral position. Depress "up" and "on" switches, and allow motor assembly to traverse upward until automatically stopped by microswitch operation.
- 3) Screw core barrel and adapter to output shaft of coring device.
- 4) Depress "down" and "on" switches, and allow motor assembly to traverse down until core bit is approximately 1/2-inch from rock face (entering drill string guide hole in base plate). Depress "off" switch.

- 5) Place coring device control lever to "down percussion" position. Depress "on" switch and monitor machine for one minute to ensure proper coring. Adjust clutch for 20-22 ampere reading on meter if required. Note: Clutch must be tightened (increased axial pressure) to increase current reading, and loosened to decrease current reading. Current reading may intermittently increase or decrease 1-4 amperes depending on rock material. Current readings above 30-33 amperes generally indicate excessive coring torque which may be caused by drill string misalignment with the coring hole (movement of coring device) or stoppage of coring debris transport to surface due to "wet spots" in the rock. This condition, which usually will not occur until the deeper depths are attained, can be corrected by pulling and cleaning the drill string.
- 6) After a time interval of approximately 20-40 minutes has elapsed, coring of the first section should be completed and machine will automatically stop by actuation of the microswitch. Place control lever in neutral position and depress "up" button. Motor assembly should traverse upward at the rate of approximately 11 inches per minute. Note: If an excessive pulling pressure requirement is evident (clutch slipping without movement of motor assembly), depress "off" button. Place control lever in "up percussion" position and depress "on" button. This will cause drill string to rotate and percuss as the motor assembly traverses upward. This, in turn, will break the core and reduce side-wall friction as the drill string moves upward. However, this remedial action should be avoided if possible, because the percussion action tends to fracture the core and cause small fragments to drop into the drill hole.
- 7) Coring device will automatically stop when motor assembly reaches the top of its traverse. Depress "off" button. Remove percussor housing restrainer top and pull entire drill string and percussion assembly upward through percussor housing. Remove core bit from core barrel using special tool if required. Tilt core barrel and remove core samples. Replace core extractor bushing and screw core bit on the core barrel. Uncouple core barrel at the 5-inch adapter section interface. Screw a core barrel extension tube to core barrel, and screw 5-inch adapter section and percussion assembly to core barrel extension tube. Guide drill string through percussor housing, down into the core hole, and seat spline of percussor into the mating drive spline of the coring device. Replace percussor housing restrainer top.
- 8) Repeat items 4 through 7.
- 9) Items 4 through 7 are to be repeated until complete ten feet of rock core is attained. Each time the drill string length is to be increased, a core barrel extension tube is added to the top side of the core barrel.

LUNAR DRILL LOAD SIMULATOR

An amendment to the basic Lunar Coring Device Design Study Contract was negotiated for the design, fabrication, and test of a Lunar Drill Load Simulator. This equipment simulates the electrical load characteristics of the breadboard model coring device, and will be utilized for a series of power system interface tests to be conducted by the LEM spacecraft contractor. A detailed description of this special-purpose equipment and tests which were performed prior to delivery are presented in Appendix I.

CONCLUSIONS AND RECOMMENDATIONS

Study Results

As a result of the studies, laboratory feasibility tests, breadboard development hardware, and field tests performed during this program, the following conclusions are submitted.

- 1) Coring Technique - The rotary percussion coring technique using tungsten carbide annular core bits best meets the requirements and restrictions for the ten-foot lunar rock coring device. The rotary diamond coring technique possesses many desirable characteristics, but coring of hard rock materials cannot be accomplished unless excessive quantities of coolant gases are available for the coring mission. Other coring techniques were studied and rejected for failure to meet one or more of the lunar operating restrictions.
- 2) Breadboard Model Coring Device Capabilities - Development, testing, and analytical studies demonstrated the following capabilities:
 - a. The employment of a rotary-impact force with controlled axial thrust from a ground level mechanism will successfully core medium-hard consolidated rock to a depth of at least twelve feet.
 - b. Dust Transport System - A mechanical spiral machined in the outer core barrel and extension tubes will successfully transport drilling debris from the face of the cutting bit to the surface without the aid of a gas flow system in the terrestrial environment. Small quantities of gaseous lubrication may be required for the lunar surface application to reduce the effects of increased dust friction and adhesion as a result of the vacuum environment.
 - c. Aluminum Extension Tubes - Percussion energy is not excessively attenuated through the use of aluminum extension tubes for transmitting energy from the surface level percussor to the subsurface core bit. Field tests conducted in marble revealed that penetration rates were relatively constant from the one-foot to ten-foot levels if proper drill string alignment was maintained.

- d. **Power Requirements** - The ten-foot core hole can be cored in a medium-hard material within the 2400 watt-hours of power allotted to the lunar drill.
- e. **Vacuum Operation** - Incorporation of an open loop, evaporative water cooling system with pressurized motor and gear case best meets the vacuum operation requirements for the coring device. Gaseous lubrication of the core bit can be accomplished if required by use of the environmental control system exhaust.
- 3) **Other Prime Mover Systems** - Study of various prime mover systems applicable for the lunar coring device has revealed that the dc electric motor system will best meet the requirements.
- 4) **Portable Power Supplies** - An evaluation of various portable, electric power supplies applicable for the lunar coring device revealed that only the rechargeable silver-zinc battery should be considered for this application. The silver-zinc battery portable power supply becomes more practical for use on LEM vehicles which employ the same primary power source because the scientific equipment payload would not be penalized for the portable power source.

Additional Study Recommendations

The current program resulted in the development of a breadboard model coring device capable of obtaining one-inch diameter cores from a variety of rock materials. However, the laboratory feasibility tests, and field evaluation tests delineated various other design areas which should be investigated prior to the development of the flight model coring devices with integrated environmental control systems. This approach would permit the additional optimization to be performed on the breadboard model thus eliminating numerous modifications to the flight models.

Rotary Percussion Core Bit - The operating efficiency (penetration rate, power consumption, and quality of core samples) of the coring device is directly influenced by the rotary-percussion core bit. Although the performance of the modified standard Pratt and Whitney core bits was superior to the rotary diamond bits, there are three additional design areas which could be further optimized:

- 1) **Cutting Kerf** - The Pratt and Whitney core bit possesses a 1/4-inch kerf (1.5" O.D. x 1.0" I.D.) which results in a cutting area of 0.981 in.². A 1/16-inch reduction of the kerf (1.5" O.D. x 1.125" I.D.) would result in a cutting area of 0.773 in.², and an approximate power consumption reduction of 22% for the same penetration rate. In addition, the resulting increased core diameter (1.125") would be more resistant to fracture.

The major problem encountered while drilling with narrow kerf percussion bits is loss of the carbide cutters due to a failure of the brazing material. Therefore, additional study should be directed at improved brazing or mechanical restraint techniques for maintaining core bit integrity.

- 2) Tungsten Carbide Cutter Geometry - An optimization program directed at improving the geometry of the tungsten carbide cutters for the lunar application will result in improved coring efficiency.
- 3) Carbide Cutter Material - The efficiency of the core bit is dependent upon the retention of a sharp cutting edge during the coring operation. Frequent replacement of dull bits will result in a burden upon the astronaut's lunar surface mission time and delivered payload weight. Therefore, additional optimization of carbide cutter material is justified.

Rotary and Rotary-Percussion Capability - The breadboard model test program revealed that the drill string can be more easily retracted from the drill hole while rotating without percussion. In addition, coring in soft materials such as pumice and tuff can be accomplished with greater ease using a pure rotary, rather than the rotary-percussion action required for hard rock materials. Therefore, a design improvement should be incorporated which will permit the astronaut to rapidly interchange the coring mode between rotary and rotary-percussion.

Variable Energy Impact Blow - The breadboard model test program revealed the desirability of employing a variable energy impact blow to the core bit which is adjustable to the hardness of the rock material. The hard, consolidated basalt requires a heavier blow to ensure carbide penetration and reduce bit "dragging" effects. The medium hard vesiculated basalt requires a medium energy blow to ensure satisfactory penetration without core fracture.

An optimization of impact frequency, carbide indexing and impact spring energy is required in order to determine the range of variable energy adjustment which should be incorporated.

Soft Rock Anchors - Further evaluation of soft rock anchors (for pumice, tuff, etc.) should be conducted in view of the possibility that consolidated rock outcrops may not be readily available on the lunar surface. In addition, the possibility of using the LEM landing gear as a mechanical restraint for the coring device should be studied.

Vacuum Operation - High vacuum rock drilling tests should be conducted to study possible problem areas such as rock/core bit cold welding effects, increased core dust friction, and adhesion of coring dust to the core bit and core barrel. These tests should be conducted in one of the large NASA facilities which possess sufficient pumping capabilities to handle the outgassing load. If gas lubrication appears mandatory for vacuum coring, additional study of an integrated gas system should be conducted. Two possible solutions for a gas requirement are: 1) utilization of exhaust steam from the evaporative environmental control system, or 2) employment of a gas turbine prime mover (such as H_2O_2), and using exhaust gas as a lubrication agent.

Prototype Coring Device Design Specifications

The design and operating principles developed for the breadboard coring device can be used to delineate the design specifications and requirements for a prototype lunar coring device. The following changes to the breadboard model coring device will be required for the prototype flight model:

- 1) Control Box - The ammeter employed in the control box was predominantly used for test purposes and could probably be deleted on the flight model. Also, the relay circuitry for automatic shutdown at the completion of an upward traverse of the motor is not required since the astronaut would be in attendance at this time. Therefore, it is recommended that the entire control box be eliminated. The "off," "on," "up," "down" and "automatic shutdown" switches, and RF filters could be incorporated in the motor housing. This modification would also eliminate the control box-to-motor power cable.
- 2) Motor and Housing - This assembly would be integrated with the gear box section to eliminate casing redundancy and reduce weight.
- 3) Percussor and Gear Box Housing - This assembly would be integrated into a single unit to eliminate casing redundancy. Also, the percussor, gear box, and motor housing would be pressurized as a single unit. Rotating labyrinth seals will be required for the spindle output shaft, gear shift control lever, vertical drive gear, and percussive energy level control (previously discussed).

The drill string feed-through technique currently employed with the breadboard model would be eliminated, and all core barrel or extension tube connections would be accomplished at the output spindle. A variable impact energy spring would be incorporated to optimally core a variety of materials ranging from pumice to basalt.

- 4) Basic Mounting Structure - A lighter material (aluminum with aluminum oxide finish) would be utilized for the geared vertical traverse column. The thickness of the base would be reduced, and the number of anchoring points would be reduced from three to two.
- 5) Extension Tubes - A modified bayonet coupling mechanism would replace the conventional threads. The inside diameter of the drill string would be maintained sufficiently large to permit accumulation of ten feet of rock core.
- 6) Environmental Control System - The environmental control system designed (Appendix C) for cooling the electric motor must be incorporated into the prototype.
- 7) Lubrication - General Electric F-50 oil will be employed for the motor and gear box bearings (sealed), and solid lubricants for the remaining exposed (low rpm) gears and bearings.

ER 13952

The weight of the flight model coring device will be reduced from the breadboard model weight of 63 pounds to approximately 40 pounds, excluding cable. Weight of the recommended 100-foot aluminum conductor cable is approximately 7 pounds, for a total system weight of 47 pounds.

Suggested Future Program Plans

It is envisioned that the program steps leading to the fabrication of space qualified lunar rock coring devices should progress as follows:

- 1) Initial Study Program resulting in breadboard model coring device - (completed)
- 2) Modifications and Further Optimization of Breadboard Model - (18-week program, October 15, 1965 through February 29, 1966).
- 3) Design, Fabrication and Test of Five (5) Prototype Flight Models - These models would include the environmental control system for the motor and the proper materials and lubrications required for lunar surface operation. The five prototype flight models would be utilized as follows:
 - a. One model for field test and preliminary environmental tests by Martin,
 - b. Two models for astronaut training and NASA evaluation,
 - c. One model for evaluation by the Geological Survey, and
 - d. One model for LEM interface tests.

This program can begin prior to the termination of 2) above, since the initial portion of this program will consist of a detailed stress analysis and state-of-the-art materials selection. (One-year program, December 1, 1965 through December 1, 1966.)

- 4) Finalization of Design - Fabrication and acceptance tests of flight hardware - (one-year program, December 1, 1966 through December 1, 1967).

BIBLIOGRAPHY

1. "Final Technical Report on Preliminary Feasibility Study of Drilling a Hole on the Moon," Hughes Tool Company, ASTIA Document AD258661 23 September 1960.
2. Peckman, V. A., and Dallas, J. P., "Development of a Lunar Rock Drill and Subsurface Sampling System," Hughes Aircraft Company, reported in IEEE Transactions on Aerospace, Vol. 2, No. 2, April 1964.
3. Brantley, J. E., "Rotary Drilling Handbook," Palmer Publications, New York, N. Y., 1952.
4. Hvorslev, M. J., "Subsurface Exploration and Sampling of Soils for Civil Engineering Purposes," Waterways Experiment Station, Vicksburg, Mississippi, November 1949.
5. Forrester, J. D., "Principles of Field and Mining Geology," John Wiley and Sons, New York, N. Y., 1946.
6. Pearl, Richard M., "Rocks and Minerals," Barnes & Noble, Inc., New York, N. Y., 1956.
7. Spencer, E. W., "Basic Concepts of Physical Geology," Thomas Crowell Co., New York, N. Y., 1962.
8. Branley, F. M., "The Moon - Earth's Natural Satellite," Thomas Crowell Co., New York, N. Y., 1960.
9. Whipple, F. L., "Earth, Moon and Planets," Grosset & Dunlap Co., New York, N. Y., 1958.
10. Cummings, C. I. and Lawrence, H. R., "Technology of Lunar Exploration," sponsored by American Institute of Aeronautics and Astronautics, Academic Press, New York, N. Y., 1963.
11. Bennett, E. C., Wood, H. L., Jaffe, L. D., Martens, H. E., "Thermal Properties of a Simulated Lunar Material in Air and in Vacuum," Jet Propulsion Laboratory, California Institute of Technology, TR 32-368, November 1962.
12. Kopal, Z., "Internal Structure of the Moon," presented at ARS Lunar Missions Meeting, Cleveland, Ohio, 17-19 July 1962.
13. Head, V. P., "A Lunar Surface Model for Engineering Purposes," presented at ARS Lunar Missions Meeting, Cleveland, Ohio, 17-19 July 1962.
14. Giberson, W. E., "Surveyor Project Status," presented at ARS Lunar Missions Meeting, Cleveland, Ohio, 17-19 July 1962.

BIBLIOGRAPHY (CONT)

15. Johnson, G.W.S., "Recommendations for Utilizations of Lunar Resources," Seminar proceedings, Jet Propulsion Laboratory, California Institute of Technology, 8 March 1963.
16. Halajian, J. D., "Vehicle-Soil Mechanics on the Moon," Paper No. 632B presented at Automotive Engineering Congress, January 1963.
17. ASTM, "Tentative Method for Thin-Walled Tube Sampling of Soils," ASTM Designation: D1587-58T, 1958.
18. ASTM, "Tentative Method for Penetration Test and Split-Barrel Sampling of Soils," ASTM Designation: D1586-58T, 1958.
19. Vey, E. and Nelson, J. D., "Studies of Lunar Soil Mechanics," Final Report for NASA Contract NASr-65(02), IITRI Project M272, July 1963.
20. Chistyakov, Yu. N., "Practice of Determining the Temperature of Individual Parts of Lunar Surface," WP-AFB Translation from Izvestiya Komissii Po Fizike Planet, NR.2, 1960.
21. Runcorn, Stanley K., "The Interior of the Moon," Jet Propulsion Laboratory, California Institute of Technology, TR 32-529, December 15, 1963.
22. Weide, D. L., "The Behavior of a Lunar Soil Model in a Vacuum," Douglas Report SM-42116, ASTIA Document AD 290608, September 1962.
23. Uren, L. C., "Petroleum Production Engineering," McGraw-Hill Book Co., Inc., New York, 1956.
24. Murray, A. S., and Eckel, J. E., "Foam Agents and Foam Drilling," The Oil and Gas Journal, February 20, 1961.
25. Shemyakin, M. M., "On Some Patterns in the Distribution of Crater Chains in the Regions of Clavius and Hipparchus Cirques," Aerospace Information Division Translation Report 62-121, 4 September 1962.
26. Sadil, J., "The Moon - The Nearest Body in the Universe," reported in NASA Document N64-24490.
27. Jet Propulsion Laboratory, California Institute of Technology, Informal Report, "Ranger 1964," reported in NASA Document N64-22461.
28. Lincoln, J. L., "The Lunar Surface," Boeing Report D2-100036 dated November 5, 1962, reported in ASTIA Document AD 601904.
29. "Lunar Drill Feasibility Study - Final Report," Texaco, Incorporated, ASTIA Document AD 258683, January 13, 1961.
30. Dundzila, A. V., and Campbell, J. A., "Lunar Drill Study Program," Armour Research Foundation of Illinois Institute of Technology, ASTIA Document AD 258618, January 1961.

BIBLIOGRAPHY (CONT)

31. Bingham, M. G., "How Rock Properties are Related to Drilling," The Oil and Gas Journal, December 14, 1964.
32. Miyamoto, S., "Magmatic Boiling and Underground Structure of the Moon," reported in NASA Document N6215744.
33. Strughold, H., "The Ecological Profile of the Moon," reported in NASA Document N6214215.
34. Bronner, F. E., "Outline of Lunar Geography and Geology," General Electric Company, ASTIA Document AD 293429, July 1962.
35. "The Internal Constitutions of the Inner Planets and the Moon," University of California Report, reported in NASA Document N6415183.
36. Fudali, R. F., "Lunar Surface Characteristics," Bellcomm, Inc., Washington, D. C., December 28, 1962.
37. Thorman, H. C., "Review of Techniques for Measuring Rock and Soil Strength Properties at the Surface of the Moon," Jet Propulsion Laboratory, California Institute of Technology, reported in NASA Document N6312922, January 1963.
38. "Studies of the Physical Properties of the Moon and Planets," Rand Corporation, reported in NASA Document N6210404, December 1961.
39. Kopal, Z., "Thermal History of the Moon and the Terrestrial Planets," Jet Propulsion Laboratory, California Institute of Technology, Technical Report No. 32-108, May 1, 1961.
40. Roddy, D. J., Rittenhouse, J. B., and Scott, R. F., "Dynamic Penetration Studies in Crushed Rock Under Atmospheric and Vacuum Conditions," Jet Propulsion Laboratory, California Institute of Technology, Technical Report No. 32-242, April 6, 1962.
41. Kulander, J., "Lunar Temperatures," Boeing Report D7-2517 dated September 22, 1959, reported in AFBMT Technical Report 59-9.
42. Schlichta, P. J., "Geological Aspects of Lunar Exploration," Jet Propulsion Laboratory, California Institute of Technology, Technical Report No. 34-8, January 25, 1960.
43. Badgley, P. C., Jaffe, F. C., Poole H. C., and Siems, P. L., "Geological and Thermodynamic Aspects of Lunar Rocks," Colorado School of Mines Research Foundation, Inc., July 1962, reported in NASA Document N6217492.
44. O'Keefe, J. A., Cameron, W. S., "Evidence From the Moon's Surface Features for the Production of Lunar Granites," reported in NASA Technical Note D-1669, May 1963.
45. Dauncey, G. B., "Setting of Diamecads in Hard Matrix Bits," Diamond Research Laboratory, Johannesburg, South Africa, reported in Canadian Mining Journal, May 1961.

BIBLIOGRAPHY (CONT)

46. Roxtrom, E., "Craelius Automatic Core Orientator," Svenska Diamantbergbörnings AB, Stockholm, Sweden, reported in Canadian Mining Journal, March 1961.
47. Shorthill, R. W., "Measurements of Lunar Temperature Variations During an Eclipse and Throughout a Lunation," Boeing Report D1-82-0196 dated August 1962, reported in ASTIA Document AD 286471.
48. Carlson, D. D., MacFarlane, G., "Engineering Problems in a Lunar Environment," reported in NASA Document N6412673, July 1963.
49. Lavik, M. T., "Ceramic Bonded Solid Film Lubricants," Midwest Research Institute, WADD Technical Report 60-530, September 1960.
50. Buckley, D. H. and Johnson, R. L., "Friction, Wear and Decomposition Mechanisms for Various Polymer Compositions in Vacuum to 10^{-9} Millimeters of Mercury," NASA-Lewis, NASA TN D-2073, December 1963.
51. Buckley, D. H., "Gallium is Useful Bearing Lubricant in High Vacuum Environment," NASA-Lewis, NASA Technical Brief 63-10337, May 1964.
52. VanVliet, R. M., "A Molecular Approach to Dry Film Lubrication in a Vacuum (Space) Environment," WADC Technical Report 59-127, July 1960.
53. Evans, H. E. and Flatley, T. W., "Bearings for Vacuum Operation," NASA Goddard, paper for SAMPE Symposium on Effect of Space Environment on Materials, St. Louis, Mo., May 7-9, 1962.
54. Freundlich, M. J. and Jagodowski, S. S., "Lubricant for High Vacuum Environment," WADD Technical Report 60-728, Part I, March 1961.
55. Bowen, P. H., "Lubrication of Bearings and Gears in Aerospace Environmental Facilities," AEDC-TDR-63-166, July 1963.
56. Buckley, D. H. and Johnson, R. L., "Influence of Microstructural Inclusions on Friction and Wear of Nickel and Iron in Vacuum to 10^{-9} mm of Mercury," NASA Technical Note D-1708, May 1963.
57. Evans, H. E. and Flatley, T. W., "High Speed Vacuum Performance of Gold Plated Miniature Ball Bearings with Various Retainer Materials and Configurations," NASA TN D-2101, December 1963.
58. Proceedings of Space Lubrication Conference (NASA-DOD-American Society of Lubrication Engineers), Biltmore Hotel, New York, May 3, 1963. Document (DDC) AD439844.
59. Adamczak, R. L., Benzing, R. J., and Schwenker, H., "Lubrication in Space Environment," paper for SAMPE Symposium on Effects of Space Environment on Materials, St. Louis, Mo., May 7-9, 1962.

BIBLIOGRAPHY (CONT)

60. Ham, J. L., "Investigation of Adhesion and Cohesion of Metals in Ultrahigh Vacuum," National Research Corporation, NASA documents N62-11137 and N62-11433.
61. Hall, R. M. and Yoshimoto, H., "Radiant Cooling or Shielding," Product Engineering, November 14, 1960.
62. Marks Mechanical Engineer's Handbook, Fifth Edition, 1951.
63. Rogers, John R., and Vaughn, Otha H., Jr., "Lunar Environment: An Interpretation of the Surface of the Moon and Its Atmosphere," NASA Technical Memorandum N65-10304, September 3, 1964.
64. Salisbury, John W. and Glaser, Peter E., "The Lunar Surface Layer, Materials and Characteristics," Academic Press, New York, 1964.
65. "Lunar Surface Controversy Rekindled," Missiles and Rockets, 26 April 1965.
66. Mitchell, James K., "Current Lunar Soil Research," reported in Proceedings of American Society of Civil Engineers, May 1964.

APPENDIX A - BASIC DATA EVALUATION

To effectively specify operating criteria for the lunar coring device, it was necessary to study current related experience, and evaluate the interface data relating to a final design. The evaluation and interpretation of this preliminary data established the initial guidelines for the coring device design and auxiliary study requirements. As additional data became available, further refinements in the approach and techniques were incorporated.

The primary interface and study areas which required a preliminary evaluation included: 1) Apollo-LEM Interfaces, 2) Lunar Geological and Environmental Factors, 3) Coring Techniques, 4) Man/Machine Interfaces, and 5) Materials Selection Criteria.

Apollo-LEM Interfaces

The design of the ten-foot lunar coring device included considerations for the restrictions imposed by the Apollo-LEM spacecraft system in addition to its rock coring requirements. Factors such as size, weight, portability, and power consumption rate are governed by the payload limitations, storage bay dimensions, and power source capacity of the LEM spacecraft.

The design specification for the LEM vehicle included a scientific payload weight of 250 pounds. Therefore, the design of the lunar coring device was required to include a maximum of weight saving features, consistent with its operational requirements. Integration of the coring device with the spacecraft systems was considered as a possible means of weight reduction. A preliminary review of the lunar coring device subsystems revealed three possible areas where integration with the spacecraft systems could result in substantial weight reductions:

- 1) Coring bit coolant and chip removal system - If the pure rotary drilling technique were utilized for the lunar coring device, a gas would be required for a coring bit coolant and chip removal agent. The rotary-percussion technique which was ultimately selected for the lunar coring device does not require a gas for use in the earth environment. However, subsequent high-vacuum coring tests may reveal that small amounts of gaseous lubrication are required to prevent excessive cutting-friction and dust adhesion to the core barrels. Therefore, utilization of the LEM descent stage pressurizing helium would result in a net payload weight reduction if a bit and core barrel gaseous lubrication is required for rock coring in the vacuum environment of the moon.
- 2) Coring device prime mover - Utilization of the LEM descent stage residual fuel as an energy source for a gas turbine was considered. The exhaust gas from this system could also serve as a bit coolant and chip removal agent if catalytic decomposition, rather than hypergolic oxidation were employed. Exhaust gas temperatures of hydrazine decomposition would range from 320° C to 430° C, as compared to the higher 1100° C to 1650° C range for hypergolic burning.
- 3) Coring device restraint system - The lunar coring device will require the structural elements necessary to maintain rigidity during the drilling operations, and to provide a tie-down means for attachment to the lunar surface.

ER 13952

However, if coring within the immediate vicinity of the LEM vehicle were considered satisfactory, or if anchoring of the device were found to be impractical because of a widespread dust layer, the structural weight of the coring device could be reduced somewhat by attaching it mechanically to the spacecraft. The lunar weight of the LEM vehicle would be more than sufficient for restraining the coring device.

A logical approach to the design of the coring device would be to: 1) Provide a self-restraining anchor system for attachment to rock outcrops which may be present in the near vicinity of the LEM landing area, and 2) Provide an alternate means of mechanically attaching the coring device to the LEM vehicle if direct anchoring to the lunar surface is impractical due to an unconsolidated upper layer of rubble or dust. It is envisioned that the coring device could be attached directly to one of the LEM landing legs in such a manner as to facilitate coring through the landing pad to the lunar surface.

The interior configuration of the LEM equipment storage bay has not been completely defined. Preliminary information indicates that the compartment may be "pie-shaped", with an outer peripheral dimension of 54 inches. The initial design specifications for the lunar coring device limited its structural members to a maximum of 30 inches. Therefore, the coring device has been designed with coupling and telescoping features which will allow it to be stowed within the required stowage area. The overall length of the coring device can remain somewhat flexible, until the final design of the LEM stowage compartment is established.

The dc LEM power source may consist of either a fuel cell or silver zinc batteries. The specified output voltage may vary over a range of 20 to 32 volts. Therefore, the lunar coring device must also be capable of operating over this voltage range. A maximum continuous power operating level of 1,000 watts, and a total power consumption of 2,400 watt-hours has been established for the coring device.

Lunar Surface Geological and Environmental Factors

A review of current lunar surface interpretations was required in order to establish the design parameters of the lunar drill which will be affected by the drilling characteristics of the anticipated lunar rocks. Although existing lunar surface information was somewhat speculative, the general opinion regarding the characteristics of surface materials was sufficient to establish general guidelines for the design of the lunar drill. Refinements can be made to the design of the drill as additional lunar surface information becomes available from the Ranger, Surveyor, Apollo and other related space programs.

The environmental conditions under which the lunar drill must operate have been determined more accurately than the geological small scale features of the lunar surface materials. These environmental factors were studied, and appropriate design considerations incorporated in the lunar drill to assure satisfactory operation.

General Inferences from Direct Lunar Measurements

Any evaluation concerning lunar surface and subsurface characteristics must take into account the origin of the materials. There is little question among authorities that meteorite impact and volcanic activity both contributed to the origin of these materials. There are, however, vast differences of opinions regarding the relative

contribution of each process. The precise nature of the lunar surface materials is also speculative.

Most of the lunar surface inferences have been predicated upon measurements and observations which were conducted from the atmospherically obstructed terrestrial surface. Salisbury⁽⁶⁴⁾ categorizes these measurements and inferences as follows:

- 1) Infrared emission - Low thermal conductivity.
- 2) Radio emission - Low thermal conductivity.
- 3) Radar reflection - Low density. Surface gradient 1 in 11 on a 1-m and 10-cm scale.
- 4) Polarization - Agglomerated powder composed of opaque grains.
- 5) Photometry - Highly porous, complex and irregular surface. Relief many times the wavelength of light.
- 6) Albedo and color - Nonterrestrial reflectivity.

To this list, the following direct visual observations should be added:

- 1) Telescopic observation - Gross lunar topography and stratigraphy.
- 2) *Ranger VII, VIII and IX photographs - Details of surface topography stratigraphy and suggestive lithologic texture.*

The design of the lunar drill was predicated initially upon a "worst-case" moon. At the present time we do not know the answers to the following cosmological problems:⁽⁶³⁾ (1) the chemical composition; (2) the exact mechanism of crater or maria formation; (3) the density and thermal distribution of the interior; (4) the existence of water or other minerals required for the sustenance of life; or (5) the true nature of the small-scale features of lunar surface, e.g., dust, vesicles, "fairy castle," surface roughness and hardness.

Interferences of Small Scale Lunar Features⁽⁶³⁾

For purposes of establishing the lunar drill design criteria, the small scale features are more important than the gross or large scale features. The drill design included the provisions required for drilling in materials implied by both the impact and volcanic mechanisms.

The ejecta, whether caused by meteorite impact or explosive volcanoes, result in widespread disposition of angular fragments on the surface. The size distribution

*It is interesting to note that most of the personal theories presented by leading lunar geologists regarding lunar surface origin and characteristics have not been significantly altered by the photographs obtained from the Ranger Program. A recent symposium at NASA's Goddard Space Flight Center (15-16 April 1965) revealed that the "dust theorists" are still "dust theorists," and the "relatively high bearing strength theorists" still maintain their previously established hypothesis.⁽⁶⁵⁾

may be logarithmic and range from clay-sized powders (0.004 mm) to angular boulders (256 mm). Block sizes as large as 10 to 15 meters in diameter may occur from a lunar crater the size of Meteor Crater, Arizona. Regardless of the size distribution, marked angularity and poor size-sorting of this material can be expected. The absence of an atmosphere and the weathering process is of great importance since the material will not have been greatly modified after it reached its final resting place except by sputtering.

The lunar maria features derived from volcanic origin are generally agreed to consist of thick deposits built up by separate lava sheets. The characteristics of the lava flow should be similar to those occurring on earth, with considerations being given to the lower gravity and vacuum conditions of the moon. The terrestrial-type examples of lava flows are aa and pahoehoe. Aa, the Hawaiian term for basaltic lava flows, is typified by a rough, jagged, spinose, clinkery surface, while pahoehoe is typified by a smooth, billowy, or ropy surface. Modifications to these types of lava flows resulting from the lower lunar gravity and vacuum may include deeper nucleation and slower rise of bubbles resulting in a highly vesicular lava. Vesicular igneous rocks such as pumice and scoria are likely to be more common than the dense basalts of earth terrains. Other interpretations include pyroclastic deposits of volcanic ash and tuff which may be found widely distributed and interbedded with the lava flows.

The array of possible lunar surface materials which is interred by the various observation and measuring techniques represents the minimum drilling capability which should be incorporated into the lunar drill. Therefore, the drilling tests should eventually include materials such as tuff, scoria, basalt, andesite, pumice, pahoehoe, aa, and rhyolite.

Characteristics of Possible Lunar Materials

The thermal conductivity, specific heat and thermal inertia of the anticipated lunar materials must be considered during the design of the lunar drill. A detailed thermal analysis is required to determine if the conducted and convected heat from the drill bit to the rock is sufficient to maintain a reasonable equilibrium temperature.

Comparative thermal characteristics of copper and possible lunar materials are listed in Table A-1. The simplified two-layer lunar surface model consists of an upper layer possessing the approximate characteristics of powder in a vacuum. The lower layer consists of rock possessing the approximate characteristics shown in Table A-1 perhaps modified somewhat by vesiculation.

It is generally conceded that the voids created in loosely packed powders in a vacuum will result in average thermal conductivities which are approximately 1% of the values obtained under a pressure of one atmosphere. However, the thermal conductivity of the lower level consolidated rock material is expected to approximate terrestrial igneous rocks.

TABLE A-1Comparative Thermal Characteristics of Possible Lunar Materials⁽⁴¹⁾

Material	Thermal Conductivity, K (cal/cm ² /sec/(°K/cm))	Density, (gm/cm ³)	Specific Heat, c (cal/gm/°K)	Thermal Inertia, (KPC) ^{-1/2} (cal/cm ² /°K/sec ^{-1/2})
Copper	0.9	9	0.09	1
Rock	5×10^{-3}	3	0.2	20
Pumice	3×10^{-4}	0.6	0.2	170
Powder in Vacuum	$3 \times 10 \times 10^{-6}$	2.0	0.2	500 to 1000

Surface Temperatures⁽⁴¹⁾

The maximum average temperature on the surface of the moon occurs at the point where the sun is directly at the zenith, or subsolar point. It has been observed that the maximum temperature occurs when the heat flux is a maximum, that is, no phase lag is apparent. The theoretical and experimental determination of this temperature is in agreement within less than 1° K at a value of 374° K. The actual temperature at a particular subsolar point may be as high as 390° K or as low as 330° K. The variation of subsolar temperature is due to the facts that the solar constant (average 1.3×10^6 ergs/sec-cm²) varies slightly depending on the moon's distance from the sun and that the actual albedo ranges from less than 5% to more than 40%.

The design of the lunar drill must include the features necessary to ensure satisfactory operation in the high temperature environment. Temperature sensitive equipment such as the electric motor will require an environmental control system to ensure satisfactory heat removal from the lunar drill system.

The minimum lunar surface temperature occurs within a few days after passage of the terminator. However, the initial temperature drop upon "black out" of the solar radiation can occur very rapidly. One observer measured a temperature drop from 374° K to 200° K over a period of 1 hour during an eclipse.

It is anticipated that operation of the lunar drill will occur during the sunlit portion of the synodic month, thus placing the emphasis on high temperature design features. However, low temperature storage must also be considered.

Subsurface Temperatures⁽⁶³⁾

The subsurface lunar temperature fluctuations with surface temperature changes decrease in magnitude proportional to the subsurface depth. One study has shown that the fluctuations essentially cease at a depth of 30 inches, and a mean temperature of approximately 235° K is attained at this depth.

Although the lunar subsurface temperatures which will be encountered by the drill bit are relatively low, the correspondingly low thermal conductivity of the rock material reduces effective heat conduction and radiation from the drill. A detailed thermal analysis was conducted to determine what percentage of the total heat generated by the coring bit would be conducted and radiated into the surrounding rock, and is included in Appendix B.

Atmosphere (63)

The lunar atmospheric pressure is estimated at 10^{-13} times the earth's mean sea level pressure. Extremely small quantities of H_2 , H_2O , CO_2 and other gases are estimated to comprise the 10^{-10} mm Hg (or lower) lunar atmosphere.

Absence of a significant lunar atmospheric pressure requires a careful selection of materials and lubricants for the lunar drill. The subject of materials is discussed in a later section of this report.

A second major problem created by the low pressure environment is that of thermal control. Since there can be no external convective cooling for the lunar drill system, heat removal must be accomplished by radiation into space.

The vacuum environment of the lunar surface may create other rock drilling problems which are not encountered in the terrestrial environment. Recent studies (64,66) have indicated that the lower pressures may result in increases in the coefficient of friction and adhesion between metallic and nonmetallic materials. Dr. S. H. Penn, Grumman Aircraft Research Department, in his soon-to-be published "Wildcatting on the Moon," postulates that use of a mechanical force drill on the moon's surface will be impossible without lubrication of the drill bit. Therefore, the problem of rock cutting and dust removal with the lunar drill system may require the use of a controlled lubricant or special core barrel surface material in order to reduce the predicted dust-metal adhesion problem. This cannot be determined until a high vacuum rock coring test can be conducted.

Radiation

In addition to temperature considerations, the possible effects of solar and cosmic radiation on material degradation must be considered for the lunar drill. Although metals are not seriously affected by radiation, the selection of plastics for seals and other applications must consider their possible breakdown under the radiation environment.

Coring Techniques

During the past several hundred years, numerous techniques have been developed for hole drilling on the terrestrial surface. The three techniques which are employed for the majority of earth drilling operations include percussion, rotary, and rotary percussion. Other methods of drilling which receive limited usage for special purpose drilling include flame drills, electric arc, chemical softeners, pellet impact, abrasive laden jets, and explosive shaped charges. A brief discussion of these techniques and their possible use for the ten-foot lunar coring device is presented below.

Flame and Electric Arc Drills. - The flame drill has been in service since 1853; the electric arc since 1874. Both techniques use high temperatures to spall the rock during cutting operations. Drilling devices employing these techniques are used predominantly for the mining of relatively small blocks of various rocks which are used for fabricating monuments and building materials.

Use of the flame or electric arc devices would be impractical for obtaining consolidated 1-inch diameter cores to ten foot depths on the lunar surface. Relatively large "cuts" would be required around the periphery of the core in order to accommodate the drilling equipment below the surface, and to provide allowances for irregular cutting. Additional mechanical devices would be required for core extraction after completion of the cutting operation. Electric arc devices inherently require large power supplies which would be in excess of the LEM capacity. In addition, proper heat control with a gas operated flame drill in the 10^{-10} mm Hg lunar atmosphere would be difficult.

It is possible that an electric arc device may prove to be feasible for deep drilling operations after the establishment of a permanent lunar base, but for the early LEM landings it appears to be prohibited.

Chemical Softeners. - The use of chemicals such as sodium carbonate or sodium hydroxide for softening rocks began in 1887. This technique is currently used to some extent for the etching of rock, but has never received wide usage for the formation of deep holes. It would appear extremely difficult to control the formation of a rock core over a 10-foot depth with a chemical softener. In addition, the low subsurface temperatures and vacuum conditions on the moon would prohibit the use of most chemicals for the hole formation process.

Pellet Impact and Abrasive Laden Jets. - Both the pellet impact and abrasive laden jet techniques employ the same principle of impacting high velocity particles against the rock at the bottom of the hole. The former technique employs the use of a fluid to supply the energy to the pellets which impinge upon the rock surface. The pellets also serve as a grinding agent at the bottom of the hole and are continuously circulated until consumed. The particles utilized in the abrasive laden jet system are smaller than the pellets, but are employed in the same manner to erode the rock.

Both systems utilize water or drilling fluids for terrestrial drilling operations which would be prohibitive on the lunar surface. A high velocity gas system could possibly be utilized to supply the energy to the abrasive particles, but the required quantities of gas would limit these systems for the lunar coring operation.

Explosive Shape Charges. - There have been extensive advances in the utilization of shaped charges for hole boring operations. Depth, orientation, and size of holes can be controlled in homogeneous materials by the proper employment of shaped charges. In order to obtain a core it is necessary to lay out a "charge pattern" on the surface of the rock outcrop which approximates the desired core size. For a one-inch diameter core an equilateral triangle (or hexagon) with two-inch sides would be employed, with the appropriate shaped charge placed at the vertices of the triangle in order to obtain the desired depth. A rotary coring device would still be required to cut through the rock material remaining between the explosively bored holes. The power required for the coring operation would be much less than for a complete hole, and a chip removal system would not be required because the finished hole would provide "storage room" for the coring chips.

Although the use of shaped charges present some advantages, they would not be particularly valuable because of the need of a rotary coring device to extract the core. Because of the high energy levels available with the shaped explosives, it is anticipated that their employment may have advantages with the advanced permanent base lunar operations. Astronaut safety, lunar surface contamination and other related factors would require investigation before final recommendation.

Rotary, Percussion, and Rotary-Percussion Devices. -The majority of present-day drilling operations are accomplished by rotary, percussion or rotary-percussion devices. Each technique possesses advantages and disadvantages, which were evaluated with respect to the task requirements.

Rotary Drilling. (30)-Rotary drilling is accomplished by boring the bit (solid or core type) along a helical path while it is being subjected to the axial thrust and rotary torque required for shearing of the rock material. Actual rock breakdown occurs in the following manner:

1. A buildup of forces and deflection of the bit takes place until a sudden fracture of the rock occurs;
2. A rapid release of stored energy in the deflected bit takes place, causing the bit to impact upon the rock;
3. A buildup of forces again occurs, with some failure of the rock along irregular lines of the fractured rock and new contact plane. This action continues until the next fracture occurs, completing the cycle.

Percussion Drilling. (30)-Percussion drilling is accomplished by a high impact energy exchange between the bit (core or chisel type) and the rock. A small portion of the rock is fractured with each impact, and the bit is indexed to a new spot before the next blow. Fragmentation of the rock occurs in the following manner:

1. Crushing of rock surface as the bit makes initial contact;
2. Elastic deformation of the rock;
3. Pulverization of rock beneath the point of contact. Concurrent with the pulverization phenomenon, a stress wave is propagated along the path of least resistance, which results in rock fracture;
4. Chip production. Fracture relieves the stress and the force between the rock and bit. Dependent upon the energy stored in the tool, the bit may continue down through the pulverized region causing a second fracture to occur, or the rock may go through elastic deformation only, causing the bit to rebound.

Rotary-Percussion. -Rotary-percussion drilling contains elements of both the rotary and percussion actions previously described. The bit is held in contact with the formation so that after each percussive blow the rotary motion of the bit will shear off the rock between the indentations, thereby giving larger cuttings and, consequently, more efficient drilling.

Summary. -All three techniques (rotary, percussion and rotary-percussion) can be employed using either "above surface" or "down-the-hole" electric, pneumatic, or hydraulic prime movers. The "down-the-hole" equipment may prove to be more practical on the lunar surface for relatively large diameter holes (greater than three inches), and where the drilling depth exceeds approximately one-hundred feet. This type of equipment reduces the power losses and excessive weight inherent with the long drill rods required with "above surface" prime movers. However, the "down-the-hole" equipment is not recommended for the relatively short ten-foot coring device.

Lunar drilling feasibility studies were conducted by the Hughes Tool Comp.⁽²⁷⁾, Armour Research Foundation of Illinois Institute of Technology⁽³⁰⁾, and Texaco⁽²⁹⁾ in 1960. These studies were oriented toward the development of a lunar drill under the following general specifications:

1. Unit to weigh less than sixty pounds and consume a minimum of power;
2. Capable of drilling a 1.0 to 1.5-inch diameter hole to a depth of five feet;
3. Maximum available thrust (restraining force) is 50 to 75 pounds;
4. Samples of the lunar surface (hole cuttings or chips) required for instrument analysis.

The purpose of the studies was to evaluate the relative advantages and disadvantages of the rotary, percussion, and rotary-percussion techniques for hole drilling within the operating restrictions for the lunar drill.

Figure A-1 (Percussive Drilling Results from Texaco Study) illustrates the penetration rates obtained in sandstone and granite using the rotary-percussion technique. This compared favorably to the penetration rates obtained by pure rotary drilling under the low axial thrust of 57 pounds using various 1.0 to 1.5-inch diameter bits. However, one test was conducted using a one-inch masonry carbide bit with an increased axial loading of 180 pounds and rotational speed of 450 RPM. This test resulted in a penetration rate of 0.5 inches per minute with a power expenditure of 250 watts, which compared favorably to the rotary-percussive penetration of 0.375 inches per minute at the same power level. The Texaco tests clearly demonstrated that relatively high axial loading is required in order to obtain satisfactory penetration rates with pure rotary drilling.

The Armour study⁽³⁰⁾ revealed results similar to those obtained by Texaco for rotary coring. Penetration rates in the soft to medium hard materials were satisfactory, and increased proportionately with increasing axial loading. No significant penetrations could be obtained in granite. The results of the diamond coring tests are tabulated in Table A-2 (Rotary Diamond Drilling Results from Armour Study). These tests were conducted at a rotational speed of 900 RPM, and the input power was maintained at 0.58 to 0.69 HP.

Rotary drilling tests were also performed using carbide tip drills in a variety of materials. In addition, several rotary-percussion tests were performed using solid bits. The results of these tests will not be analyzed since they are not related to the coring requirement for the current lunar drill program. However, it was interesting to note that rotary-percussion penetration rates of 0.51 to 1.14 inches per minute were

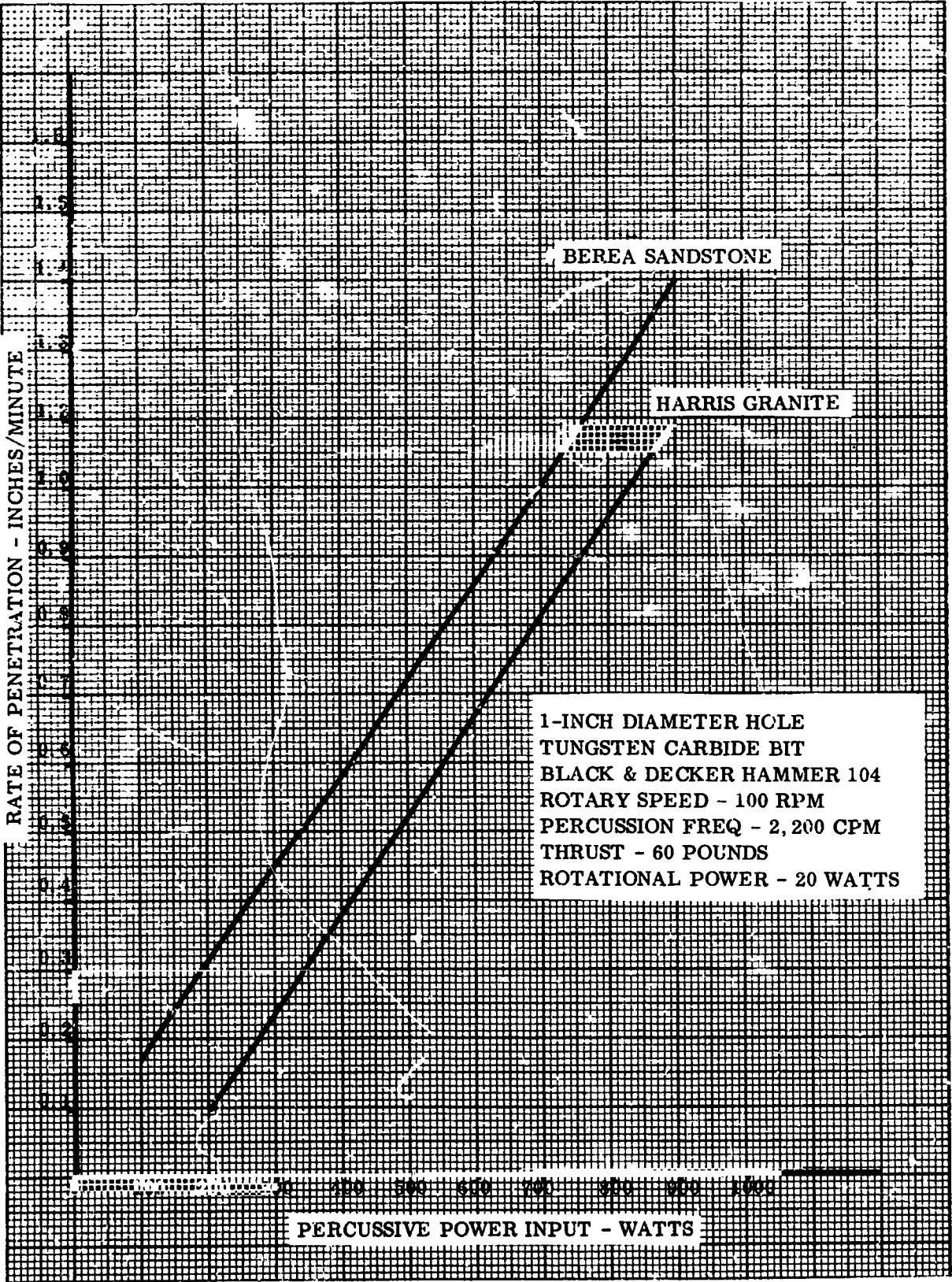


Figure A.1. Percussive Drilling Results from Texaco Study⁽²⁹⁾

ER 13952

obtained with the solid bits at power input levels of 550 to 940 watts. This represented a significant improvement over the pure rotary diamond coring penetration rates in granite.

The majority of the Hughes Tool Company feasibility penetration tests were oriented toward the pure percussive devices. This technique was recommended as the most feasible method for drilling a complete hole on the lunar surface within the restrictions of their study. Most of the coring bits evaluated were of the standard, wide kerf type which require power levels greater than that available for the ten-foot coring device.

Table A-3 (Comparison of Rotary and Rotary-Percussion Systems) presents a tabulation of preliminary trade-off data. The higher penetration rates in granite and absence of core bit temperature problems are desirable features in the rotary percussion systems. However, the requirements for granite penetration appears unlikely for the marial regions of the lunar surface. The relative simplicity, reliability, and core retrieval characteristics of the rotary coring system initially appeared most desirable for the ten-foot coring device. Therefore, initial feasibility tests were conducted with diamond core bits (see Feasibility Test Section). The testing was directed toward thin-wall bits in an effort to conserve power.

TABLE A-2. ROTARY DIAMOND DRILLING RESULTS FROM ARMOUR STUDY

Material	1-Inch Diamond Core Bit			2-Inch Diamond Core Bit		
	25 lbs.	35 lbs.	45 lbs.	25 lbs.	35 lbs.	45 lbs.
Concrete	1.5 in/min	3.1 in/min	3.3 in/min	0.89 in/min	1.14 in/min	1.60 in/min
Limestone	1.2 in/min	1.3 in/min	2.2 in/min	1.4 in/min	1.6 in/min	1.8 in/min
Hornblend Schist	0.36 in/min	0.55 in/min	0.75 in/min	0.215 in/min	0.375 in/min	0.60 in/min
Marble	1.25 in/min	1.66 in/min	2.22 in/min	0.48 in/min	0.85 in/min	1.0 in/min
Granite	None	None	None	---	---	---

TABLE A-3. COMPARISON OF ROTARY AND ROTARY-PERCUSSION SYSTEMS

Comparative Items	Diamond Rotary Core Drill	Carbide Rotary-Percussion Core Drill
Recovery of Solid Cores	Controlled-diameter cores can be obtained with relative ease, although use of single-shell core barrels sometimes results in core shearing due to friction.	Difficult to obtain due to fracture tendencies.
Complexity and Reliability	Most simple mechanism available for rock coring.	Additional mechanism required for percussive action.
Weight of Equipment	30-40 pound range, exclusive of bit cooling gas system. Use of residual LEM gas or fuel possible.	Additional weight required for percussive mechanism. Heavier drill rods required to withstand and transmit the rotary-percussion energy to the drill bit.
Dust and Chip Transport System	Relatively simple system due to the small particle size and amounts produced during the cutting operation.	Additional complexity due to larger particle size and amounts of rock material produced during the cutting operation.
Penetration Rates	Satisfactory in soft to medium hardness rock materials. Penetration difficult in extremely tough granites due to diamond wear-out.	Reasonable penetration rates can be obtained in the granites.
Core Bit Cooling	Relatively high bit temperatures may occur, especially if bit is improperly "loaded". Temperature can be controlled by operation cycling or gas.	Low operating temperature of bit requires no special consideration.

ER 13952

Man/Machine Interfaces

The ability of the astronaut to safely employ the rock coring device on the lunar surface will depend on a large number of factors including, but not limited to the following general functions:

1. Selection of work site;
2. Removal of equipment from the LEM, and transport to the work site;
3. Preparation of equipment for operation at the work site;
4. Initiation of the coring sequence;
5. Periodic removal of core sections and addition of drill rod extensions;
6. Core preparation for return to LEM;
7. Shutdown, disassembly, and packaging of equipment for movement to new area if required;
8. Transport of specimens and equipment back to the LEM;
9. Available working time of the life support system;
10. Astronaut mobility and dexterity with full pressure ensemble in a 1/6-G lunar environment.

The primary function of the rock coring device is to obtain segmented lunar core samples down to a depth of ten feet. Obtaining such a sample on earth with commercial equipment is a time consuming task, requiring hours as opposed to minutes to accomplish. Operation of the commercial coring equipment usually requires full-time attendance by one or more operators. However, a continuous monitoring operation of a lunar coring device by an astronaut cannot be afforded. Therefore, a maximum of automatic features were incorporated into the design of the coring device, commensurate with weight and size restrictions.

Relatively large forces are required to restrain the drill when coring to depths of ten feet. Preliminary testing, employing the Martin Lunar Gravity Simulator, indicated that an unrestrained operator can be expected to exert 18 to 22 pounds of downward force in line with the vertical axis of the body before losing footing with the surface. Employing the same criteria, a maximum torque restraint capability range of 13 to 16 foot-pounds resulted. In view of the anticipated coring time and reaction force required, it was logical to assume that the coring device would not be hand-restrained, but instead, anchored to the lunar surface. During the actual coring process the astronauts' primary attention should be devoted to other lunar surface tasks.

The breadboard model coring device, and associated equipment was designed and packaged so that it would be easily transported to and from the work site. Thus, a minimum weight and size for the equipment was required. The maximum limits specified by permissible LEM payload, and influenced by the 1/6-G lunar environment appear adequate to facilitate astronaut handling of the coring device.

Previous testing and evaluation by Human Factors, using subjects suited in the Gemini and prototype Apollo spacesuits, indicate that it is very difficult to stoop down or squat close to the standing surface in the pressurized ensemble. Subjects found it necessary to kneel on one leg before retrieving an item dropped on the floor. An astronaut would not be expected to assume low crouching or squatting work positions on the lunar surface with present day spacesuits. Securing the leg supports of the coring device to the lunar surface does not require an astronaut to apply forces or perform an excessive number of tasks from a low work position.

In view of the overall height restriction of the basic unit (approximately 30 inches), all controls and displays were located as close as possible to the top of the device. However, weight trade-off considerations may require some compromise to this criteria on subsequent flight models.

Excessive stooping and bending may be required during assembly and disassembly of the unit if components are placed on the lunar surface upon arrival at the drilling site. It may be desirable on subsequent flight models to supply an equipment container with extendable legs to facilitate temporary storage, assembly and disassembly of the subsystem components. Again, weight trade-off considerations may require some compromise of this approach.

The inherent design of the device provides for the operator's visual detection of coring depth and rate. Once the coring operation commences, the astronaut's tasks will be reduced to primarily that of periodic monitoring. While an electrical rate display would be desirable, a simpler method of accomplishing the same function is to maintain an accounting of drill rod extensions coupled into the drill string by subtraction of the unused drill extensions from the original total number.

The foregoing represents a cursory study of design objectives and operator restrictions for the lunar coring device. Spacesuited operators were used to evaluate the final prototype coring device model to ensure that the man/machine interface problems were adequately solved or identified for subsequent correction. The results of the spacesuit interface tests are presented elsewhere in this report.

Materials Selection Criteria

The selection of materials and lubricants for the lunar drill is an important consideration. Environmental conditions⁽⁶³⁾ under which the coring device may operate include a vacuum of 10^{-10} mm Hg or higher, and a lunar surface temperature range of $389^{\circ} \pm 5^{\circ}$ K to $120^{\circ} \pm 2^{\circ}$ K throughout the synodic month. The drilling operations will initially be restricted to the "lunar day" which will involve only the upper portion of the synodic monthly temperature range.

Much effort has been expended by Martin and others in the investigation of materials and lubricants for use in the vacuum of space. A wide variety of lubricants has been employed in the mechanical systems of U. S. satellites and spacecraft. Oils and greases having low vapor pressures have worked quite well in these applications. Sealed or partially sealed units have been employed to prevent vaporization of lubricants. The recent trend has been to use materials that have built-in lubricants, or to employ solid lubricants such as fluorocarbons, and solid film lubricants (e.g., MoS_2 and WSe_2).

Ball bearings suitable for use in vacuum are readily available. These bearings are manufactured from standard bearing steels, 440C or 52100, with bearing retainers containing a lubricating material. Retainers made of Duroid 5813 (60% Teflon, 40% glass fibers impregnated with MoS_2) have performed satisfactorily in satellite applications. Recently developed, improved retainer materials contain mixtures of: (1) 60% copper and a 40% mixture of 3 parts Teflon and 1 part WSe_2 , or (2) 70% silver and a 30% mixture of 3 parts Teflon and 1 part WSe_2 . Ball bearings containing one of the above improved retainer materials will be considered for use in the lunar drill. If the lower operating lunar surface temperatures are encountered (lunar night), additional problems are created for the hard bearing steels, as their toughness is reduced at the extreme low temperatures. Nickel-containing steels, such as case hardened 9310 (3.25% nickel, 1.2% chromium with a slight molybdenum additive), are satisfactory for the low temperature operation. Ball bearings with smallest possible ball size will be selected to minimize lubrication problems in vacuum.

Gears for the lunar drill may be constructed from self-lubricating materials such as the sulfur-bearing steels. Sulfur-bearing, free-machining steels are readily available. Sulfurized steels in both carbon and low alloy grades are also available. A wide variation of hardness can be obtained by proper selection of composition and by heat treatment.

Materials for parts that have sliding motion can be made either as metal-to-metal or metal-to-nonmetal combinations. For heavy loads, a properly selected steel-to-steel combination can be used. Sulfurized steels should be selected to provide a built-in lubricant and a solid film lubricant, such as MoS_2 , applied by burnishing or by vacuum deposition. A vacuum coating method for MoS_2 , known as CLD 5940, has been developed by the Columbia Broadcasting System Laboratories. Steel versus aluminum can also be employed if the aluminum is hard coated by the Martin, Alumite, or similar process. A new method that impregnates Martin hard coating with Teflon ("Tufram" coating by the Magnaplate Company) is another applicable process. Metals versus non-metals can be used if the mechanical loads are light. Steel versus Teflon is a satisfactory combination for light sliding motion.

Development of roller bearings for space application has not progressed as extensively as that of ball bearings. However, the same material fundamentals apply for the roller bearings as for the ball bearings. The usual bearing steels, when lubricated by solid lubricants, may be satisfactory for roller bearings if their use is required in the lunar drill.

When designing the lunar drill for use in the near vacuum environment of the lunar surface, the possible galling and seizing (cold welding) problem must be considered. It is desirable to design for light loading of any combination of metals which have relative motion. Light loads will lessen the tendency for the metals to gall and seize in service.

The possible lower surface temperatures for the lunar drill must be considered for the selection of materials for day and night operations. Carbon steel and some low alloy steels are embrittled at the low temperatures, especially when they are stressed in the presence of slots, notches, threads, or other stress raisers. All parts subjected to high stresses must be fabricated from steels having sufficient nickel content to assure toughness at the lower operating temperatures.

ER 13952

Lubricants for the lunar coring device are required to work in high vacuum and elevated temperatures. For high temperature lubrication greases and oils are not satisfactory, and dry lubricants must be employed. Molybdenum disulfide is an effective lubricant in vacuum to 1500 F or above. For this application the solid film lubricant could be bonded to the required surfaces by means of a stable inorganic compound. The fluorides of calcium and strontium have been used as lubricants at very high temperatures. The following are possible lubricating systems for the moving parts of the coring device:

1. Dry film lubricants such as MoS_2 or WSe_2 , bonded with sodium silicate or B_2O_3 .
2. CaF_2 or SrF_2 bonded with a stable oxide.
3. Flame sprayed or plasma arc sprayed mixtures of solid film lubricants (example MoS_2) and metals (nickel or silver).

ER 13952

APPENDIX B - ROTARY CORING PRELIMINARY ANALYTICAL MODEL

Anticipated Drill Drive-Motor:

13000 R.P.M.

Geared 24-1 540 R.P.M. output

Efficiency within Voltage Range 60%

600 Watts input Power to Motor

360 Watts Maximum output work

Friction work generates heat 788.2 Ft.-Lbs./BTU

Friction is basically proportional to pull down force:

Friction Load, $F = N f$ Normal Load
multiplied by coefficient of friction of materials.

f , Sliding Friction on Hardest Rock = .50 (approx.)

Minimum pressure load to product diamond drill cutting
of hard rock = 200 Lb. Est.

Anticipated Friction

$F = 200 \times .5 = 100 \text{ Lb.}$

Cutting Load = 2 x Pull Down Load
per Ref. 1

Total Peripheral Force

500 Lb.

Ft.-Lbs. Per Rev. $\frac{2 \pi \times .6}{12} \times 500 = 157.2$

Pull-down H.P. may be stored intermittently

Total available H.P. x Mech. Eff.

$33000 \times \frac{360 \text{ Watts}}{746 \text{ Watts}} \times .9 = 157.2 \times \text{R.P.M.}; \text{R.P.M.} = 91$

ER 13952

This is an indication of possible insufficient horse power available for drilling hard rock with diamond bit, since 500 R.P.M. is nearer to the speed requirement for drilling rate.

Using a 500 Lb. down pull = N

A cutting load coefficient of 1.5

(The torque resistance load factor to down-pull load for a specific configuration of bit and type of rock)

Total Peripheral Force = $F_{\text{Drill}} = n f + 1.5 N$

$F_{\text{Drill}} = 100$

Ft.-Lbs. per revolution = 60

R.P.M. = $\frac{360}{746} \times .9 \times \frac{33000}{60}$

R.P.M. = 238.5

(Note greater R.P.M. increases power used)

Friction ratio $\frac{100}{500} = 20\%$ (Example 1)

$\frac{25}{100} = \frac{1}{4} = 25\%$ (Example 2)

Since the diamond drill wears during cutting a safe friction value even under optimized drilling conditions would be 25 to 30%.
Using 30% component:

360 Watts x .9 x .30 = 97.3 Watts

(Maximum condition for one hour or'y).

Worse condition: -

1 Watt Hour = 3.413 B.T.U.

97.3 x 3.413 = 332 BTU/Hr.

(Maximum Drill Bit Heat)

ER 13952

Assume 39000 P.S.I. to be the highest strength value for summarized compressive strength of lunar rock. Applying this to rotary diamond drilling, an estimation of drilling parameters can be made as follows; see Fig. B.1. Stone cutting is basically failure of the stone in local compressive strength.

$$\begin{aligned}\text{Peripheral load} &= 39000 \times \frac{.016}{.707} \times \pi \times 1.15 \times .150 \\ &= 475 \text{ Lb.}\end{aligned}$$

The pull down force is also 475 Lbs.

Assuming 332 BRU (or 97.3 Watt-Hour)

generated by friction, the equivalent peripheral load would be

$$\frac{332 \times 778.2 \times 12}{90 \times 60 \times 1.15} = 159 \text{ Lb. friction}$$

The total peripheral load for very hard rock could be 634 Lb. but if .010 depth of cut were used this load would be 500 Lb.

The torque load, of example 1, of 500 Lb. $\times \frac{1.15}{2} = 228 \text{ In-Lb.}$ must be carried up the pipe which attaches to the bit. The heat generated must be prevented from raising temperature levels to the point of damaging the diamonds. The diamonds begin to deteriorate at 1400°F and the annealing temperature of stainless steel is 1350°F.

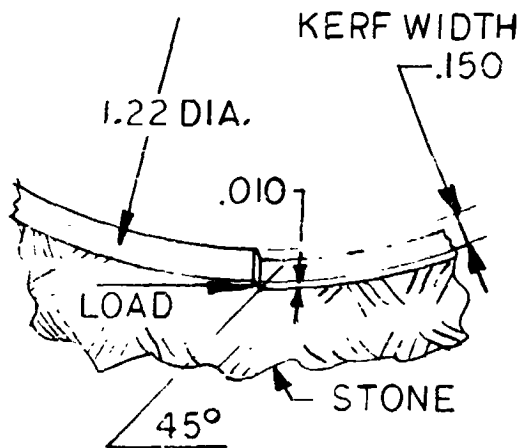
Heat dissipation can be obtained from the following:

- (a) Radiation and conduction in the rock
(to maintain heat flow from drill bit by radiation.)
- (b) Conduction of heat away from the bit up the shaft
and into the drill structure (where radiation
maintains heat flow from drill.)

Table B-1
E.R. = Half-Hard

Item	Metal Alloy Type No.	Heat Conductivity Btu/hr/ft ² /°F/ft	Specific Heat 32° to 212° F Btu/lb/°F	Thermal Expansion 32° to 212° F 10 ⁻⁶ in./in./°F	Mod. of Elasticity x 10 ⁵ lb./sq. in. (tension)	Spec. Stiffness x 10 ⁵ lb./sq. in.	Melting Temperature (°F)	Annealing Temperature (°F)	Yield Strength (psi x 1000)	Shear Strength (psi x 1000)	Elongation in 2" Percent	Ultimate Tensile Strength (psi x 1000)	Density lb per cu. in.	Remarks
1	Copper	226 to 196	0.092	9.3	170	53	1912	700						Anneal temperature too low
2	Phosphorus bronze	120 to 29	0.09	10.2	170	53	1900	900						Anneal temperature too low
3	Beryllium copper 172	100	0.10	9.2	170	64	1600	1400	80	50	7	110	0.297	0.1/5 Be 2.5 Co + Cu
4	Aluminum alloy	92 to 51	0.22	12.6 13.2	100	105	1185	775						Anneal temperature too low
5	Alloy steel	38.5 to 22	0.10	6.5	300	106	2550	1000	132	95	18.5	150	0.283	Rust?
6	Beryllium	87	0.45 0.66	6.4	420	657	2332	1400	20		5	85	0.066	No tapping powder met. † = shock load
7	Tungsten carbide cermet	50 to 26	0.034	2.5 3.9	943	185		2100	2		2			
8	Martimetic stainless steel	14.4	0.11	5.5	300	104	2675	1700	45 fatigue		13.5	220	0.281	38.5 impa.†
9	Ferritic stainless steel	15.1	0.11	5.8	290	104	2700	1350			25	60	0.280	
10	Nickel alloy 800	36.	0.13	6.6	300	93	2615	1500	75		15.2	90	0.321	Spring grade
11	Monel 411	15.5	0.13	9.17	230	82	2400	--	35 cast		25 cast	65	0.312	
12	Cupro nickel 715	17	0.09	9.0	220	68.1	2140	1800	68 H.f.		12	73	0.323	
13	Manganese bronze A	61	0.09	11.2	150	66	1590	800	60 H.H.		19 H.H.	84	0.302	Temperature to anneal = low

*at 1000° F



STONE CUTTING KERF

FIGURE B.1

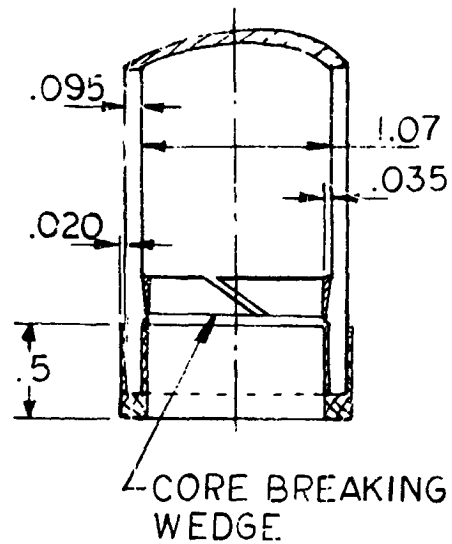
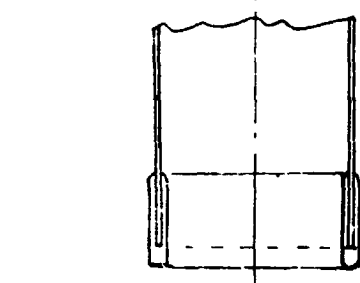


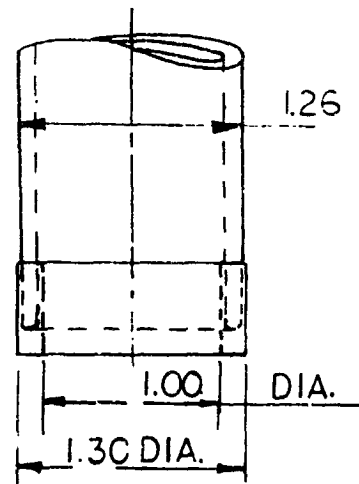
FIGURE B.4



I.D.=1 IN.
O.D.=1.188 IN.
KERF=.095 IN.

TEST DRILL BIT $\frac{135''}{HR}$

FIGURE B.2



REQ'D DRILL RATE $\frac{17.2''}{HR}$

FIGURE B.3

ER 13952

$$\text{Total Heat } Q = q_{RR} + q_{CR} + q_{CB} + q_{CCH}$$

q_{RR} = Heat Radiated into Rock

q_{CR} = Heat Conducted into Rock

q_{CB} = Heat Conducted into Drill Barrel

q_{CCH} = Heat Removed by Conduction and Convection into Helium Gas.

Eventual dissipation of heat

$$Q_{\text{total}} = Q_{\text{Lunar}} + Q_{\text{Radiation on Surface Rock}}$$

q_{CCH} can be considered to cool the rock also where its surface may pick-up heat by radiation from the hot drill barrel.

Where the rock is not consolidated, its heat of radiation from the drill will not be conducted away from immediate rock surface. The radiation of heat then equalizes and the drill receives as much radiated heat as it expels by radiation.

The gas wall thickness is relatively thin and it can be safely assumed that heat by conduction through the gas thickness is complete. The only significant factor is the heat capacity of the gas. Constant pressure condition would mostly represent steady flow

$$(\text{Flow}) W = Avp \quad (\text{Area} \times \text{Velocity})$$

$$\text{Heat Capacity, } C = C_p$$

$$C_p = 1.25 \text{ BTU/Lb/}^\circ\text{F for He}$$

The temperature along the drill barrel will first be influenced by the conductivity of the beryllium copper. Heat radiation into the rock will become relatively stable due to the low conductivity of the rock.

ER 13952

Dissipation of 332 BTU at Drill Bit, Fig. B.3 & B.4:-

Since insufficient data is available for establishing heat flow criteria, an approximation study is thought useful as a preliminary to drilling tests and drill design. From Table B-1 select beryllium copper.

Drill bit consists of .095 beryllium copper with tungsten carbide matrix holding diamond cutters.

If K_B = Heat conductivity of beryllium copper metal

K_R = Heat conductivity of consolidated rock

K_t = Heat conductivity of tungsten carbide

K = BTU/Hr/Ft²/°F/Ft (See Table)

Maximum temp. at bit = 1200°F to prevent damage to diamonds and softening of beryllium copper.

Values for K are necessarily approximate for this study.

K_R For Granite = 1.0 to 2.3

K_R For Lava = 0.49 Porous Material

K_R For Sandstone = 1.1

K_R For Marble = 1.2

Assume K_R = 1.1

K_t = 26

K_B = 100

Conductivity of rock at temperature -70°F
(Lunar subsurface 3CM depth - 54.4 to -207.4°F)

The actual heat absorbed by the rock will depend on its diffusivity which takes into account heat storage and temperature differentials.

$$q_{CR} = \frac{K A \Delta t}{L}$$

ER 13952

Estimated Rock Temperature and BTU Flow into Rock:

$$\text{Radiated Heat } Q = \sigma F_e F_A A (T_1^4 - T_2^4) \text{ BTU/Hr}$$

σ = Stefan-Boltzmann Constant

$$= .173 \times 10^{-8} \text{ BTU/Hr. Ft}^2 \text{ } ^\circ\text{F}^4 \quad (\text{Ref. 61})$$

$$F_e = \frac{1}{\epsilon + \frac{1}{\epsilon} - 1} = .15 \text{ from chart}$$

$$\text{Ext. } \epsilon_1 = .2 \text{ for drill}$$

$$\epsilon_2 = .4 \text{ for rock in vacuum}$$

$$F_A = \text{Configuration Factor} = .9$$

$$A = \text{Emitting Area} = \frac{12" \times \pi \times 1.26}{144} = .33 \text{ Ft.}^2$$

$$T_1 = \text{Temperature of Bit} = 1200^\circ\text{F} + 460 = 1660^\circ\text{R}$$

$$T_2 = \text{Temperature of Walls of Hole for Steady State Condition}$$

$$\text{Steady State Temperature of Lunar Rock} = 131^\circ - 329^\circ\text{R}$$

Temperature T_2 depends on conductivity of rock heat conductivity BTU/Hr.Ft².°F. Ft.

Estimating rock temperature close to drill rod in steady state: (From Ref. 41)

$(K\rho c)^{-1/2}$ has been found large indicating poor conductivity of lunar surface material

$(K\rho c)^{-1/2}$ was found to be 1000

For rock on earth this value was found to be as follows:

ER 13952

Table B-2

	K	ρ	C	$(K\rho C)^{-1/2}$
	CAL/CM ² /SEC/(°K/C _m)	g _m /C _m ³	CAL/g _m °K	CAL/C _m ² /°K(SEC ^{1/2})
Rock	5 x 10 ⁻³	3	0.2	20
Power in Vacuum	3-10 x 10 ⁻⁶	2.0	0.2	500 - 1000
	BTU/Ft ² /SEC/°K/Ft	Lb/Ft ³	BTU/Lb/°K	BTU/Ft ² /°K/SEC ^{1/2}
Rock	.561	187.29	.36	67.4
Power in Vacuum	.0001683 .000561	124.86	.36	1635 - 3370

If α = absorbtivity

r = reflectivity

τ = transmissivity

$\alpha + r + \tau = 1$ For heat received by the rock from the drill barrel.

τ may be zero because rock is opaque

r is returned heat by reradiation.

$$\alpha = \frac{K}{\rho C_p} \quad \text{where } K = \text{conductivity}$$

ρ = density

C_p = heat capacity

$$\alpha = \frac{.561}{187.29 \times .36} = .00833 \quad \frac{\text{Ft}^2}{\text{SEC}} = \frac{1}{120}$$

ER 13952

$$\frac{Q_{\alpha}}{Q_{\text{Total}}} = \alpha = \frac{1}{120} = \text{Thermal diffusivity}$$

$$\text{Radiated Heat} = Q = \sigma F_{\epsilon} F_A A (T_1^4 - T_2^4) \text{ BTU/Hr.}$$

$$\text{Est. } Q = .173 \times 10^{-8} \times .15 \times .9 \times .33 \left(\frac{1}{1660}^4 - T_2^4 \right)$$

$$\text{Also } \approx \frac{\text{Heat Conducted}}{\text{Heat Storage}}$$

$$\text{Heat conducted by rock} = q_{\text{CR}} = \frac{K_R A (T_1 - T_2)}{L}$$

$$\text{Let } L = x = 1" \text{ or } .0833 \text{ Ft.}$$

$$A = A \quad q_{\text{CR}} = \frac{.561 \times .33}{.0833} (1660 - T_2) = \frac{1}{120} \times 332$$

Let us check for 1/120 diffusivity of 332 BTU/Hr into rock to learn rock T_2 estimated

$$T_2 = \frac{-\frac{332}{120} + \frac{1660 \times .561 \times .33}{.0833}}{\frac{.561 \times .33}{.0833}} = \frac{-2.765 + 3685}{2.222}$$

$$T_2 = \frac{3682}{2.22} = 1658 \text{ } ^\circ\text{K} \quad \text{Then}$$

$$\text{Est. radiation } Q_R = .173 \times 10^{-8} \times .15 \times 9 \times .33 \left(\frac{1}{1660}^4 - \frac{1}{1658}^4 \right)$$

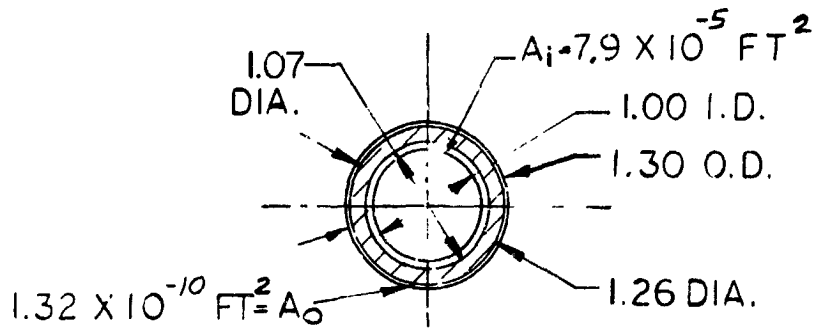
Q_R (When rock reradiates 12" of drill is inside of consolidated rock)

$$= .0359 \times 10^2 = 3.59$$

$$= 3.6 \text{ BTU}$$

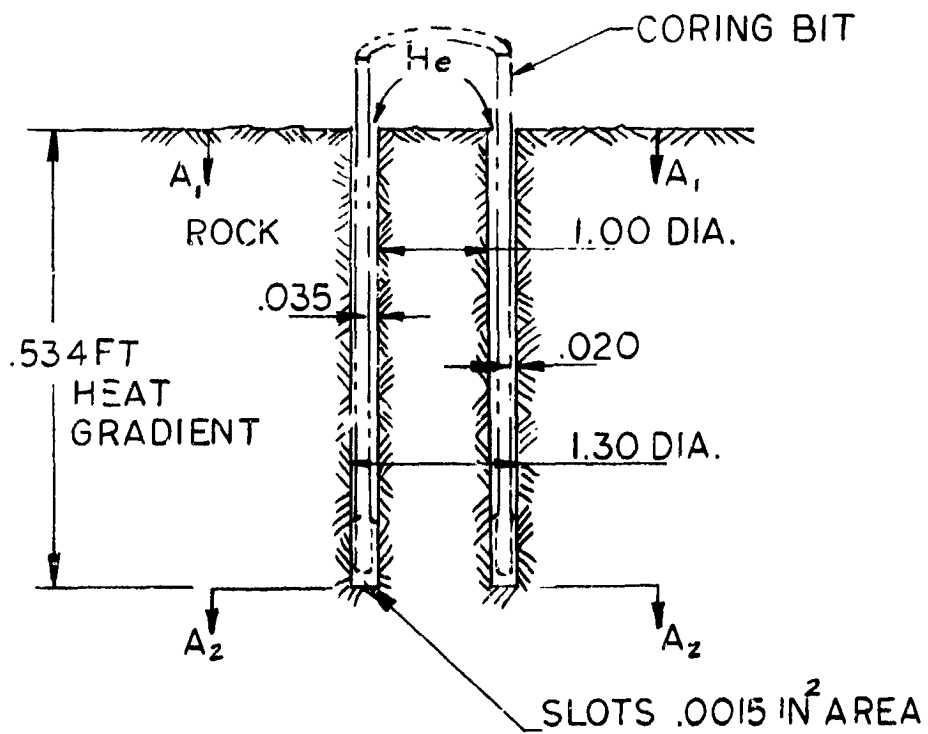
Heat stored in rock surface would be high, which accounts for the low heat dissipation by radiation to the rock from the drill barrel.

ER 13952



DRILL KERF
& CROSS SECTION

FIGURE B.5



CORE MODEL

FIGURE B.6

ER 13952

Heat conduction through the tungsten carbide matrix and into the beryllium copper drill bit tube is the important heat flow path. The area of tungsten is $A_t = .7854 (1.3^2 - 1^2) = .543 \text{ in}^2$

The beryllium tube cross-sectional area $A_B = .348 \text{ in}^2$

Temperature gradients can be estimated:

$$q_{\text{Tungsten Carbide}} = q - q_R = 328.4$$

$$q_t = \frac{K_t (t_1 - t_o)}{x} A_t \quad \text{where } x = .095$$

$$t_o = t_1 - \frac{q_t x}{K_t A} = 1200 - \frac{328.4 \times .095}{25 \times 12} \times \frac{144}{.543}$$

$$\frac{q_t x}{K_t A} = -276 \text{ } ^\circ\text{F}$$

A beryllium copper tube maximum length for total temperature gradient:

$$\frac{q_B x}{K_B A_B} = 924^\circ\text{F}$$

$$\frac{924 \times 100 \times 0.02415}{328.4} = .882 \text{ Ft.}$$

t_o will not reach zero degrees F and this temperature will be approximately that of the cooling gas being blown down the pipe for steady state drilling worse condition,

$$t_o = 660^\circ\text{R} \quad \text{see Figures B.5 and B.6}$$

ER 13952

t For tungsten-beryllium interface is 1660°F
conductance distance $x = \Delta t \ K_B \ A_B / q$

$$x = [(1660 - 276) - 660] \frac{100 \times .002415}{328.4}$$

$$x = .534 \text{ Ft}; \quad t = 724^\circ\text{F}$$

$$\text{Wetted Area Inside } A_{1-2} = \pi \times \frac{1.06}{12} \times .534 = .1235 \text{ Ft}^2$$

$$\text{Wetted Area Outside } A_{2-1} = \pi \times \frac{1.26}{12} \times .534 = .145 \text{ Ft}^2$$

Heat conduction and convection of the helium gas is mostly unknown. Experimental measurement of gas flowing through a heated drill-bit so as to obtain flow pressure drop, change in the density of gas, gas flow velocity, and the differential temperature may be made.

$$q = UA (\Delta t)_m = UA \left[\Delta t_{01} - \Delta t_{02} \right] \ln \Delta t_{01} / \Delta t_{02}$$

U = conductivity - convection

$$\frac{1}{UA} = \frac{1}{h_i A_i} + \frac{x}{KA_m} + \frac{1}{h_s A_s} + \frac{1}{h_o A_o}$$

A_o = Outside area; A_i = inside area

h_s = Heat transfer coefficient thru scale deposits

h_m = For entire surface based on Δt_m

Mean local Coefficient of heat transfer
BTU per hour: Ft² OF differential

G = Mass velocity W/s Lb/Hr. Ft² of cross section

μ_f = Viscosity at bulk temperature Lb/Hr.Ft
Arithmetic mean between wall and fluid

K_f = K at the film temp. $t_f \ (t + t_o) / 2$

ER 13952

D = Diameter in feet

D_i = Clearance inches

$$h_m = .024 C_p G^{.8} / (D_i)^{.2} \quad \text{Estimating (Simplified Eq)}$$

D_i = Clearance (inches)

$$G = \frac{4.5 \text{ Lb/Hr.}}{.534 \times \frac{1.07}{12}} = 30 \text{ Lb/Hr.Ft.}^2 \quad \text{(Mass Vel.)}$$

$$D_i = .035$$

$$h_m = \frac{.024 \times 1.25 \times (30)^{.8}}{(.035)^{.2}} = 8.92 \quad \text{BTU/Hr.Ft.}^2 \text{ of}$$

$$\frac{1}{UA} = \frac{1}{h_m A_i} = \frac{1}{8.92 \times .15}$$

$$UA = 1.37$$

Temperature inside is that of the beryllium bulk temperature (being supplied heat from drilling by conduction)

The quantity of gas required is taken from electric motor requirement

T₁ of gas entering is 660°R

T₂ of gas at drill matrix = 1022°F

Coefficient BTU taken by gas per h_m = 8.92

$$q = \frac{\text{BTU}}{\text{HR Ft.}^2 \text{ of}} 8.92 \times .15 \times 247 \frac{\text{Ft.}^2 \text{ of}}{\text{HR}} = 330 \frac{\text{BTU}}{\text{HR}}$$

$$\text{Let } \Delta t_{o2} = 50^\circ$$

ER 13952

$$\Delta t_m = \frac{\Delta t_{01} - \Delta t_{02}}{\ln \frac{\Delta t_{01}}{\Delta t_{02}}}$$

$$\Delta t_m = \frac{362 - 50}{362 - 50} = \frac{312}{5.8917 - 3.9120}$$

$$\Delta t_m = \frac{312}{1.9797} = 157.6$$

$$q_{12} = U A \Delta t_m$$

$$= 1.37 \times 157.6 = 218$$

$$q_{21} = \text{Approx. } 1/2 \text{ due to return flow}$$

$$q_{12} + q_{21} = 218 + 109 = 327 \text{ BTU}$$

Roughly estimating the drill conditions in vacuum would suggest supersonic velocity of flow except as modified by drill chip loading of the gas. This minimum flow velocity can be estimated from Ref. 1 for preliminary study.

There are no empirical formulae for heat transfer involving helium in any Standard Handbook. The usual heat considerations involving fluid flow in a round pipe do not apply to the torus area for fluid flow in the lunar drill. The rock will heat-up from radiation and provide heat force to the gas conduction from two directions simultaneously. It therefore seems logical to assume 80 per cent heat capacity effective.

The quantity of gas and its condition must first be estimated from the overall drill system. See Fig. B.7.

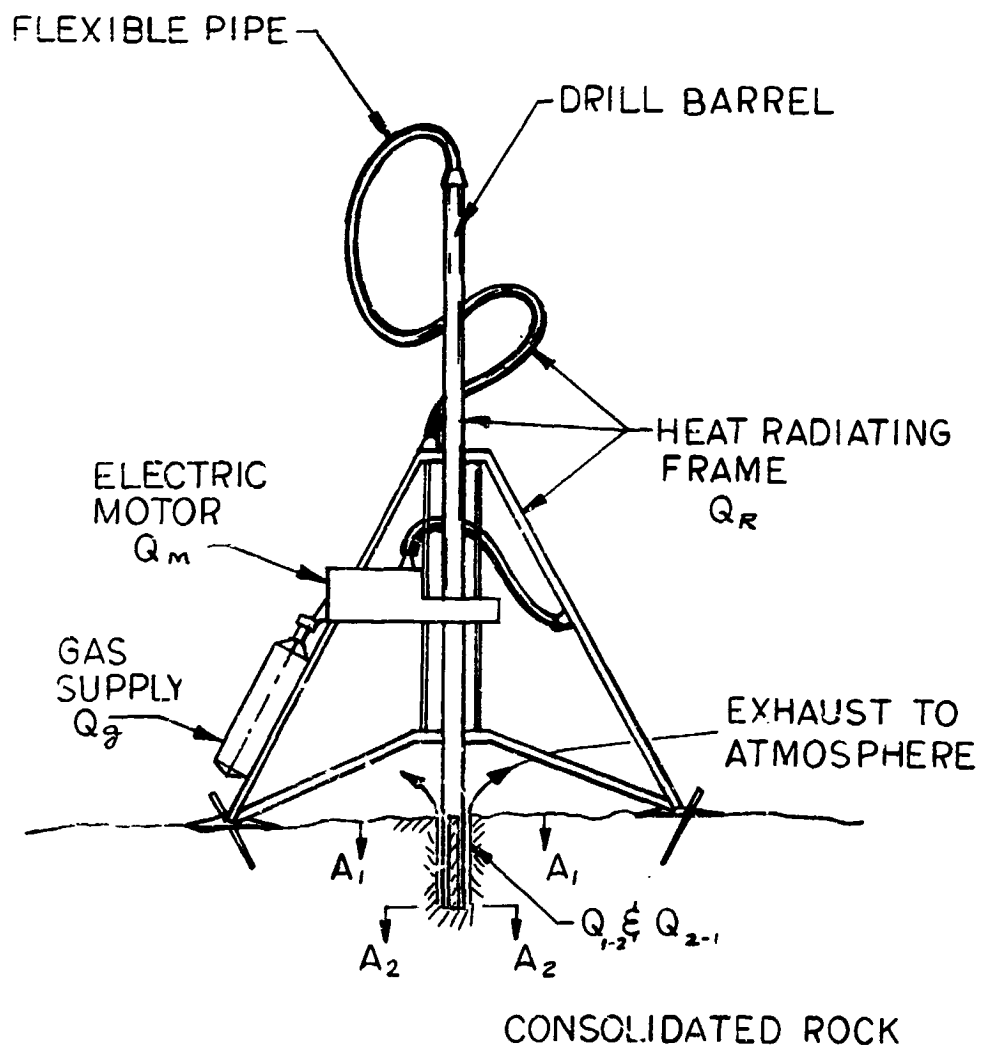


Figure B.7. Preliminary Sketch Installation

Lunar Coring Device

ER 13952

A Inlet area to each state, Ft.²
 (See Fig. B.7)

V Mean velocity in Ft./Sec

v Vol. Cu.Ft. per Lb.

p Pressure, p.s.i.

U Internal energy of fluid, BTU/Lb.

h Heat content, BTU/Lb.

Q_G & q_g BTU/Lb Heat of gas in state "g"

Q_M & q_m BTU/Lb Heat of gas from electric motor

Q_R & q_R BTU/Lb from drill rod

$Q_{A_{12}}$ & $q_{A_{12}}$ BTU/Lb from bit heater

$Q_{A_{21}}$ & q_{21} BTU/Lb from bit heater outside

$R(G - A_{O_1})$ Energy expended in friction

$R_{A_{21}}$ Energy of lifting debris from drilling bit

At points G, M, R, 1 and 2, the notations

V, v p and U are velocity, volume, pressure and energy at each section

ER 13952

By evaluating the gas flow at the bit first for flow rate estimate to keep bit clean

Hughes Tool Co. (Ref. 1)
Preliminary feasibility study Pg. C-5

$$V = 8.41 \text{ Ft./Sec.}$$

$$\rho_b = 16 \quad \text{From Chart}$$

$$R = 9$$

$$\beta = \frac{\text{Diam. Bit}}{\text{Diam. Shaft}} = \frac{1.300}{1.260} = 1.032$$

$$\beta^2 = 1.065$$

$$V_s = \frac{R}{\rho_b} = \frac{9}{16} = .5625 \quad (\text{Particles are dense})$$

$$V_0 = \text{Gas velocity (for air)}$$

$$V_s = \text{Particle velocity}$$

$$V_R = \text{Relative velocity}$$

$$(\text{Eq. C-4}) \quad Q_f = V_0 A_n \quad \text{Ft.}^3/\text{Sec}$$

$$\frac{A_H}{A_m} = \frac{\beta^2}{\beta^2 - 1} \quad A_H = A_{02} = 1.32 \times 10^{-5} \text{ Ft.}^2$$

$$A_n = \frac{A_H (\beta^2 - 1)}{\beta^2} = 1.32 \times 10^{-5} \times \frac{.065}{1.065} = 8.07 \times 10^{-7}$$

$$Q_f = V_0 A_n$$

$$= 8.41 \times 8.07 \times 10^{-7} \times 3600 = .0244 \text{ Ft.}^3/\text{Hr.}$$

Standard air

ER 13952

If we ratio air to helium on the basis of Reynold's number

$$\frac{(Air)}{(H)} \frac{R_N}{R_N} = \frac{1549}{193.5} = 8$$

$$Q_f \text{ (Helium)} = .0244 \times 8 = .196 \text{ Ft}^3/\text{Hr.}$$

Standard conditions

$$\text{Weight } H_e = 4 \text{ Lb}/359 \text{ Ft}^3$$

$$Q_f = \frac{4 \times .196}{359} = .00218 \text{ Lb.}/\text{Hr.}$$

This will not be the controlling quantity of gas needed by the drill system.

Gas required to cool the electric motor will exceed all other requirements due to the estimated heat loss of the motor:-

$$700 \text{ Watts} - 360 \text{ Watts (Work)}$$

$$340 \times 3.413 = 1160 \text{ BTU}/\text{Hr.}$$

The heat of the motor will be absorbed by the gas flow. The gas will then be cooled by radiation from the R section of Fig. B.7. It will then pass down into the drill bit picking-up heat and debris which it will exhaust into the vacuum of the lunar environment.

The gas supply is assumed at -40°F and 14.7 p.s.i. The quantity required is estimated to hold motor temperature below 300°F or 760°R .

Gas energy equation

$$h_m - h_g = C_p (T_g - T_m)$$

ER 13952

Helium Data:

$$\begin{aligned}\text{Critical } t_c &= 450.2^\circ\text{F (or } 9.8^\circ\text{K)} \\ p_c &= 2.26 \text{ ATM (33.222 p.s.i.)} \\ v_c &= .231 \text{ Ft.}^3/\text{Lb.}\end{aligned}$$

Gaseous Helium

$$w = .01039 \text{ Lb/Ft.}^3 \text{ at } 68^\circ\text{F and } 14.7 \text{ p.s.i.}$$

$$\text{Gas constant } R = 386.3$$

$$P V = R T$$

$$\frac{P_1 V_1}{T_1} = \frac{P_g v_g}{T_g} \quad \text{ref. Fig. A.7}$$

$$\frac{14.7 \times 144 \times \frac{1}{.01039}}{528} = \frac{14.7 \times 144 \times V_g}{500}$$

$$V_g = 91.3 \text{ Ft.}^3 \text{ Per Lb}$$

$$h_g = C_p T = 1.25 \times 500 = 625 \text{ BTU/Lb.}$$

The electric motor cooling will depend on the values of heat transfer coefficients which will be designed into the assembly. These may incorporate fins as needed to accomplish such criteria as 300°F maximum temperature for the electric motor working at maximum condition for one hour at 700 Watt input power.

The quantity of gas is here estimated from drill bit requirements $A_{12} - A_{21}$ as a start.

ER 13952

Minimum velocity of 8.41 ft per sec for V_{21} flow continuity:

$$w = \frac{A_g V_g}{g} = \frac{A_M V_M}{M} = \frac{A_R V_R}{R} = \frac{A_{12} V_{21}}{12} = \frac{A_{21} V_{21}}{21}$$

v is volume per unit weight

V is velocity

Let S = volume of section

A is cross sectional reas
restriction is in A_{21}

$$S_{21} = A_{21} L_{21} = .00071 \text{ ft}^3 \times .534 = .000378 \text{ ft}^3$$

$$S_{12} = A_{12} L_{12} = .000793 \text{ ft}^3 \times .534 = .000423 \text{ ft}^3$$

$$S_R = A_R L_R$$

$$S_M = A_M L_M \quad (\text{est. requirement})$$

$$S_g = A_g L_g \quad (\text{est.})$$

Because A_{21} is most likely choke point for flow of gas if 14.7 psi system is used this will provide constant pressure throughout system.

$$C_p = 1.25 \text{ Btu/lb/}^\circ\text{F} \quad \text{Heat capacity}$$

$$h = u + APV$$

$$T = \text{Temperature} \quad (\text{desired}) \quad \text{Ref. Fig. B.7}$$

ER 13952

System Section	S(ft ³) Volume	Changes per sec.	Btu/chg. (req'd.)	lb. Weight per change	H _e Estimated h	Design T °R
G	.076	1	-	1.668 x 10 ⁻³	1.048	500
M	.0432 .05	4.0	add +.0805	3.6 x 10 ⁻⁴	.341	760
R	25.7	.012	remove -26.8	.214	26.8	660
A ₁₂	.000423	14.1		2.27 x 10 ⁻⁶	2.16 x 10 ⁻²	1022 Avg.
A ₂₁	.000378	15.75 (min.)		2.03 x 10 ⁻⁶	1.93 x 10 ⁻³	1660

Calculations

Weight per change may be estimated from A₂₁ maximum allowed T₂₁ = 1660° R (max. to protect material). The weight per change criteria is used for this study in lieu of heat transfer coefficients as a scheme to roughly estimate quantity of gas required. Therefore design requirements start with bit velocity 8.41 ft/sec. Number of changes per sec = $\frac{8.41}{.534}$ of V₂₁ = .00071 ft³ x .534 (effective heater volume) = .000378 x $\frac{8.41}{.534}$ = .006 ft³/sec., 5.27 x 10⁻⁵ lb/sec.

The corresponding V₁₂ = .000423 ft³ but the gas per change will be modified by temperature difference. Cooling data for the bit can be referred to time in seconds.

The conduction and forced convection heat removal from the drill bit must take into account the temperature rise becoming uniform throughout the thickness of cooling air. The stone surface temperature will be practically the same as that of the bit due to heat

ER 13952

radiation stability on these surfaces. The cooling air thickness of .020 and .035 for V_{21} and V_{12} respectively will have a temperature gradient from both walls and a heater efficiency of 80 per cent would be conservative at these velocities.

$$\frac{332 - 3.6}{3600} = .0915 \text{ BTU/Sec.}$$

$$q_{21} = \frac{1}{.80} \times \frac{.000378}{.000378 \cdot .000423} \times .0915 = .00542 \text{ BTU/Sec.}$$

$$\text{Required BTU for } A_{21} = \frac{.00542}{15.75} = .000345 \text{ BTU/Chg.}$$

$$\text{For } A_{12} = \frac{.0915 - .00542}{7.56} = .0495 \text{ BTU/Chg.}$$

The volume .0071 x .54 is calculated to be 1022°F when it leaves A_{21}

$$\frac{P_1 V_1}{T_1} = \frac{P_2 V_2}{T_2} ; \quad T_2 = \frac{1384 + 660}{2} = 1022^\circ \text{R}$$

$$W = \text{Weight per Ch.} = \frac{14.7 \times 144 \times .000378}{1022} \times .01039$$

$$\frac{14.7 \times 144 \times 1}{528}$$

$$= \frac{.01039 \times .000378 \times 528}{1022} = 2.03 \times 10^{-6} \text{ Lb.}$$

$$h_{21} \text{ of Helium} = C_p T_W$$

$$= 1.25 \times 1022^\circ \times \frac{2.03 \times 10^{-6}}{.8 \text{ (Eff.)}}$$

$$= 1.93 \times 10^{-3} \text{ Heat content}$$

estimated from design (arbitrary) conditions

ER 13852

$$h_{12} = C_p T_w = 1.25 \times 1022 \times \frac{.000423}{.000378} 2.03 \times 10^{-6} = 2.155 \times 10^{-3} \text{ BTU(Heat)}$$

Then: - $h_{21} - h_{12} = C_p (T_{21} - T_{12})$

Since the maximum temperature is 1316°R at the matrix of the bit and 660°R at the top or section A₁ - A₁ of Fig. B.7 there is a heat loss which may be offset by work done on particles of debris during velocity in A₂₁.

Calculating against the stream of gas cooling to 660°R is assumed.

The weight of helium has now been established as 15.75 changes per sec. x 2.03 x 10⁻⁶ Lb. = 3.51 x 10⁻⁵ Lb./Sec.

$$= .1265 \text{ Lb. Per Hour}$$

Compare a design temperature and volume for helium as it leaves the electric motor

$$T_M = 300^\circ\text{F} + 460 = 760^\circ\text{R}$$

Cooling then takes place until the drill barrel penetrates the lunar surface.

- (a) Minimum length 3 Ft. of drill extension pipe
1.25 O.D. Outside area = .982 Ft.².
This pipe and the entire drill-rig will radiate heat. Some additional heat will be generated by the geared drive and pulldown. Allowance is made and a conservative estimate follows from assumptions as follows. (Elect.Motor Max. Temp. 200°F)

- (1) The hot temperature is 660°R throughout the drill pipe and stanchion
- (2) Temperature gradient (Fig. B.7)

ER 13952

Heat conducted through 321 Stainless Steel = q_s

$$q_s = K_m \frac{A_m (t_1 - t_0)}{x}$$

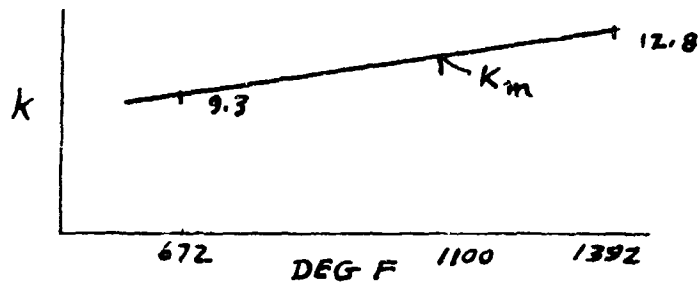


Figure B.8

Let $K_m = y$ and:-

$$\frac{x_2 - x_1}{y_2 - y_1} = \frac{x - x_1}{y - y_1}$$

$$y = \frac{(x - x_1)(y_2 - y_1) + y_1(x_2 - x_1)}{x_2 - x_1}$$

$$y = \frac{(1100 - 672)(12.8 - 9.3 \times 720)}{(1392 - 672)}$$

$$K_m = 11.85 \quad (\text{Figure B.8})$$

$$A_m = \frac{A_1 - A_0}{\frac{1}{n} \frac{A_1}{A_0}} \quad \begin{array}{l} A_0 = .982 \text{ Ft.}^2 \\ A_1 = .943 \text{ Ft.}^2 \end{array} \quad (.025 \text{ Wall})$$

$$A_m = \frac{.982 - .943}{\frac{1}{n} \frac{.943}{.982}} = \frac{.039}{.9413 - .9818} = .964 \text{ Ft.}^2$$

ER 13952

$$q_s = \frac{11.85 \times .964 (700 - t_0)}{\frac{.025}{12}}; \quad \frac{760 + 660}{2} = 700^\circ \text{ Avg.}$$

If the lunar temperature is taken as 374°K (Ref. 41)

t_0 may be found from (Ref. 1)

$$Q = \sigma F_A A (T_1^4 - T_2^4) \text{ BTU/Hr. (Ref. 61)}$$

where T_1 is equal to t_0 (Outside temp. of pipe)

$$q_s = Q$$

$$q_s = \frac{\Delta t}{R} \quad \text{where} \quad R = \frac{L}{KA} = \frac{.025}{11.85 \times .964 \times 12} = .000182$$

$$\text{Est. } q_s = \frac{700}{3600 \times .012} = .0162 \text{ BTU/Chg.}$$

$$\Delta t = .0162 \times .000182 \quad (\text{Est.})$$

$$= 2.95 \times 10^{-6} \text{ negligible}$$

$$t_0 = 760^\circ\text{F} = T_1 \quad \text{Ref. 61}$$

$$T_2 = 374^\circ\text{K}$$

From Chart Ref. 61

$$\text{if } \epsilon_1 = .53 \quad F_e = .4$$

$$\epsilon_2 = .6 \quad F_A = .9$$

$Q = 1160 \text{ BTU/Hr. from electric motor}$

$$Q = .173 \times 10^{-6} \times .4 \times .9 \times A (760^4 - 374^4)$$

Total Area = Large pipe frame etc.
Solve for area.

ER 13952

$$A = \frac{1160 \text{ BTU/Hr.}}{.173 \times 10^{-8} \times .9 \times (760^4 - 374^4)} \\ (3140.57 \times 10^{-8})$$

$A = 9.6 \text{ Ft.}^2$ which can be done, see below.

The value $h_m - h_R$ depends on the number of charges of gas per hour which will share in the total $Q = 1160 \text{ BTU}$

First trial 4 changes per sec. allows the area to be $9.6/4 = 2.4 \text{ Ft.}^2$ radiating.

$$\frac{1160 \text{ BTU/Hr.}}{3600 \times .012 \text{ (From Chart)}} = 26.8 \text{ BTU/Change of Gas}$$

$$h_m - h_R = 26.8 = C_p (T_n - T_R)(w/\text{Chg.})$$

$$26.8 = 1.25 (760 - 660) w$$

$$w = \frac{26.8}{1.25 \times 100} = .214 \text{ Lb.}$$

The volume required

Since 1 cu. ft. at 68°F and 14.4 p.s.i. = .01039 Lb.

$$\frac{\frac{PV}{T}}{\frac{PV}{T}} = \frac{\frac{14.7 \times 144 \times}{660}}{\frac{14.4 \times 14.7 \times 1}{528}} = \frac{.214 \text{ Lb/x Cu.Ft.}}{.01039 \text{ Lb/Cu.Ft.}} \\ = \frac{.214 \times 660}{.01039 \times 528} = 25.7 \text{ Ft.}^3 \\ \text{Volume/Chg.}$$

The motor, M, may be installed with a characteristic heat exchanger design and some knowledge of overall heat transfer coefficients gained from tests or extrapolation of existing heat exchangers. For this preliminary study heat conduction alone

ER 13952

at 70% system efficiency may produce rough values

say .05 Ft.³ around motor

70% efficient for heat conduction-convection

$$h_m - h_g = C_p (T_m - T_g)(w/\text{change})$$

$$\frac{1160 \text{ BTU/Er}}{3600 \times 4 \times .8} = .1002 = 1.25 (760 - 500) w$$

$$w = .00031$$

$$\frac{\frac{14.7 \times 144 \times v}{760}}{\frac{144 \times 14.7 \times 1}{528}} = \frac{.00031}{.01039}$$

$$v = .0432$$

$$h_M = 1.25 \times 760 \times .00031$$

$$= .341 \text{ BTU}$$

Required gas for each design condition: -

$$M \quad .00031 \text{ Lb/Change} \times 4 = .00124 \text{ Lb./Sec.}$$

$$R \quad .214 \text{ Lb/Change} \times .012 = .002568 \text{ Lb./Sec.}$$

$$A_{12} \quad .00000227 \text{ Lb/Change} \times 14.1 = .000032 \text{ Lb./Sec.}$$

$$A_{21} \quad .00000203 \text{ Lb/Change} \times 15.75 = .00003197 \text{ Lb./Sec.}$$

Obviously the flow will have to be uniform throughout the system. Since the "R" condition can be made to follow the system by varying the reflecting area this need only be reduced as needed. The motor heat flow depends on the .05 volume and the weight of helium per second which is critical to maintain a maximum of 760°R at the motor.

NR 13952

Corrected values for flow should be made on the basis of

$$.00124 \times 3600 = 4.5 \text{ Lb. for 1 Hr.}$$

$$\text{and 6 hours at } \frac{286}{700} \times 5.2 = .41 \times 4.5 \\ = 1.85$$

$$\text{Total weight of helium} = 11.10 + 4.5 \\ = 15.6 \text{ Lb. Est.}$$

The helium gas container will weigh approximately 10 Lb./Lb.-He resulting in a total tankage weight of 156 Lb. Therefore, if helium stored in the LEM is not available for use in the lunar drill, some other gas having a lower overall total weight must be considered if rotary diamond coring is employed.

APPENDIX C - ROTARY DIAMOND CORING FEASIBILITY TESTS

The mechanics of rotary core drilling are difficult to precisely analyze due to the nonhomogeneity of rock materials. Factors such as basic composition, mineralogy, grain interlock (texture), structure and other factors influence the drilling toughness of the rock material. As a result, the power and optimum drilling parameters required for drilling a block of rock may vary significantly, depending on the drilling direction with respect to the rock grain structure.

One theoretical approach to the prediction of rock shear strength as related to compressive strength is given by the formula:

$$s = \sigma \tan \phi$$

where s = shear strength

σ = compressive strength

ϕ = angle of internal friction or shearing resistance,

ϕ may be obtained from the following relation:

$$\alpha = 45 + \frac{\phi}{2}$$

where α = angle between the horizontal and the failure plane.

Both compressive strength (σ) and shear strength (s) depend on properties of the rock such as interlock of grains in the igneous and metamorphic rocks, and bonding or cement in sedimentary rocks. In addition, the value of ϕ is not a characteristic of the rock, but depends on the character of the shear phenomenon, especially the rate at which the shear force is applied.

Another more practical, but empirical formula ⁽¹⁾ for relating drilling penetration rate to axial load, shaft rpm, cutting area, and rock characteristics is given by:

$$P_r = K_{pr} \frac{PN}{\Delta D_b}$$

where P_r = Penetration rate (feet per hour)

P = Axial load on bit (pounds)

N = Shaft speed (rpm)

ΔD_b = Difference between OD and ID of core bit (inches)

K_{pr} = Rock constant ($\frac{\text{ft.}}{\text{hr.}} \frac{\text{in.}}{\text{lb.}} - \text{rpm}$)

Various rock constant values (K_{pr}) have been experimentally obtained by several testers ⁽¹⁾ under a variety of operating conditions. Results of these tests indicate the difficulty of obtaining precise factors required to adequately predict the drillability of rock material. In addition to the rock characteristics, the orientation and condition of the diamonds within the drill matrix will also affect the K_{pr} factor. However, this equation will be subsequently used for comparison purposes with the drilling penetration rates obtained during the feasibility tests.

Standard Wide Kerf Core Bits

General. - The first series of tests were performed using wide kerf "set" and "impregnated" type bits. The advantage of this type bit is that the wide cutting kerf allows clearance for the use of an inner and outer core barrel; the outer barrel transmits the driving torque to the bit, while the inner barrel slides over the core during the drilling operation and protects it from the shearing action of the outer rotating core barrel. The inner core barrel remains stationary with respect to the core, and the rotating outer barrel is rotationally load isolated from the inner barrel by means of roller or ball bearings.

Modified Set Diamond Core Bit 16925-1 (7/8-inch core x 5/16-inch kerf). - The maximum granite biotite gneiss penetration rate attained with this bit was 20.6 inches per hour with a rotational speed of 1160 rpm, an axial bit pressure of 411 pounds, and a power expenditure of 2200 watts. Use of these parameters in the empirical formula with a granite K_{pr} of 1.5×10^{-6} reveals a theoretical penetration rate of 13.7 inches per hour. Although the actual penetration rate was higher than the predicted rate, neither is satisfactory for the ten-foot coring device due to the excessive power and bit pressures required.

Modified Impregnated Diamond Core Bit 16925-2 (7/8-inch core x 5/16-inch kerf). - The penetration rates attained with the wide kerf impregnated diamond bit were also unsatisfactory. With marble, a penetration rate of 10.8 inches per hour was attained at a power expenditure of 1500 to 1800 watts. The granite biotite gneiss penetration rate was found to be 7.5 inches per hour.

Conclusions. - It was concluded from the wide kerf bit tests that acceptable penetration rates cannot be attained within the power restrictions of the LEM vehicle. Therefore, the remaining feasibility tests were conducted with the narrow kerf (thin-wall) core bits. Use of this type bit, however, reduced the total cutting area clearance thus prohibiting the use of a double core barrel.

Special Design Narrow Kerf Core Bits

General. - The second series of tests were performed using set diamond, thin-wall bits. The advantages of this type bit are: less driving power required; less axial bit pressure; and reduction of heat generated. The disadvantages of this type bit are: smaller cutting clearances which result in higher frictional loading between the hole wall and core barrel; and the incorporation of a core catcher becomes more difficult.

The driving power for the thin-wall bit feasibility tests was supplied by a nominal 500-watt, 24 vdc motor which was capable of operating within a range of 300 to 1000 watts. The preliminary design for the rotary lunar coring device was designed at a power input level within this range. Typical test results from the thin-wall bit coring tests are presented below.

Thin-Wall Bit No. F62990-4 (1-3/16-inch OD x 1-inch ID). -Two marble penetration rate tests were performed with this bit which resulted in 134 and 135 inches per hour respectively. Bit pressures of 50 pounds, speeds of 1400 rpm and power input levels of 600 to 648 watts were required. These parameters are well within the acceptable limits for the ten-foot coring device.

Subsequent granite biotite gneiss tests with this bit resulted in reasonable penetration rates for a short period of time. At a bit pressure of 50 pounds, rotational speed of 2200 rpm, and power input level of 950 watts, a penetration rate of 60 inches per hour was obtained. However, dulling began to occur after two inches of drilling in the granite biotite gneiss, and the penetration rate dropped to 19, and later to 7 inches per hour. Complete dulling of the diamonds was evident at this time.

Thin-Wall Bit No. F62990-5 (1-3/16-inch OD x 1-inch ID). -Granite biotite gneiss penetration rates were obtained at a lower rotational speed of 1450 rpm, axial bit pressure of 50 pounds, and power input level of 600 watts. The drill rate of 5.9 inches per hour was considered unsatisfactory. The core bit diamonds dulled after two inches of drilling.

Thin-Wall Bit No. F62990-1 (1-5/16-inch OD x 1.120-inch ID). -The rotational speed was reduced to 600 rpm, and the axial bit pressure increased to 300-400 pounds while maintaining a 600 watt power input level. The initial granite biotite gneiss penetration rate was 30 inches per hour, but soon dropped to 7 inches per hour after diamond dulling commenced.

Thin-Wall Bit No. F62990-6 (1.145-inch OD x 1.035-inch ID). -Penetration in granite biotite gneiss was conducted at a rotational speed of 2400 rpm, axial bit pressure of 50 pounds, and input power level of 690 watts. A penetration rate of 30 inches per hour was obtained for the first several inches until the core bit diamonds dulled.

Thin-Wall Bit No. F62990-2 (1-5/16-inch OD x 1.120-inch ID). -A series of high speed tests were performed with this bit using softer materials such as marble and sandstone. A rotational speed of 2650 rpm, axial bit pressure of 48 pounds, and power input level of 600 watts was maintained during these tests. A penetration rate of 76 inches per hour was attained with the sandstone, and 34 inches per hour with the marble. The core bit dulling was much less severe with this material as compared to the granite biotite gneiss.

A series of biotite schist penetration tests were also performed with this bit as a rotational speed of 2620 rpm, axial bit pressure of approximately 50 pounds, and a power input level of 600 watts. Initial penetration rates of 39 to 58 inches per hour were attained. However, bit dulling occurred after four inches of drilling, and the penetration rate decreased rapidly to 6 inches per hour.

Thin-Wall Bit No. T-13951, C-18725-5 and C-18724-6. -A series of tests were conducted using the special design Anton Smit thin-wall bits as tabulated in Table C-7. The three bits are fabricated with impregnated matrices possessing soft, medium soft, and very soft alloyed materials. Again, the core bit matrix materials would not abrade satisfactorily to expose new diamonds, and rapid dulling of the outer layer of diamonds occurred.

Conclusions. -It can be concluded from the initial thin-wall bit feasibility tests that satisfactory penetration rates can be obtained within the power limitations of the LEM vehicle providing the diamonds remain sharp. However, diamond dulling occurs within the first several inches of drilling in the harder materials such as biotite schist and granite biotite gneiss, thus reducing the penetration rate to an unacceptable level. The best penetration rates were obtained at the higher rotational speeds with nominal axial bit pressures.

The initial lunar coring device was designed with the above parameters incorporated. However, the feasibility tests subsequently demonstrated that the pure rotary diamond approach would not be usable within the restrictions of a lunar operation.

FEASIBILITY CORING TESTS

Tables C-1 and C-2 include the results of the standard, wide kerf coring bit feasibility tests. Tables C-3 through C-7 include the results of the initial thin-wall bit feasibility tests.

TABLE C-1. TEN-FOOT LUNAR CORING DEVICE FEASIBILITY TESTS

Type of Test: Drill Bit Penetration
 Drill Motor: B&D Experimental 2.5 HP, 115 VAC
 Material Tested: Granite Biotite Gneiss
 Coring Bit Data: Trucon #16925-1 (Set Diamond) Modified Standard EXM (New)
 Date & Place of Test: 4-5 December 1964, B&D Laboratory

Test No.	Remarks	Bit Press. Lbs.	Motor				Coolant Air				Bit Temp °F	Drill Rate In/Hr
			Volts	Amps	Watts	RPM	PSI	CFM	Temp In °F	Temp Out °F		
1	Motor No-Load Test (Low Speed)	N/A	115	8.0	800	920	10	3.3	82	82	N/A	N/A
2	Motor No-Load Test (High Speed)	N/A	115	9.2	960	1760	10	3.3	82	82	N/A	N/A
3	Drill Penetration	185	115	10.4	1120	500	10	3.4	82	100	130	None
4	Repeat #3 With Increased Bit Pressure	335	115	12.4	1380	483	10	3.3	82	113	200	4.4
5	Repeat #4 With Increased	335	115	17.0	1880	1190 to 1220	10	3.1 to 1.7	82	125	400	8.8

TABLE C-1. TEN-FOOT LUNAR CORING DEVICE FEASIBILITY TESTS (Cont.)

Test No.	Remarks	Bit Press. Lbs.	Motor			RPM	Coolant Air			Bit Temp °F	Drill Rate in/Hr
			Volts	Amps	Watts		PSI	CFM	Temp In °F	Temp Out °F	
6	Repeat #5 With Increased Bit Pressure	411	115	20.0	2000	1160	10	3.3 to 1.4	82	142	20.6
7	Repeat #6	411	115	20.5	2200	1120	10	3.3 to 1.4	82	145	16.9
8	Decrease RPM and Increase Bit Pressure	690	115	17.0 to 18.0	1850 to 1950	400 to 417	10	3.1 to 0.9	82	140 to 145	13.2
9	Increase Air Flow Rate	690	115	17.0 to 18.0	1800 to 1900	408	20	18.7	78	125	7.02

- Notes:
1. Bit temperature measured immediately upon removal from hole.
 2. Test indicates that standard type bit (1.460"O.D. x 845" I.D., 5/16" kerf) requires too much pressure and power for ten-foot lunar coring device.
 3. Diamonds showed evidence of polishing.

TABLE C-2. TEN-FOOT LUNAR CORING DEVICE FEASIBILITY TESTS

Type of Test: Drill Bit PenetrationDrill Motor: B&D Experimental 2.5 HP, 115 VACMaterial Tested: Granite, Biotite Gneiss and MarbleCoring Bit Data: Truco #16925-2 (Impregnated Diamond) Modified Standard EXM (New)Date & Place of Test: 7 December 1964

Test No.	Remarks	Bit Press. Lbs.	Motor				Coolant Air			Bit Temp of	Drill Rate In/Hr
			Volts	Amps	Watts	RPM	PSI	CFM	Temp In °F	Temp Out °F	
1	Penetration Test in Granite Biotite Gneiss	678	115	15.0 to 16.0	1600 to 1700	455 to 430	20	20.5 to 17.5	78	114	7.5
2	Penetration Test in Marble	778	115	17.0 to 14.0	1800 to 1500	410 to 418	20	19.0 to 7.8	89	117 to 120	10.8

Notes: 1. Penetration rate less with impregnated diamond as compared to set diamond standard bits. Neither is satisfactory for ten-foot lunar coring device.

TABLE C-3. TEN-FOOT LUNAR CORING DEVICE FEASIBILITY TESTS

Type of Test: Drill Bit Penetration
 Drill Motor: B&D Experimental 24 VDC, 20 AMPS
 Material Tested: Granite Biotite Gneiss
 Coring Bit Data: Trusco #F62990-5 Diamond Thin Wall - 1-3/16"O.D. x 1" I.D. (New)
 Date & Place of Test: 18 December 1964, B&D Laboratory

Test No.	Remarks	Bit Press. Lbs.	Motor			Coolant Air			Bit Temp °F	Drill Rate In/Hr
			Volts	Amps	Watts	RPM	PSI	CFM	Temp In °F	Temp Out °F
1	Motor No-Load Test	N/A	24.0	12.0	288	1500	19	14.0	73	73
2	Initial Penetration Test (Electrical Load Held Constant at 25 AMT)	50	24.0	25.0	600	1450	20	12 to 15	73	79
									N/A	N/A
									100	5.9

Notes: 1. Diamonds showed evidence of polishing. Granite Biotite Gneiss testing discontinued until motor can be regreared for slower RPM and increased bit pressure.
 2. Bit temperature measured immediately upon removal from hole.

TABLE C-4. TEN-FOOT LUNAR CORING DEVICE FEASIBILITY TESTS

Type of Test: Drill Bit PenetrationDrill Motor: B&D Experimental - 24 VDC, 20 AMPSMaterial Tested: MarbleCoring Bit Data: Truco #F62990-4 Diamond Thin Wall - 1-3/16" O.D. x 1" I.D. (New)Date & Place of Test: 18 December 1964, B&D Laboratory

Test No.	Remarks	Bit Press. Lbs.	Motor				Coolant Air				Bit Temp °F	Drill Rate In/Hr
			Volts	Amps	Watts	RPM	PSI	CFM	Temp In °F	Temp Out °F		
1	Penetration Test	50	24.0	27.0	648	1400	20	12	73	77	100	135
2	Repeat Test #1	50	24.0	25.0	600	1415	20	13	73	79	100	134

Notes: 1. Bit Temperature measured immediately upon removal from hole.
 2. Penetration rate equivalent to 90 feet in 8 hours with this material.

TABLE C-5. TEN-FOOT LUNAR CORING DEVICE FEASIBILITY TESTS

Type of Test: Drill Bit Penetration

Drill Motor: B&D Experimental - 24 VDC, 20 AMPS

Material Tested: Granite Biotite Gneiss

Coring Bit Data: See Remarks Section

Date & Place of Test: 11 January 1965, B&D Laboratory

Test No.	Remarks	Bit Press. Lbs.	Motor				Coolant Air			Bit Temp °F	Drill Rate In/Hr
			Volts	Amps	Watts	RPM	PSI	CFM	Temp In °F	Temp Out °F	
1	No Load Test	N/A	24	12	288	1550	-	-	-	-	-
2	Penetration Test Truco #F62990-5 (1-3/16" O.D. x 1" I.D.)	50	24	25	600	1450	-	-	-	-	6
3	Penetration Test Truco #F-62990-4 (1-3/16" O.D. x 1" I.D.)	50	38	25	950	2200	-	-	-	-	60
4	No Load Test	N/A	26	5.5	143	3750	-	-	-	-	-
5	Penetration Test Truco #F62990-4	50	26	25	650	2900	-	-	-	-	19
6	Repeat #5	50	23	30	690	2200	-	-	-	-	7
7	Truco #F-62990-6 (1.145" O.D. x 1.035" I.D.)	50	23	30	690	2400	-	-	-	-	30

TABLE C-5. TEN-FOOT LUNAR CORING DEVICE FEASIBILITY TESTS (Cont.)

Test No.	Remarks	Bit Press. Lbs.	Motor				Coolant Air			Bit Temp °F	Drill Rate In/Hr
			Volts	Amps	Watts	RPM	PSI	CFM	Temp In °F	Temp Out °F	
8	No Load Test	50	24	8	190	350	-	-	-	-	-
9	Truco #F-62990-1 (1-5/16" O.D. x 1.120" I.D.)	300- 400	24	25	600	280	-	-	-	-	30
10	Repeat #9	300 - 400	24	25	600	280	-	-	-	-	7

Notes: Granite Biotite Gneiss penetration rates acceptable during tests #3, #7, and #9. However, bits tended to dull too rapidly.

TABLE C-6. TEN-FOOT LUNAR CORING DEVICE FEASIBILITY TESTS

Type of Test: Drill Bit Penetration

Drill Motor: B&D Experimental - 24 VDC, 20 AMPS

Material Tested: See Remarks Section

Coring Bit Data: Truco #F-62990-2 - 1-5/16" O.D. x 1.120" I.D.

Date & Place of Test: 21-22 January 1965, B&D Laboratory

Test No.	Remarks	Bit Press. Lbs.	Motor			Coolant Air			Bit Temp °F	Drill Rate In/Hr
			Volts	Amps	Watts	RPM	PSI	CFM	Temp In °F	Temp Out °F
1	No Load Test	N/A	24	9.5	228	3100	-	-	-	-
2	Biotite Schist Penetration	48	24	25	600	2620	20	10	-	-
3	Sandstone Penetration	48	24	25	600	2650	20	10	-	-
4	Marble Penetration	48	24	25	600	2620	20	10	-	-
5	Biotite Schist Penetration	48	24	25	600	2620	20	10	-	-
6	Biotite Schist Penetration	53	24	30	720	2480	20	10	-	-
7	Biotite Schist Penetration	55	24	35	840	2300	20	10	-	-
8	Biotite Schist Penetration	58	24	40	960	2150	20	10	-	-
9	Biotite Schist Penetration	48	24	25	600	2440	20	10	-	-

Notes: Penetration rates acceptable while coring sandstone and marble with very little dulling of core bit. However, the bit dulling rate was excessive in the Biotite Schist after 2 or 3 inches of drilling.

TABLE C-7. TEN-FOOT LUNAR CORING DEVICE FEASIBILITY TESTS

Type of Test: Drill Bit Penetration - Shallow Hole Tests
 Drill Motor: B&D Experimental - 24 VDC; 20 Amps
 Material Tested: Biotite Schist
 Coring Bit Data: Anton-Smit Co. New York (See Notes)
 Date & Place of Test: 3 February 1965, B&D Laboratory

Test No.	Remarks	Bit Press. Lbs	Motor			Coolant Air			Bit Temp of F	Drill Rate In/Hr
			Volts	Amps	Watts	RPM	PSI	CFM	Temp In of F	Temp Out of F
1	1 1/4" Bit T-13951	100	24	20-25	480-600	625	20	5		8.4
2	1 1/4" Bit T-13951	180	24	25-30	600-720	600	20	5		18.7
3	1 1/4" Bit T-13951 (Speed too high for effective cutting)					2200				
4	1 1/4" Bit T-13951	60	24	15	360	330	20	5		16.0
5	1 1/4" Bit C-18725-5	175	24	30-35	720-840	550	20	5		34.0
6	1 1/4" Bit C-18725-5	175	24	40	960	500	20	5		26.2
7	1 1/4" Bit C-1825-5	175	24	35-40	840-960	560	20	5		18.7

TABLE C-7. TEN-FOOT LUNAR CORING DEVICE FEASIBILITY TESTS (Cont.)

Test No.	Remarks	Bit Press. Lbs	Motor			Coolant Air			Bit Temp °F	Drill Rate In/Hr
			Volts	Amps	Watts	RPM	PSI	CFM	Temp In °F	Temp Out °F
8	C-18725-5 (Resharpened)	175	24	35-45	840-1080	560	20	5		20.6
9	C-18725-5 (Resharpened)	60	24	11-20	264-480	280	20	5		16.0
10	C-18725-5 (Resharpened)	140	24	20	480	280	20	5		8.4
11	1 1/4" B17 C-18724-6	60	24	15	360	330	20	5		10.3
12	1 1/4" B17 C-18724-6	80	24	15-20	360-480	300	20	5		8.4
13	1 1/4" B17 C-18724-6	100	24	20-25	480-600	650	20	5		8.4

- Notes: 1. Core Bit T-13951 Thin-Wall Diamond, Soft Impregnated Matrix, 60-80 grit
2. Core Bit C-18725-5 Thin-Wall Diamond, Medium Soft Impregnated Matrix, 30-40 grit
3. Core Bit C-18724-6 Thin-Wall Diamond, Very Soft Impregnated Matrix, 60-80 grit
4. Performance of C-18725-5 was satisfactory when sharp. Matrix material did not abrade sufficiently to expose new diamonds.

APPENDIX D

PRELIMINARY DESIGN PARAMETERS FOR ROTARY CORING DEVICE

Several design approaches for the mechanization of the initial lunar coring device were studied. The primary factors governing the preliminary design approach included reliability, astronaut dexterity and handling capability, available power, weight, and the preliminary results of the coring bit feasibility tests. A brief discussion of the three major design categories (refer to Figure D-1) which could be utilized for the coring device is presented below.

Direct Drive Device

The simplest, and perhaps the most reliable, approach to the design of the coring device would be to mechanize the technique employed in standard commercial, hand-operated drilling machines. With this approach, the driving motor would be mounted to a vertical column approximately thirty (30) inches in length. A low rpm, high torque gear and slip clutch assembly would be employed to drive the motor vertically on the geared column. The motor would then drive the drill rods and core barrel down through the lunar surface while simultaneously providing the required rotation for effective drilling.

The major disadvantages of this technique are, 1) the maximum depth of continuous drilling is limited by the length of the vertical drive column, and 2) the astronaut would be required to add new sections of drill rod each time the motor completes a vertical translation along the drive column. The uncoupling of the original drill rod, and coupling of the new drill rod would be required at ground level which would be extremely difficult for the spacesuited astronaut.

Continuous Feed Device

A more complicated approach to the design of the coring device would be to incorporate a continuous feed mechanism. With this arrangement, the motor would remain stationary near the ground level of the device, and its mechanisms would be capable of driving and rotating the drill rods and core barrel down through the lunar surface. The major advantage with this technique is that the coupling or uncoupling of drill rod sections could be accomplished at waist level by the astronaut, rather than at the ground level required by the previously described method. The disadvantage with this method is that a drive means (gear teeth, spiral, etc.) must be machined into the core barrel or drill rods. This, in turn, would result in heavier drill rods, and a wider kerf coring bit would be required in order to obtain the required clearance in the subsurface hole for the thick-wall drill rods. The feasibility tests have shown that the wide kerf coring bits cannot be used within the electrical power limitations of the LEM spacecraft.

Intermittent Feed Device

The intermittent feed technique represents a compromise between the two previously described methods. With this approach, a vertical drive column would be employed to allow vertical translation of the drive motor. However, the drill rod driving mechanism would be located in such a manner that coupling and uncoupling could be accomplished from the top of the device (waist level) rather than at ground level. A one-way clutch and drive device can be incorporated which will enable the thin-wall

ER 13952

core barrel and drill rods to be rotated and driven into the lunar surface. Therefore, the need for a geared or screw feed system machined into the core barrel is eliminated.

The preliminary design for the rotary lunar coring device incorporated the intermittent feed technique. The core barrel and drill rods would be sectioned into thirty (30) inch segments for compatibility with the LEM stowage compartment. The core barrel and first drill rod would be assembled and "fed" into the driving mechanism of the coring device. During each drilling cycle the motor would initially start at the top of the vertical drive column. Upon actuation, the one-way clutch and drive device would "clamp" the drill rod, and the entire motor assembly would traverse vertically down the drive column while simultaneously rotating and applying axial pressure to the drill rods. The driving motor would automatically stop at the end of its vertical traverse (approximately 30 inches). Breakage of the rock core, reverse vertical traverse of the drive motor, and removal of the 30 inch core would require the attention of the astronaut. The core barrel and drill rod would then be inserted back into the subsurface hole, another 30 inch drill rod would be coupled, and another cycle initiated. Four such cycles would be required to attain a total depth of ten feet.

The coring device will incorporate a low speed, high torque gear and slip clutch assembly for traversing the vertical drive column. Use of an adjustable slip clutch will allow the axial bit pressure to adjust automatically with the hardness of the material being drilled. A maximum unrestrained vertical traverse of approximately eleven inches per minute will be attainable for core extraction. Two rotational speeds of 2400 rpm and 600 rpm will be provided for the coring operation. The motor will operate at an approximate power level of 600-800 watts, with a basic rotational speed of 12,000 rpm. The drive motor, clutch mechanisms, and vertical drive column will be restrained by a tripod frame anchored to the lunar surface.

Subsequent feasibility tests using diamond core bits revealed that the rotary technique was not feasible for lunar application. The rotary diamond study was discontinued, and the remainder of the program devoted to rotary-percussion coring.

ER 13952

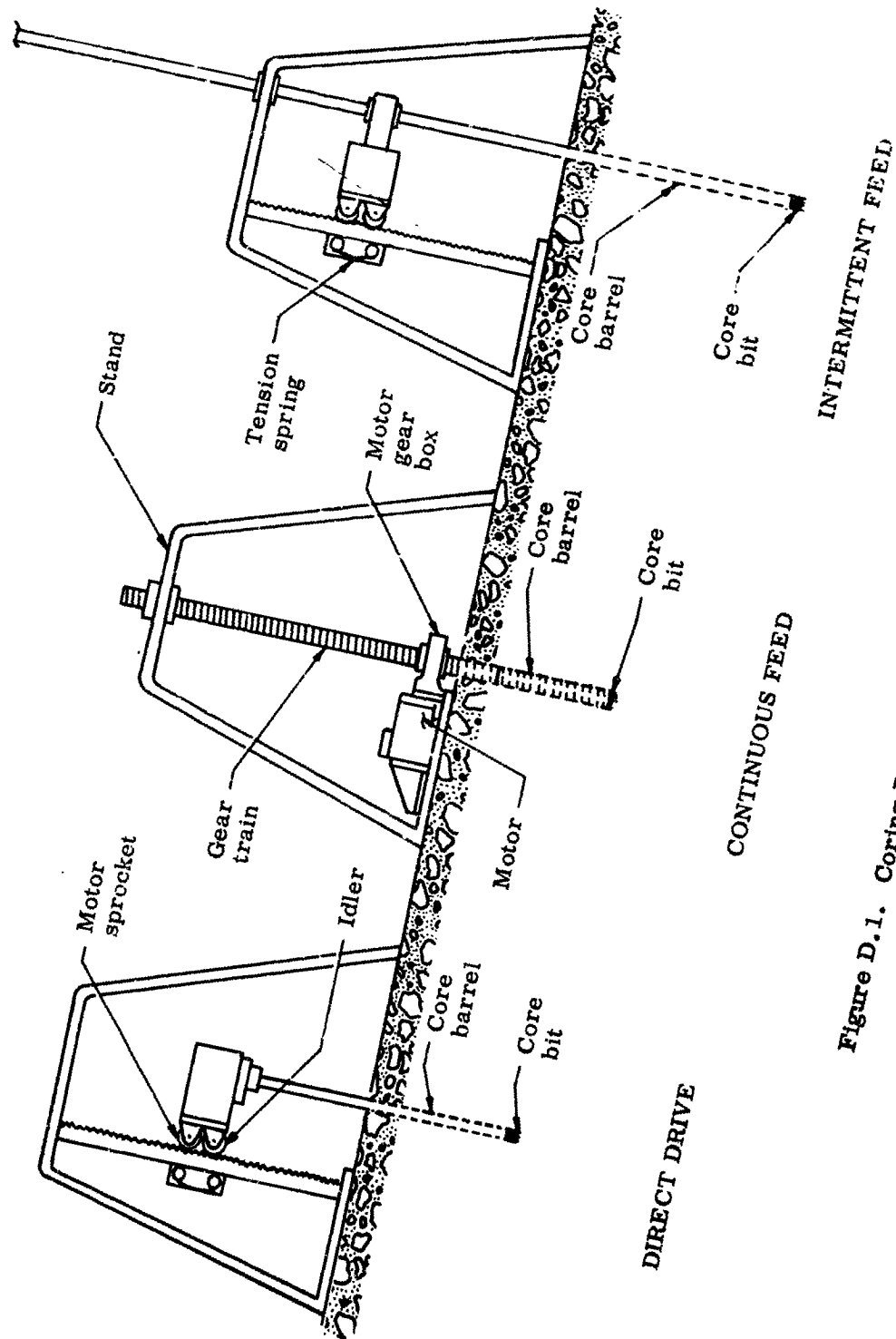


Figure D.1. Coring Device Design Approaches

APPENDIX E - PRIME MOVER SYSTEMS

Gas Turbine. -The possibility of excess aerazine 50 fuel remaining in the LEM descent stage after landing on the moon warrants the evaluation of a gas turbine as a power source for the lunar coring device. This fuel would normally be abandoned upon take-off of the ascent stage for return to the Apollo spacecraft. The fuel consists of a mixture of 50 percent hydrazine and UDMH (Unsymmetrical Dimethyl Hydrazine). There is also a quantity of oxidizer available at a ratio of 1.6:1 to the residual fuel. If this nitrogen tetroxide oxidizer is used at approximately a one to one ratio, the gases generated will be at a cooler temperature.

The temperature may be held to approximately 2110° R and a turbine designed for 1200° R exhaust to supply from .06 to .08 HP per hour per pound of fuel. At approximately 0.5 HP required per hour for the lunar drill, 6.7 pounds of fuel per hour or 47 to 50 pounds of fuel total would be required for a seven-hour mission.

The possibility of using residual fuel located in the LEM descent stage may warrant additional study effort. The high temperature gases could possibly be expanded and cooled to lower temperatures before blowing into the drill cavity for cleaning and cooling of the bit. A dual injection piston type motor using equal parts of aerazine and nitrogen tetroxide timed for injection at piston top dead-center may be possible with proper cooling. However, any process involving hypergolic burning of aerazine fuel and an oxidizer is not recommended if the astronaut must work in the immediate vicinity of the exhaust gases.

Pneumatic or Steam Drive Motor. -Use of a pneumatic power unit would provide exhaust gas to blow chips out of the drilled hole and for cooling of the diamond bit. The use of steam as an energy source is not desirable because the drilling debris is a rock flour material which may jam the drill should water from the saturated steam wet this material. Consequently, steam type power units will not be considered in this discussion.

Similarly, a standard internal combustion engine must be eliminated because of uncertain starting characteristics. Fuel and oxygen would become additional weight items to a 5 to 7 pound per horsepower engine. Engine cooling gas would be required to blow chips from the drill and cool the bit. This would require large radiation heat exchanger surfaces. The overall weight accumulation greatly exceeds that for fuel cell power.

Pneumatic power might be generated from cryogenic gas heated and expanded in a pressure vessel receiving heat from the sun.

The gas quantity, Q , per second, corresponding to a required output work of 286 watt-hours of power may be determined from turbine requirements. A power turbine using a gas of 30 psia, and possessing a 35% efficiency factor is possible with careful design. A gas nozzle efficiency of 98% is feasible, and a pressure drop down-steam of 50% may be used for maximum flow of gas. A brief analysis of this system is presented below. The conclusions drawn from this estimation of probable parameters indicate that solar heat is insufficient by itself to provide the necessary heat energy. If a supplemental heat source were to be supplied, the weight of necessary hardware configurations exceeds the LEM power source weight. This system is therefore not recommended.

ER 13952

Turbine Power Drive Analytical Model

$$\text{Turbine power required} = 286 \times \frac{2656}{3600} = \frac{\text{ft-lb}}{\text{sec}} = 231$$

turbine gas flow: -

$$P = 30 \text{ lb} = P/2 ; P = 60 \text{ psia required}$$

$$\text{Flow thru nozzle } Q_n = .98 \times A \left(\frac{2 \times 30}{\rho} \right)^{1/2} = \frac{7.6A}{\rho^{.5}} \text{ area} \times \text{volume}$$

ρ at 4 grams/sec (estimate for job)

$$\rho = 4 \times \frac{2.205}{32.2} \times 10^{-3} = 2.74 \times 10^{-4} \text{ lb/sec}$$

$$\rho^{.5} = .01655 \text{ slugs}$$

If the area of the nozzle is designed for .005 ft²

$$q_n \text{ per second} = \frac{7.6 \times .005}{.01655} = 2.29 \frac{\text{ft}^3}{\text{sec}}$$

$$q_{\text{turbine}} = \frac{2.29}{.35} = 6.36 \frac{\text{ft}^3}{\text{sec}} \text{ from } 8.82 \times 10^{-3} \frac{\text{lb}}{\text{sec}} \text{ gas.}$$

If helium were used,

Helium at the critical state:

$$+ 9.8^\circ\text{R } h = 12.25 \text{ Btu/lb}$$

$$2.26 \text{ atmospheres} = 29.4 \text{ psia}$$

$$.231 \text{ cu ft per lb}$$

$$\text{Heat capacity of helium at } 168^\circ\text{R} \approx 14.7 \text{ psi}$$

$$= 1.25 \text{ Btu/lb/}^\circ\text{F}$$

Helium supply

$$\frac{14.7 \times 144 \text{ }^\circ\text{R}}{168} = \text{vol/lb} \quad \frac{29.4 \times 144 \times .231}{9.8}$$

ER 13952

$$= \frac{29.4 \times 144 \times .231}{9.8} \times \frac{168}{14.7 \times 144} = .791 \text{ cu ft/lb}$$

$$n_1 = C_p (T_1) = 1.25 \times 168 \\ = 210 \text{ Btu/lb}$$

Pressure 29.4 psia

$$2.74 \times 10^{-4} \text{ lb/sec}$$

$$T = 168^\circ\text{R}$$

$$v = .791 \text{ ft}^3/\text{lb}$$

Required pressure is 60 psi.

$$\text{Required } V = 6.36 \text{ ft}^3/\text{sec}$$

$$8.82 \times 10^{-3} \text{ lb/sec}$$

$$T_2 = \frac{P_2 V_2 T_1}{P_1 V_1} = \frac{60 \times 6.36 \times 168}{14.7 \times 791}$$

$$T_2 = 551^\circ\text{R} \text{ temperature required at nozzle}$$

Total solar input to a point at spec. latitude (sun radiant heat) (Ref. 41)

$$E_o = 1.37 \times 10^6 \text{ ERGS/cm}^2/\text{sec} = 0.1205 \text{ Btu/ft}^2/\text{sec}$$

A fan should be used to improve heat conduction-convection and storage to maintain 551°R. A preheater for the supply gas would be advisable so as to assist the process of energy storage from the sun's rays.

Available energy from the sun for a 45° angle of the total is

$$E_o \text{ max} = 1.37 \times 10^6 \text{ erg/cm}^2/\text{sec} \times \frac{337}{375}$$

$$\frac{T_{45^\circ}}{T_{\text{equator}}} = \frac{337}{375} \text{ (Ref. 41)}$$

$$E_o = .1085 \text{ Btu/ft}^2/\text{sec for } 45^\circ \text{ Radian.}$$

ER 13952

If conduction and convection resistance is $R = \frac{L}{KA} = 2.5$

$$\text{Estimated } q = \frac{\Delta t}{R} = \frac{551 - 168}{2.5} = 153 \text{ Btu/sec/ft}^2$$

$$q_{\text{storage}} = \rho C_p V \frac{\Delta t}{\Delta \tau}$$

$$q_{\text{storage}} = 2.74 \times 10^{-4} \times 1.2 \times 383 \\ = .126 \text{ BTU/Sec for helium.}$$

$$h_2 - h_1 = c_p (T_2 - T_1) w \quad \text{Ref. 62}$$

$$h_2 = 1.2 \times 551 \times 2.74 \times 10^{-4} \\ = 2.41 \text{ BTU}$$

$$h_1 = 210 \times 2.74 \times 10^{-4} = .0575$$

$$h_2 - h_1 = 2.3525$$

$$q = 2.3535 \quad \text{Heat that must be absorbed.}$$

$$\frac{2.3525}{.126} = 18.65 \text{ times as much required heat as can be stored (approximately)}$$

Solar heat alone is not adequate using helium gas.
It could be supplemented with electrical or chemical heat if such a design were to become necessary.

Electric Motor Systems. -An analysis of general AC and DC electric motor systems must be conducted in order to determine their relative efficiencies operating from the basic LEM DC power source at various radii from the vehicle.

The DC electric motor systems exhibit many inherent characteristics which are readily adaptable to operation directly from the basic LEM power source. The primary advantage is that a DC motor can be designed for direct operation from the power source without the requirement for additional power conversion equipment. Any associated equipment required for power conversion will result in power losses, weight increases, and additional complexity which must be compared with the advantages to be gained by its employment.

Preliminary information regarding the characteristics and capabilities of the LEM power source indicate that the available power allocated to the lunar drill system will be limited, and output voltage levels may fluctuate over a wide range. These factors further increase the desirability of a simple DC system.

The primary advantage of an AC system is that the equipment weight may be less than that for a comparable DC system if the operating distance from the power source to its utilization point is relatively long. The DC voltage would be converted to a relatively high AC voltage at the fuel cell by use of an inverter, and transmitted over a light power cable to the drill motor. Use of a low voltage DC motor requires higher line currents and heavier cables in order to transmit the same power load as the higher voltage AC system. Therefore, the additional inverter weight and power loss of the AC system must be compared to the higher line weight of the DC system in order to determine relative efficiencies.

Four motor systems were selected for this analysis, one of which will approximate the operating parameters of the final design for the lunar coring device. These representative systems include:

- 26VDC Motor (3,800: 200 rpm, low speed)
- 26VDC Motor (28,000: 200 rpm, high speed)
- 208V, 400 CPS, 3-Phase Delta Motor (3,800: 200 rpm, low speed)
- 208V, 400 CPS, 3-Phase Delta Motor (28,000: 200 rpm, high speed)

The 208V, 400 CPS, 3-Phase Delta system was chosen to represent the AC systems analysis because its power-density efficiency is greater than the lower 30, 50, and 60 CPS AC systems.

A constant LEM power source output of 26VDC at 500 watts (0.67 horsepower) was assumed as the input for each system. The objective of the analysis was to determine the power-weight transfer efficiency (HP per pound of system weight) of each system with the lunar drill located at various distances from the LEM vehicle.

Table E-1 (DC and AC Motor Systems Equipment) itemizes the equipment and parameters used during the analysis of each of the four motor systems, including weights, efficiencies, and power losses. Figure E-1 (DC and AC Motor Systems Weight) illustrates the weight of each motor system (excluding drill support frame, core barrels, etc.) operating at various distances from the LEM vehicle. The increasing weight with increasing operating distances results from the weight of the power cables for all systems, and slight changes in motor design with the DC systems

to compensate for the relatively large line losses. Figure E-2 (DC and AC Motor Systems Power Output) illustrates the actual horsepower delivered to the drill by each system operating with an input of 500 watts (0.67 horsepower) from the LEM power source. This graph reveals that the DC low speed system is the most efficient (exclusive of weight) for operating distances up to approximately 400 feet. This distance represents the efficiency cross-over point, and the AC low speed system becomes more efficient for distances greater than 400 feet.

Figure E-3 (DC and AC Motor Systems Power Density) is a normalization of Figures E-1 and E-2, illustrating the horsepower delivered to the lunar drill per pound of system weight. The DC low speed system is again shown to be the most efficient for distances up to 350 feet. However, the power losses in both systems at the 350-400 foot range represent nearly half of the total power delivered by the LEM fuel cell. This relatively large power loss would probably be unacceptable for the lunar coring device application. Operating ranges of the order of 0 to 100 feet appear more appropriate, unless subsequent analysis reveals that a self-contained power source is feasible.

As a result of this analysis, the following conclusions can be made:

1. A DC low speed motor system is recommended for the lunar coring device within the weight and power restrictions of the LEM vehicle. However, this preliminary analysis is based on an assumed output rotational speed of 200 rpm. It is possible that the recommended basic motor rpm for the final model may differ somewhat from the 3,800 rpm used in this analysis, depending on the results of the optimum rotation speed feasibility drilling tests.
2. In order to minimize power losses, the operating radius of the coring device should not exceed approximately 100 to 150 feet. This can be defined more accurately upon completion of the coring feasibility and power requirement tests.

Equipment Parameters	Motor System		
	Low Speed-DC	High Speed-DC	Low Speed-AC
LEM Power Source	500 (.67 HP)	500 (.67 HP)	500 (.67 HP)
Output-Watts			
Three-Phase Inverter	N/A	N/A	208, 3 ϕ - Δ
Output Voltage	N/A	N/A	7.95
Weight-Pounds	N/A	N/A	0.73
Efficiency			
Inverter Cooling Pump			
Weight-Pounds	N/A	N/A	4.8
Power-Watts	N/A	N/A	20
Power Cable	2 wire, #6	2 wire, #6	3 wire, #14, 1 wire, #20
Type	Aluminum	Aluminum	Aluminum
Weight-Pounds	51 lbs/1000 ft	51 lbs/1000 ft	14,493 lbs/ 1000 ft.
Resistance-Each Wire	0.648 Ω /1000 ft	0.648 Ω /1000 ft	4.14 Ω /1000 ft
Drill Motor	DC, 3800 rpm	DC, 28,000 rpm	AC, 3800 rpm
Weight-Pounds	11.5 to 15.0	2.4 to 2.9	11.8
Efficiency	0.87	0.73	0.89
Gear Box	2-Stage	5-Stage	2-Stage
Step-Down Ratio	19	144	19
Weight-Pounds	2.7 to 3.0	4.0 to 7.5	2.8
Efficiency	0.95	0.73	0.905
Motor Cooling Pump			
Weight-Pounds	4.0 to 4.3	4.6 to 5.4	4.2
Power-Watts	20	20	20
Miscellaneous Fittings			
Weight-Pounds	1.3	1.3	0.9

Table E-1. DC and AC Motor Systems Equipment

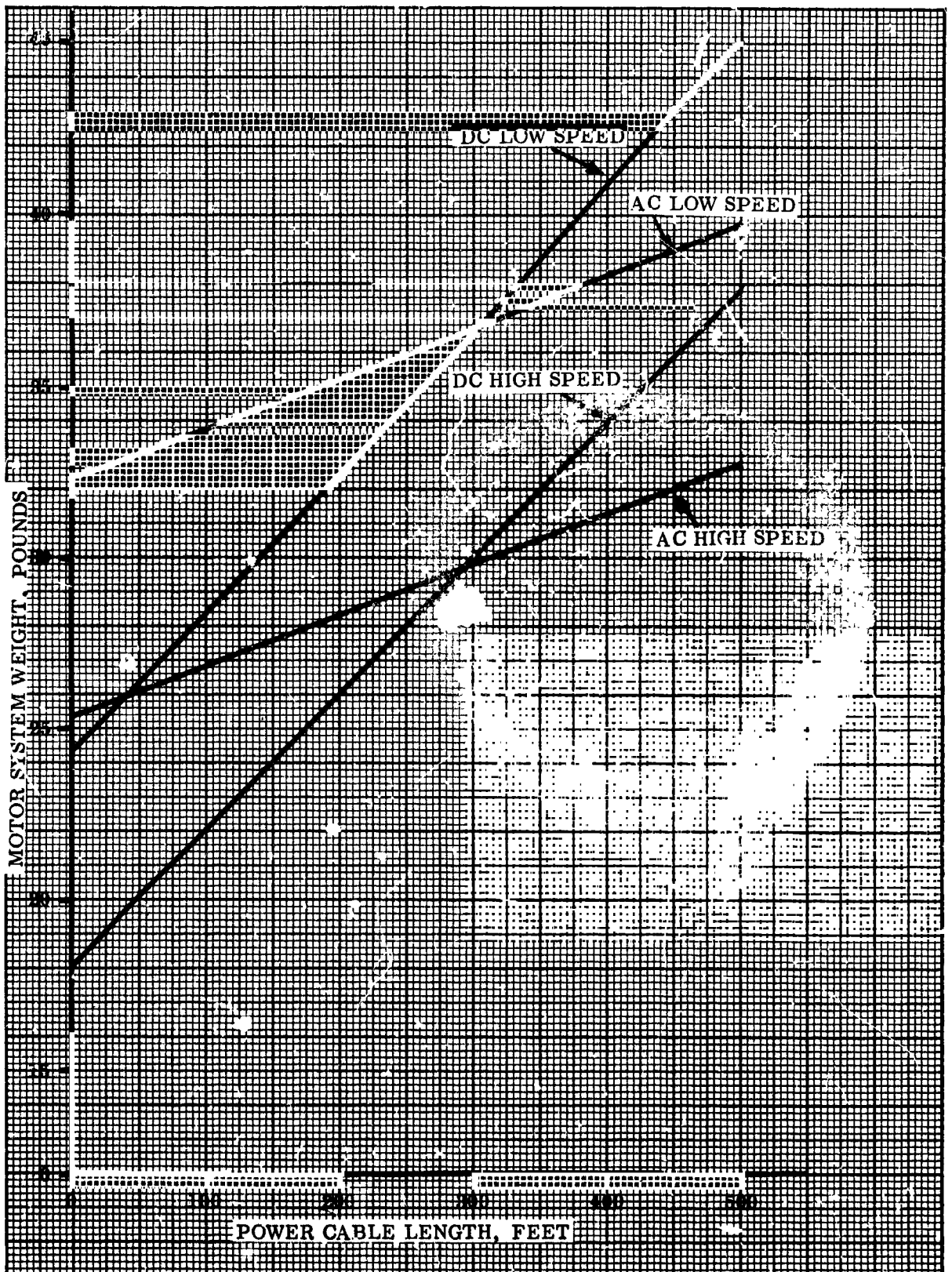


Figure E.1. DC and AC Motor Systems Weight

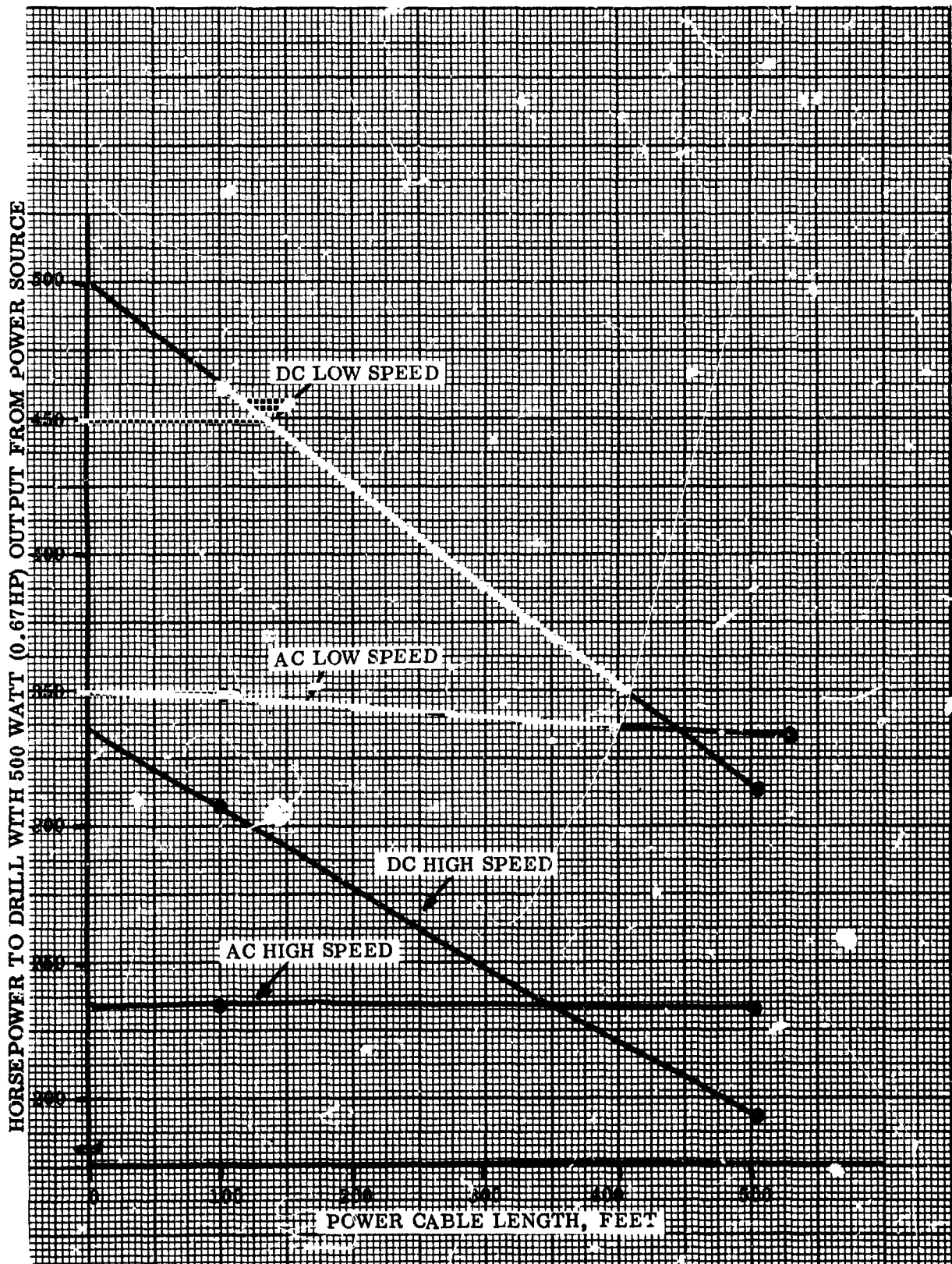


Figure E.2. DC and AC Motor Systems Power Outputs

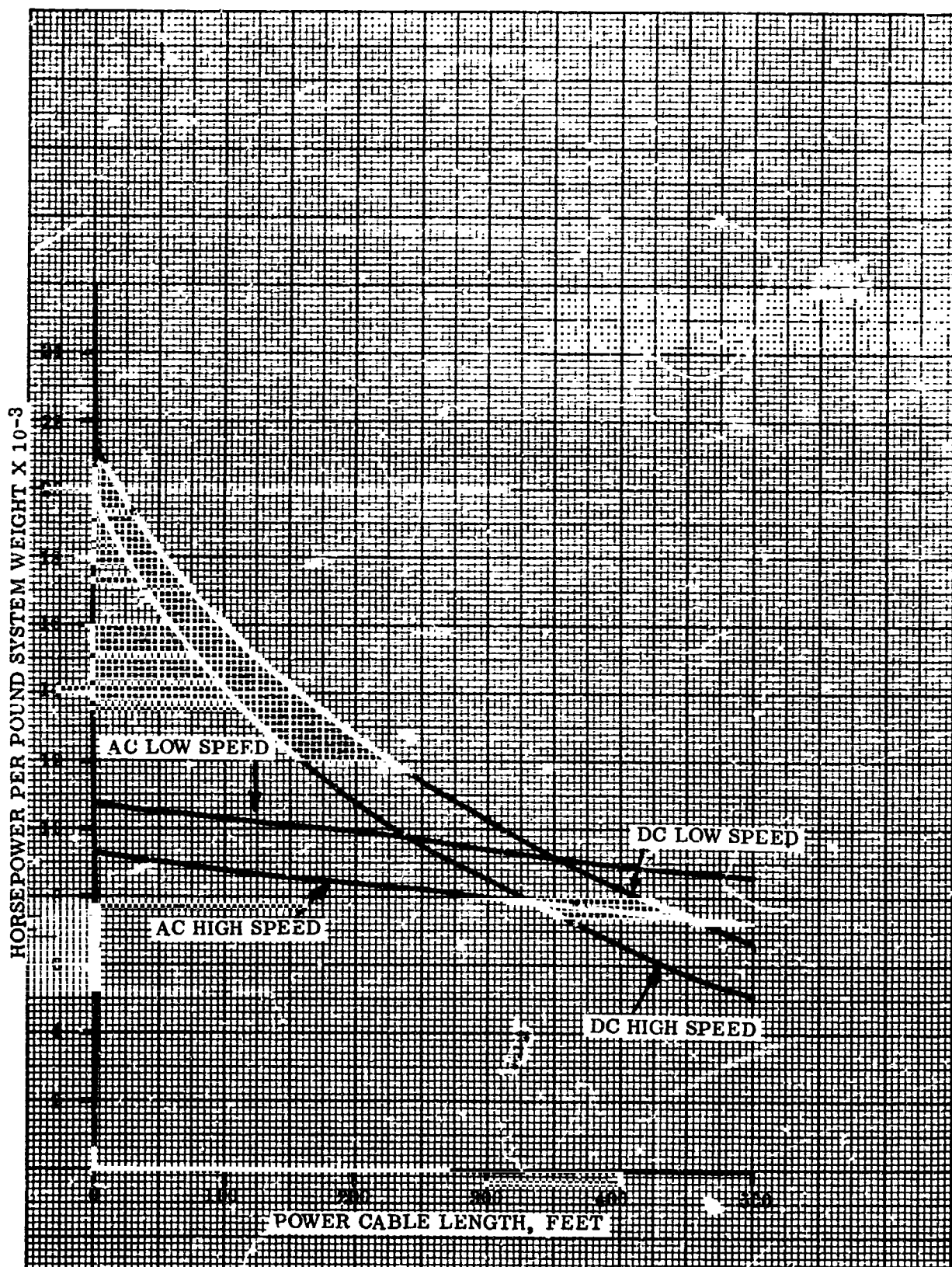


Figure E.3. DC and AC Motor Systems Power Density

APPENDIX F - SELF-CONTAINED ELECTRICAL POWER SOURCES

Operation of the lunar coring device from the LEM power source presents obvious restrictions on the operating radius and available drilling time. The incorporation of a self-contained power source would alleviate these restrictions if the additional penalties incurred are not prohibitive. Based on current and previous analyses of various space systems, potential power sources are reviewed below.

Power supplies can be generally classified into two categories: 1) chemical reaction systems which are time-limited and rated in kilowatt hours, such as batteries, fuel cells and chemical dynamic systems; and 2) continuous heat sources which are not restrictively time-limited, such as solar concentrators, radioisotopes, and nuclear systems. These, together with energy conversion systems, such as the photovoltaic devices, are generally employed in applications requiring operating times greater than a month.

Figure F-1 (Power System Selection Curves) illustrates the general power output range and operating times for which the various power sources can most efficiently be employed. Other power source selection criteria are based on weight, ease of integration with other systems, simplicity and reliability, and growth potential.

Batteries. -The simple battery is a desirable power source choice for applications of relatively short durations and modest power demands, such as the lunar coring device. The battery exhibits a maximum in reliability, while requiring a minimum of checkout time, possesses a relatively long shelf life, and does not require a thermal radiator in the spatial environment. Figure F-2 (Power Density of Battery Systems) illustrates the relative weights for various types of batteries. The nickel-cadmium and silver-cadmium batteries are somewhat heavier, but their potential recharge cycles are greater than the lighter weight silver-zinc batteries. However, the lunar coring device battery would require few, if any, recharges on the lunar surface and the silver-zinc battery would be adequate.

A typical silver-zinc battery system applicable for the lunar coring device could consist of four (4) parallel sets of fourteen (14) series connected Electric Storage Battery Company SS-25B cells. The power density of these cells, encapsulated and sealed for the lunar environment, is 37 watt-hours per pound. The system would be rated at 24 vdc, with a total power capacity of 2100 watt-hours. The package would occupy approximately 0.6 cubic feet and would weigh 70 pounds.

Low discharge rate silver-zinc batteries are currently available which possess power densities of 100 watt-hours per pound. Although these batteries are not currently usable with the lunar coring device, projected technical advances with high discharge rate cells are anticipated to obtain power densities of 50 watt-hours per pound. This would allow a weight reduction of the 2000 watt-hour battery to the 40-50 pound range.

The magnesium meta-dinitrobenzene "tape battery" system under development for NASA by the Monsanto Research Company is currently in an experimental stage. Its developers foresee a possible system power density of 245 watt-hours per pound. If the device proves to be practical for applications similar to the lunar coring device, the 2,000 watt-hour power supply weight could possibly be reduced to approximately ten pounds provided no thermal problems arise.

Fuel Cells. -The relatively high efficiency of a cryogenic hydrogen-oxygen fuel cell is second only to a battery system. Fuel energy conversion efficiencies of 1.2 pounds per kilowatt-hour are attainable, but this is partially negated by a fixed system weight of 210 pounds per kilowatt operating level. The fuel cell contains very few moving parts, the no-load losses are relatively small, and the system is reliable for operating periods ranging from several days to several weeks. However, use of the fuel cell incurs disadvantages which are not inherent with the battery system, such as a relatively elaborate shutdown system, and a radiator is required to dissipate excess heat.

Figure F-3 (Power Density of Fuel Cells) illustrates the "fixed" and "variable" weight-power characteristics of various power-level fuel cells. It can be seen that a 500-watt fuel cell applicable for the lunar coring device would have a fixed system weight of approximately 105 pounds, and a total weight of 107.4 pounds would be required for a total power capacity of 2,000 watt-hours. This, of course, does not compare favorably with the 70-pound silver-zinc battery required for the same total power capacity. However, the total power capacity of the fuel cell can easily be increased from 500 to 10,000 watt-hours by the addition of 12 pounds of fuel for a total system weight of 117 pounds. This compares very favorably to a corresponding silver-zinc battery system which would weigh approximately 350 pounds.

Chemical Dynamic Systems. -Figure F-4 (Power Density of Chemical Dynamic Systems) illustrates the system weights of various power-level turbine alternators. It can be seen that the fixed system weight of 25 to 60 pounds per kilowatt-hour compares favorably to the fuel cell. A 2,000 watt hour capacity system would weigh approximately 65 pounds. However, the relative complexity, bearing lubrication, heat rejection, and other problems associated with the chemical dynamic systems negate the weight advantages over the fuel cell and battery systems.

Photovoltaic Devices. -The solar cells employed in the photovoltaic devices convert solar flux directly into electrical energy at efficiencies of 8 to 12 percent. The efficiencies can be improved by employing reflectors or orienting devices. However, the performance of these systems can be degraded by high energy radiation and micro-meteorite bombardment. The "N" on "P" type cells are about three times as radiation-resistant as the "P" on "N" type and are most generally employed for spatial applications.

Figure F-5 (Power Density of Nuclear, Solar and Radioisotope Systems) illustrates comparative power-weight data for the various "continuous operation" systems. A solar cell system with a continuous operating capacity of 500 watts would weigh approximately 115 pounds. This would represent an absolute minimum for the lunar coring device; a 700 watt continuous source weighing approximately 160 pounds would be more appropriate.

Solar Concentrators. -These systems provide the energy to generate power directly by employing thermionic and thermoelectric devices, or indirectly by the use of turbo-generators. With the possible exception of radiation effects, the disadvantages cited above for the solar cells also apply to the solar concentrator systems. Orientation of the concentrator system toward the sun must be more precise (accuracies of ± 0.1 degrees are required), thus resulting in a heavy system even though the theoretical efficiencies are high. In addition, the static solar power systems require power conversion equipment while the dynamic systems can be designed to generate power at the utilization voltages.

It can be seen from Table F-1 (Comparative Characteristics of Power Sources) that a 500 watt thermionic solar concentrator would weigh approximately 100 pounds. The higher power 700 watt power source recommended for the lunar drill would probably require a dynamic system weighing approximately 175 pounds.

Nuclear Powered Devices. -These systems can be divided into two types: 1) those which use radioisotopes; and 2) those which employ nuclear reactors. The radioisotope is a low temperature heat source and is readily adaptable for use with the thermoelectric devices. The operating temperature of the nuclear reactor is limited by the materials used in the power generating devices. The higher the inlet temperature to these devices, the higher the power generating efficiency which subsequently results in reduced radiator surface area requirements.

Nuclear reactor and radioisotope systems offer very compact and long duration energy sources. The resultant radiation, however, dictates the use of heavy shielding and possibly a remote location for the reactor on the lunar surface. Also, the selection of materials and components for other subsystems will be influenced.

Examination of Table F-1 (Comparative Characteristics of Power Sources) and Figure F-5 (Power Density of Nuclear, Solar and Radioisotope Systems) reveals that the weight penalties incurred by the use of radioisotope or nuclear reactors employing thermoelectric elements would be prohibitive. A 500-watt radioisotope device employing thermoelectric elements would weigh 300 to 500 pounds; a nuclear reactor employing the thermoelectric elements would weigh approximately 1000 pounds. The minimum operating range for the thermionic and dynamic nuclear reactors is above that allowable for the lunar coring device.

The radioisotope generator employing thermionic elements is the only nuclear system which could potentially serve as a portable power supply for the lunar coring device. A 500-watt device could be expected to weigh approximately 175 pounds. However, the weight of this device is also considered to be excessive in view of the LEM payload restrictions and limited astronaut capabilities.

Tradeoffs and Conclusions. -As a result of this analysis of potential self-contained power sources for the lunar coring device, the following conclusions have been made:

1. The incorporation of a self-contained power source for the lunar coring device will require that a relatively large portion of the LEM 250 pound payload be utilized for this purpose.
2. The continuous heat source devices (radioisotope generators, nuclear reactors, solar concentrators, photovoltaic devices) are not feasible for use on the early LEM missions which will not exceed two or three days. The minimum weight penalty incurred by use of any of these devices would be approximately 100 pounds, and it is doubtful that they could be transported and operated on the lunar surface by one astronaut. These power systems will be more practical for the follow-on lunar missions when powered transporters such as the MOLAB are employed.
3. The chemical dynamic systems (turbo-alternators) are considered to be somewhat complex for operation by the astronaut on the lunar surface, although the power-density characteristics are superior to the continuous heat source devices for short duration missions.

ER 13952

4. The most feasible approach for increasing the operating range of the coring device is to utilize a rechargeable silver-zinc storage battery(ies) with a capacity of 1000 to 2000 watt-hours. The storage battery power supply presents the ultimate in simplicity and can be transported and operated anywhere within the anticipated exploration range of the lunar astronaut.

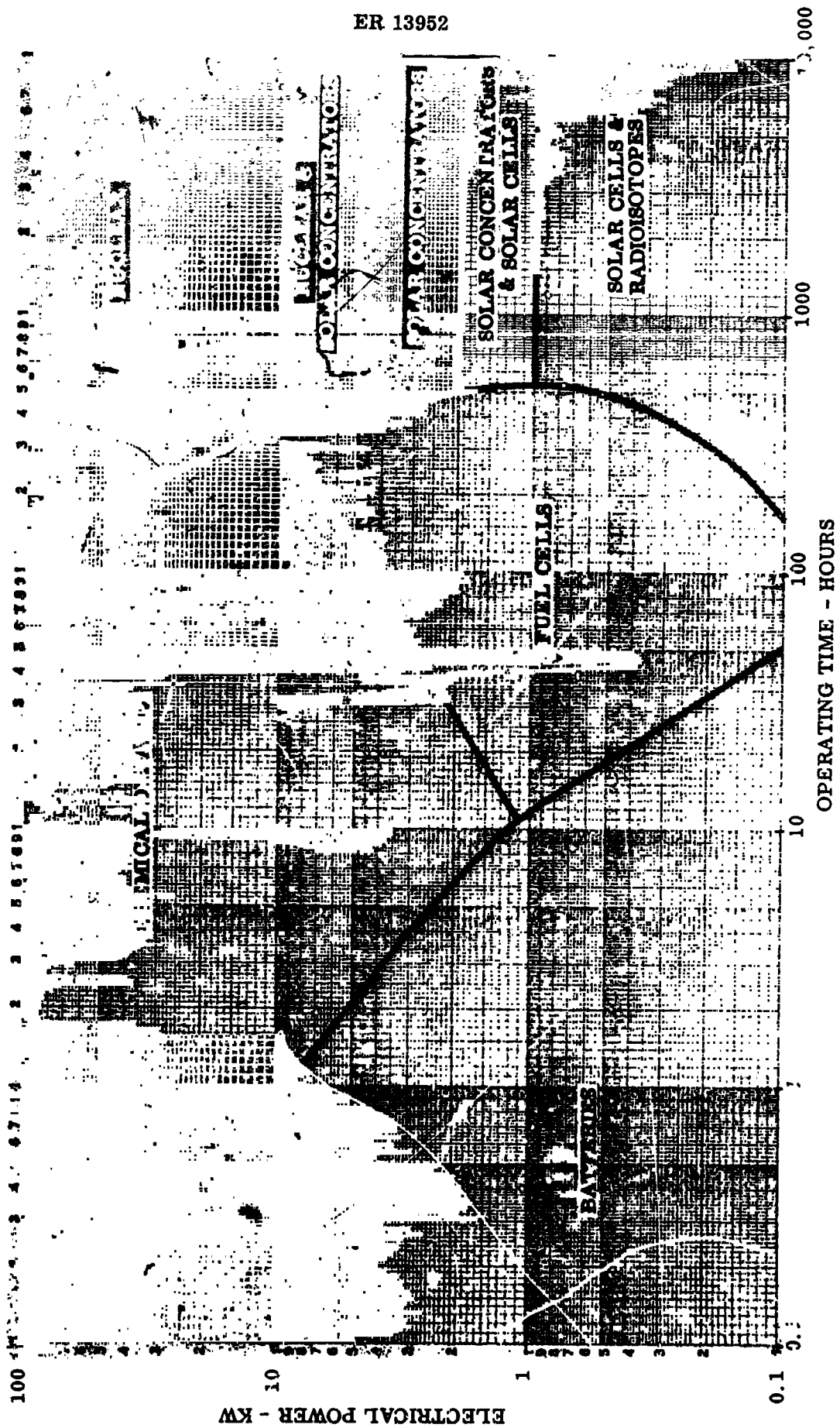


Figure F.1. Power System Selection Curves

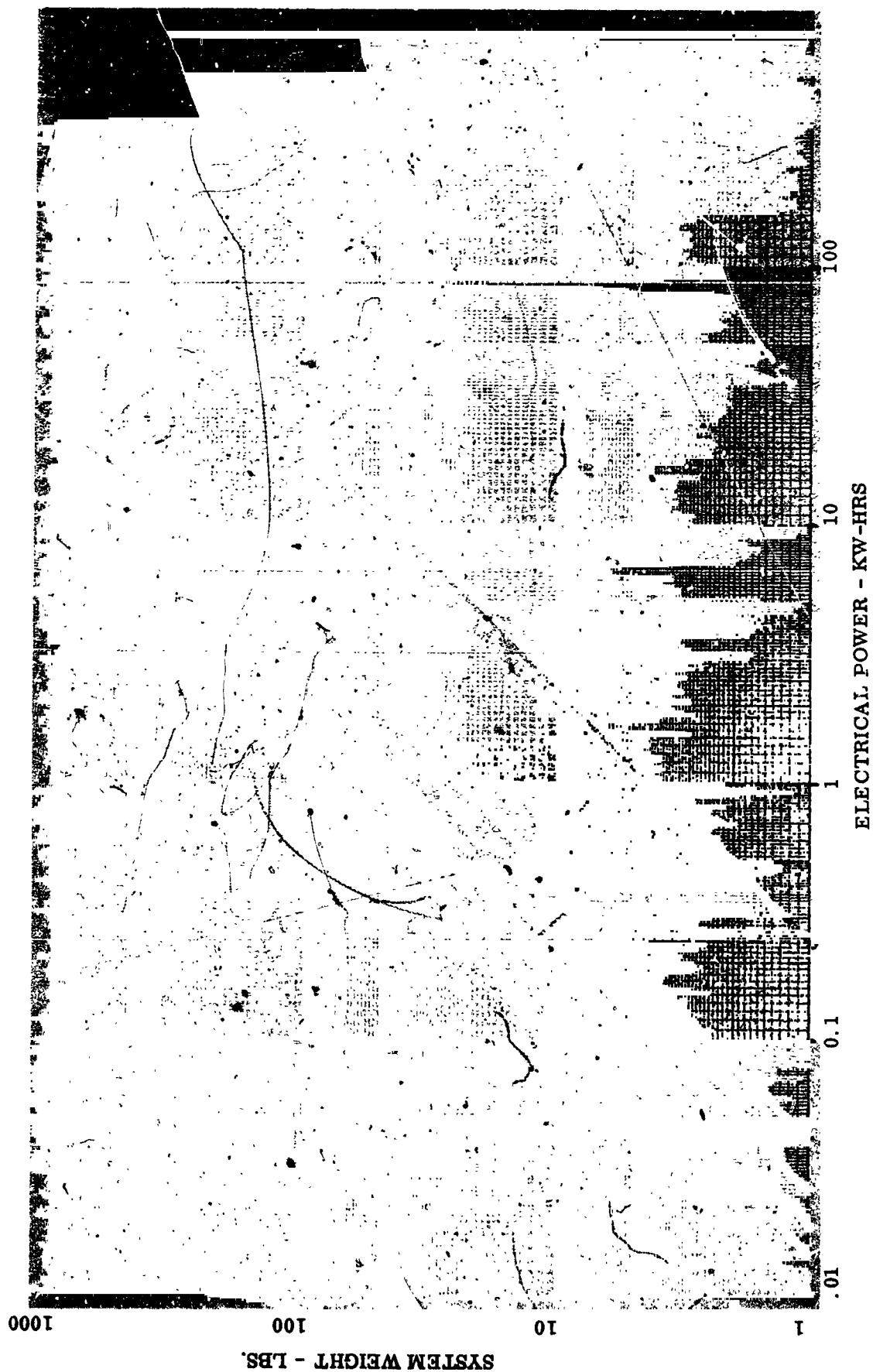


Figure F.2. Power Density of Battery Systems

ER 13952

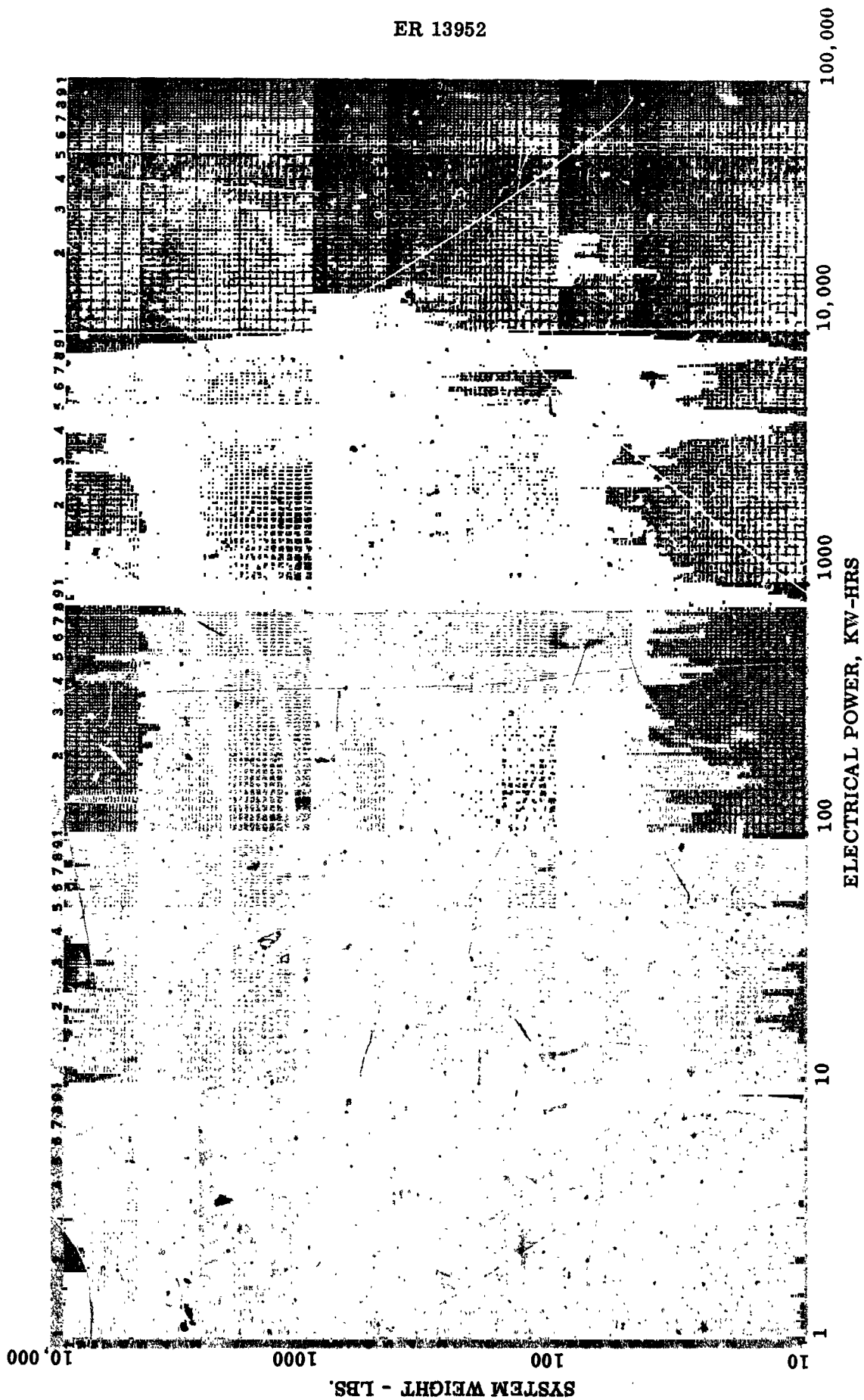


Figure F.3. Power Density of Fuel Cells

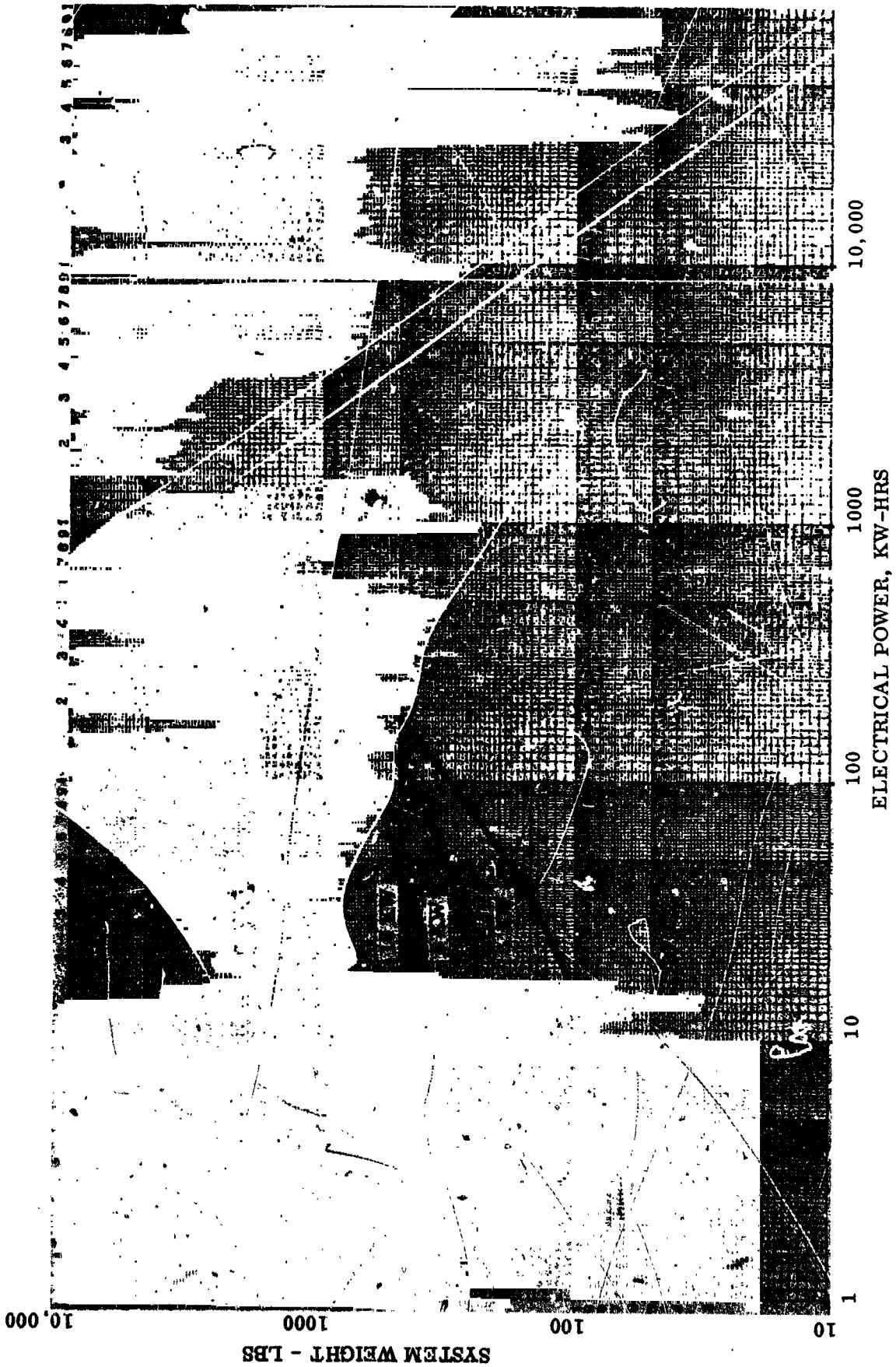


Figure F.4. Power Density of Chemical Dynamic Systems

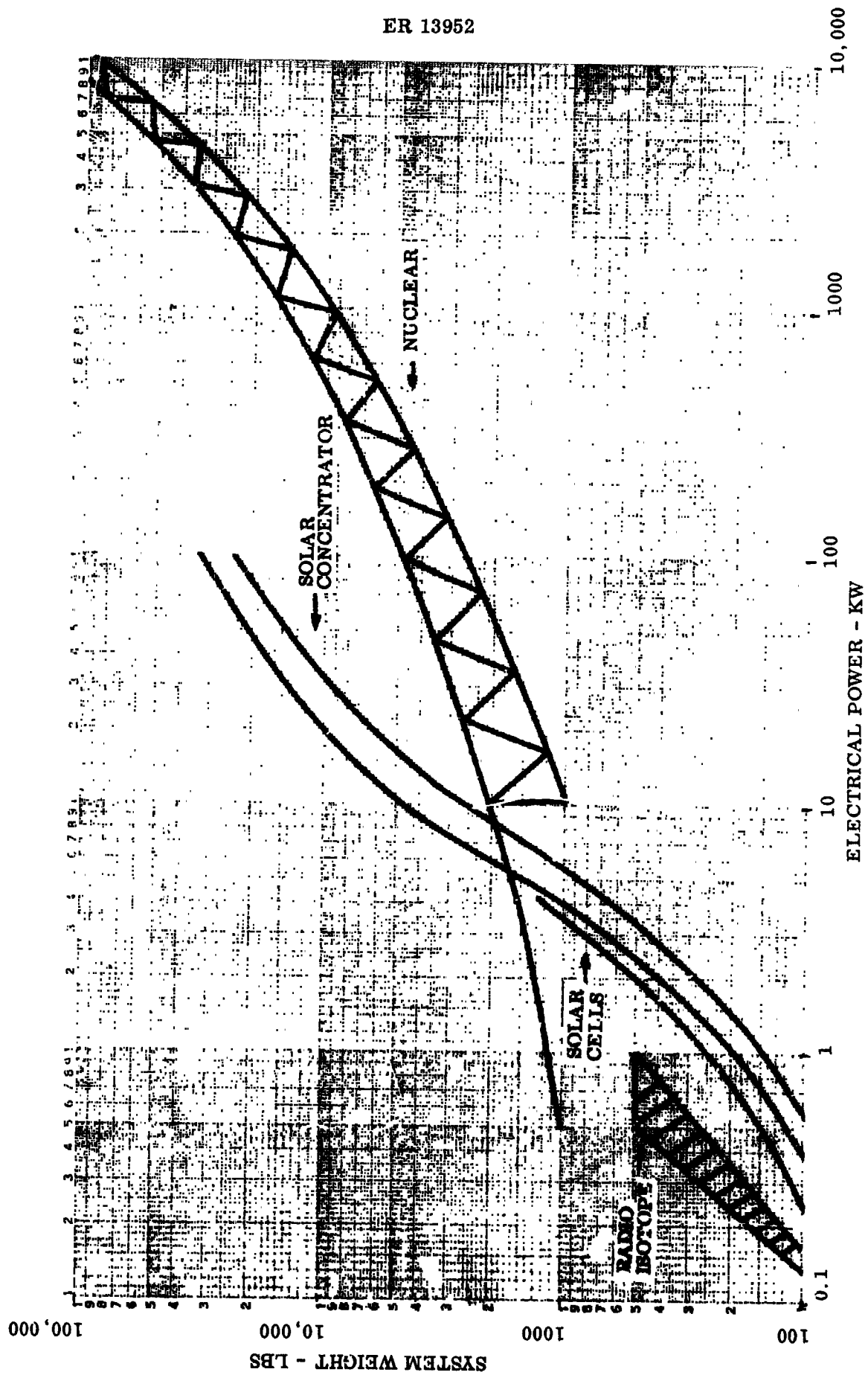


Figure F.5. Power Density of Nuclear, Solar & Radioisotope Systems

TABLE F-1. COMPARATIVE CHARACTERISTICS OF POWER SOURCES

ENERGY SOURCE	POWER CONVERSION DEVICES	OUTPUT POWER RANGE	EFFICIENCY	POWER DENSITY	OPERATING LIFETIME	REMARKS
Chemical Systems	Fuel Cells	500W to 10KW	60-70%	210 lb/KW fixed plus 1.2 lbs/KW Hr.	Weeks	Lifetime may be extended to months.
	Batteries	to 10KW	70-80%	9-14 W Hrs/Lb	6000 partial recharges	Lifetime is a function of depth of discharge.
	Silver-Cad.	to 10KW	70-80%	14-20 W Hrs/Lb	2000 partial recharges	
	Silver-Zinc	to 10KW	70-80%	25-40 W Hrs/Lb	100 partial recharges	
Photovoltaic Devices	Turbo- Alternator	.5KW to 100KW	30%	25-60 lb/KW fixed plus 2.4 lb/KW Hr	Days	
	Solar Cells N on P type	to 4KW	8-12%	230 lb/KW	Months to Years	Weight does not include energy storage system.
	Thin Film Solar Cells	200W	2%	70 lb/KW	Months to Years	
	Thermo- Electric	25W to 500W	2%	500 lb to 1000 lb/KW	Months to Years	
Thermal (Contin- uous Heat Sources)	Thermionic	1 KW	4-15%	350 lb/KW	Months to Years	
	Thermo- Electric	500W	2%	2000 lb/KW	Years	
	Thermionic	10 KW to 30 MW	4-15%	10 lb to 100 lb/KW	Years	
	Dynamic	10 KW to 1MW	25%	10 lb to 500 lb/KW	Years	
	Thermionic	500W	4-15%	200 lb/KW	Years	Weight does not include energy storage system.
	Dynamic	1-30 KW	25%	250 lb/KW	Years	

APPENDIX G - MOTOR ENVIRONMENTAL CONTROL SYSTEM

The following preliminary analysis was performed to establish the design requirements for an open-loop, liquid boil-off type environmental control system for the lunar coring device motor. Figure G-1 illustrates the major components of the environmental control system.

Electric Motor Heat Load:

Assumptions:

1. Motor performance characteristics as per Figure 1.2.
2. Range of torque = 3.2 - 7.0 ft.-oz. depending on rock hardness
3. Total heat load = $\frac{\text{Watts output}}{\text{Efficiency}} - \text{Watts output}$
4. Winding resistance = .278 ohms (measured experimentally)

TABLE G-1. ELECTRIC MOTOR HEAT LOADS

Torque (Ft.-Oz)	Input Current (AMP)	Output Power (Watt)	Efficiency	Input Power (Watt)	Total Heat (Watt)	I ² R Loss (Watt)	I ² R Loss (% of total)	Speed (RPM)
3.2	11	197	.72	274	77	34	44	6700
4.0	14	245	.74	331	86	54	63	6500
4.8	17	290	.74	392	102	80	78	6350
5.7	20	330	.71	465	135	111	82	6200
7.0	25	382	.64	597	215	174	81	6000

Conclusions:

1. Heat load ranges between 77 and 215 watts
2. At the higher heat loads, over 80% of the heat is generated in the windings (when eddy currents and windage are added to the I²R loss)

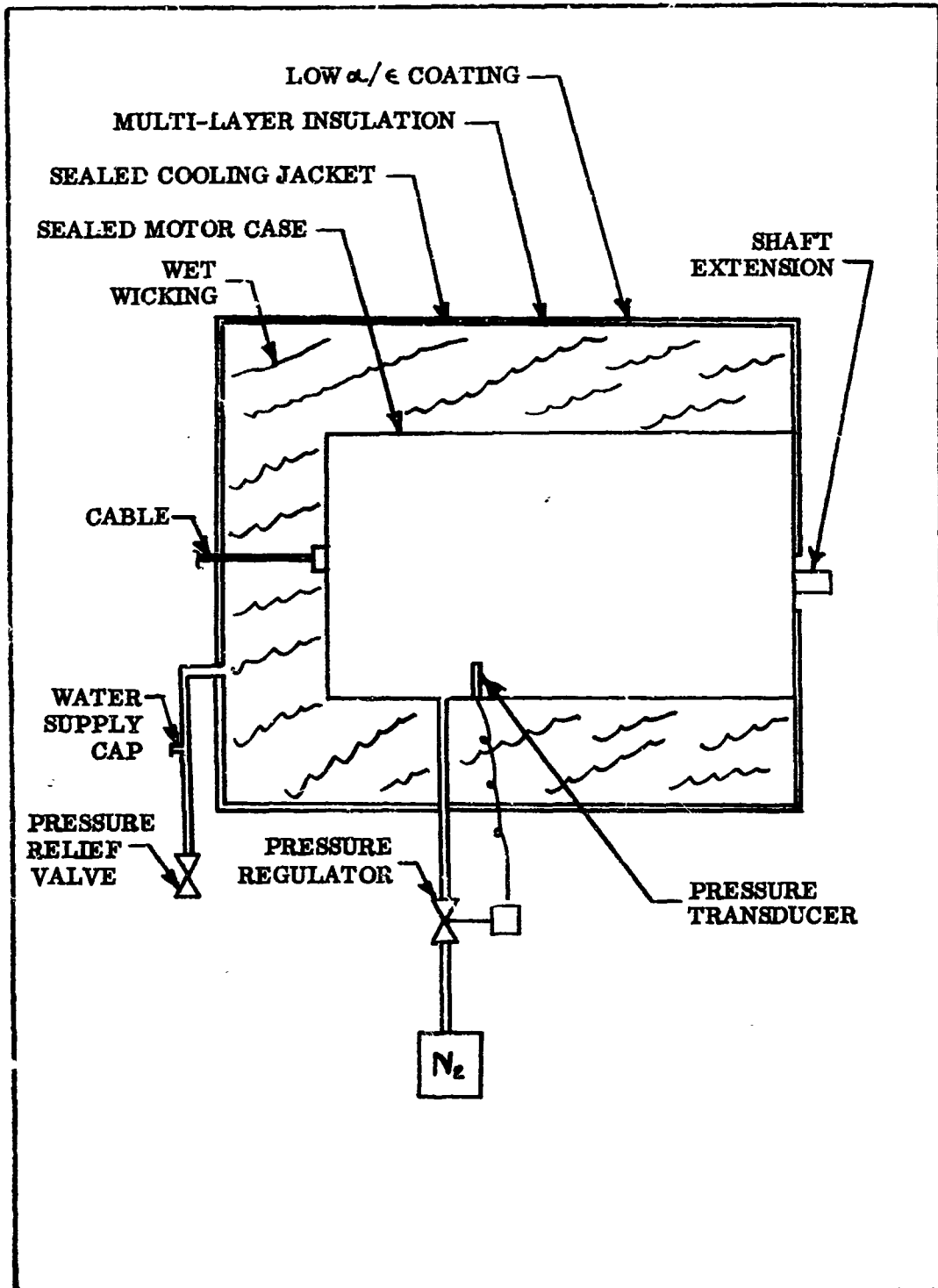


Figure G.1. Schematic Diagram of Motor Cooling System

HEAT STORAGE CAPACITY OF MOTOR (TRANSIENT COOLING):Assumptions:

1. Envelope dimensions are 3 1/4" diameter x 6" long.
2. 50% of the gross volume consists of solids, of which 80% is steel and 20% is aluminum.
3. Initial temperature is 200° F.
4. Maximum allowable temperature is 400° F.
5. Nominal heat dissipation is 135 watts.

Computations:

$$\text{Gross volume} = \frac{\pi}{4} \times 3.25^2 \times 6 \times \frac{1}{1728} = .0288 \text{ ft.}^3$$

$$\text{Volume of steel} = .5 \times .8 \times .0288 = .0115 \text{ ft.}^3$$

$$\text{Volume of aluminum} = .5 \times .2 \times .0288 = .0029 \text{ ft.}^3$$

$$\text{Thermal capacity of steel} = .0115 \text{ ft.}^3 \times 480 \frac{\text{lb}}{\text{ft.}^3} \times .12 \frac{\text{Btu}}{\text{lb}^\circ\text{F}} = .66 \frac{\text{Btu}}{^\circ\text{F}}$$

$$\text{Thermal capacity of al} = .0029 \times 165 \times .22 = .11$$

$$\text{Total thermal capacity} = .77 \text{ Btu}/^\circ\text{F}$$

Assuming no heat transfer to ambient (conservative), time to reach maximum allowable temperature is =

$$\frac{.77 (400-200)}{135 \times 3.41} = .33 \text{ hour}$$

Conclusion:

Since the motor is to operate for 8 hours, a cooling system is required because the thermal capacity of the motor is inadequate.

UNPRESSURIZED MOTOR HEAT TRANSFER:Assumptions:

1. Internal heat load = 135 watts (nominal)
2. Heat transfer by radiation exclusively

(Continued)

3. View factor from internal elements to case, $F_{ic} = 1.0$
4. Emittance of all internal surfaces = 0.9
5. Surface area of internal elements = 60% of case area
6. Maximum allowable temperature of internal elements = 400° F
7. Internal dimensions of motor case are 3" diam. & 5" long

Computations:

$$A_c = \text{Internal surface area of case} = \frac{(\pi \times 3 \times 5 + 2 \times \pi \times 1.5^2)}{144} = .425 \text{ ft.}^2$$

$$A_i = \text{Surface area of internal elements} = .6 \times .425 = .255 \text{ ft.}^2$$

$$Q_{\text{radiation}} = A_i F_{ic} \epsilon_i \epsilon_c \sigma (T_i^4 - T_c^4)$$

$$135 \times 3.41 = .255 \times 1 \times .9 \times .9 \times .173 \left[\left(\frac{860}{100} \right)^4 - \left(\frac{T_c}{100} \right)^4 \right]$$

$$\text{or } 12900 = 5470 - \left(\frac{T_c}{100} \right)^4 \quad \text{or } \left(\frac{T_c}{100} \right)^4 = -7430$$

The above means that for the internal elements to be at 400° F under vacuum, the case temperature would have to be under 0° absolute temperature, which is impossible to achieve.

If the case temperature is assumed to be 220° F = 680° R, then:

$$12900 = \left(\frac{T_i}{100} \right)^4 - \left(\frac{680}{100} \right)^4 \quad T_i = 1107^\circ \text{ R} = 747^\circ \text{ F}$$

Conclusions:

1. If the motor is unpressurized and the case maintained at 220° F by water evaporative cooling at 14.7 psia, the internal elements operating temperature would be approximately 527° F higher or 747° F.
2. Since the maximum allowable temperature of the windings is currently assumed to be 400° F it is imperative that the motor be pressurized.

PRESSURIZED MOTOR HEAT TRANSFER:Assumptions:

1. Nominal armature speed = 6200 RPM
2. Pressurizing gas: nitrogen at 15 psia
3. Diameter of armature = 2.16" = .18 ft.
4. Maximum allowable temperature of armature $T_a = 860^\circ \text{R}$
5. Nominal heat load = 135 watts
6. Surface area of armature = .255 ft.²
7. Internal surface area of case = .425 ft.²

Computations:

Velocity of armature relative to case = πD (RPS)

$$= \pi \times \frac{2.16}{12} \times \frac{6200}{60} = 58 \text{ ft/sec}$$

It is reasonable to assume that the velocity of nitrogen relative to either the armature or the case is = 29 ft/sec

Properties of nitrogen at $\sim 300^\circ \text{F}$ and 15 psia are:

ρ = Density = .051 lb/ft³, k = thermal conductivity = .02 Btu/hr ft $^\circ\text{F}$

μ = Viscosity = 1.55×10^{-5} lb/ft sec, C_p = Specific heat = .26 Btu/lb $^\circ\text{F}$

$$\frac{h D}{k} = .023 \left(\frac{D \rho v}{\mu} \right)^{.8} \left(\frac{C_p \mu}{k} \right)^{.4}$$

$$\frac{h \times .18}{.02} = .023 \left(\frac{.18 \times 29 \times .051}{1.55 \times 10^{-5}} \right)^{.8} \left(\frac{.26 \times 1.55 \times 10^{-5} \times 3600}{.02} \right)^{.4}$$

$h = 5.5 \text{ Btu/hr ft}^2 \text{ } ^\circ\text{F} = \text{convective heat transfer coefficient}$

Considering heat transfer by both convection and radiation from the armature to the case:

$$135 \times 3.41 = \left(\frac{1}{\frac{1}{5.5} + \frac{1}{5.5}} \right) \left(\frac{.255 + .425}{2} \right) (860 - T_{\text{case}}) \\ + .255 \times 1 \times .9 \times .9 \times .173 \left[\left(\frac{860}{100} \right)^4 - \left(\frac{T_{\text{case}}}{100} \right)^4 \right]$$

$$T_{\text{case}} = 544^\circ \text{R} = 84^\circ \text{F}$$

(Continued)

In order to maintain the case temperature at 84° F, it is proposed to surround the case with a wicking material which is kept moist by water supplied from a connecting reservoir.

Conclusion:

By pressurizing the sealed motor case with nitrogen at 15 psia, the temperature difference between the armature and the case is reduced to 316° F when the former is maintained at a maximum temperature of 400° F.

PRESSURIZATION SYSTEM:

Although the motor case will have welded construction for maximum sealability, some leakage will occur through the rotary shaft seal and the static wire feed-through. Therefore, a leakage make-up system must be provided.

Assumptions:

1. Rotating shaft seal (silicone element) has a leakage rate of approximately .009 ft³/hr
2. Static seal for electrical conductor has a leakage rate of approximately .002 ft³/hr
3. Void volume = .0144 ft³
4. Operation period = 8 hours
5. Storage pressure = 200 psia

Computations:

$$\text{Leakage make-up required} = (.009 + .002) 8 = .088 \text{ ft}^3$$

$$\text{Density of nitrogen at 15 psia and 240° F} = \frac{P}{RT}$$

$$= \frac{15 \times 144}{55.2 \times 700} = .056 \frac{\text{lb}}{\text{ft}^3}$$

$$\text{Total volume of nitrogen} = .088 + .0144 = .1024 \text{ ft}^3$$

$$\text{Total mass of nitrogen} = .1024 \times .056 = .0057 \text{ lbs.}$$

$$\text{Volume of storage tank} = .1024 \times \frac{15}{200} \times 1728 = 13.25 \text{ cu. in.}$$

(Continued)

If spherical, radius of sphere = $\left(\frac{13.25 \times 3}{4 \pi}\right)^{1/3} = 1.47 \text{ inch}$

Using 1/8" thick aluminum shell, weight = $4\pi \times 1.47^2 \times .125 \times .1 = .34 \text{ lb}$

As an alternate, a commercial high pressure cylinder, 5.953 inches long x 2.376 diameter can be used.

In addition to the storage tank, a pressure regulating valve and a transducer to control its operation is required.

Conclusion:

The pressurization system will consist of a nitrogen storage tank (approx. 3-inch diameter sphere or 2 3/8" diameter x 6" long cylinder), a pressure transducer, a pressure regulating valve and the necessary piping.

BOILING HEAT TRANSFER:

Assumptions:

1. Outer surface area of case in contact with wick = $.483 \text{ ft}^2$
2. Maximum temperature of case = 544° R
3. Nominal heat load = 135 watts
4. Volume of wicking material = 20% of volume of water
5. Density of wicking material = 30 lb/ft^3

Computations:

From equation (4), Table 9, Chapter 4 of ASHRAE Guide (1961):

$$h_{\text{boiling}} = .37 \left(T_{\text{surface}} - T_{\text{water}}\right)^3$$

$$135 \times 3.41 = .37 \left(544 - T_{\text{water}}\right)^3 (.483) \left(544 - T_{\text{water}}\right)$$

$$T_{\text{water}} = 537^\circ \text{ R} = 77^\circ \text{ F}$$

$$h_{\text{boiling}} = .37 (544 - 537)^3 = 125 \text{ Btu/hr ft}^2 \text{ } ^\circ \text{ F}$$

Saturation pressure corresponding to 77° F saturation temperature = .46 psia

Latent heat of evaporation at 77° F saturation temperature = 1050 Btu/lb.

(Continued)

$$\text{Boiling rate} = \frac{135 \times 3.41}{1050} = .44 \text{ lb/hour}$$

For an operation period of 8 hours, the water reservoir should have a capacity of $8 \times .44 = 3.52 \text{ lbs.}$

$$\text{Volume of water required} = \frac{3.52 \times 1728}{62.4} = 97.6 \text{ cu. in.}$$

$$\text{Volume of wicking} = .20 \times 97.6 = 19.5 \text{ cu. in.}$$

$$\text{Weight of wicking} = 30 \times 19.5/1728 = .34 \text{ lb.}$$

$$\text{Specific volume of water vapor} = 695 \text{ ft.}^3/\text{lb.}$$

$$\text{Vapor generation rate} = \frac{.44 \times 695}{3600} = .0845 \text{ ft.}^3/\text{sec.}$$

$$\text{Sonic velocity in water vapor at } 77^\circ \text{ F} = 1320 \text{ ft./sec.}$$

$$\begin{aligned} \text{Minimum cross section of exhaust nozzle} &= \frac{.0845 \times 144}{1320} \\ &= .0092 \text{ in.}^2 \end{aligned}$$

$$\text{Minimum diameter of exhaust nozzle} = \frac{4 \times .0092}{\pi}^{1/2} = .117 \text{ inch}$$

$$\text{Volume of coolant jacket} = 97.6 \times 1.20 = 117 \text{ cu. in.}$$

$$117 = \left[\frac{\pi}{4} (3.25 \times 2x)^2 - 3.25^2 \right] \times 6$$

$$\text{Thus } x = 1.35 \text{ inch} = \text{required depth of jacket}$$

To allow some vapor to accumulate within the jacket, make the jacket internal diameter $6 \frac{1}{4}$ inches.

$$\text{Using .040" thick aluminum sheet, weight of jacket} = (\pi \times 6.25 \times 7.5 + \frac{\pi}{2} \times 6.25^2)$$

$$\times .040 \times .1 = .83 \text{ lb.}$$

Conclusion:

In order to dissipate the heat generated within the motor, it is recommended that the motor case be surrounded by a well sealed coolant jacket $6 \frac{1}{4}$ inches in diameter x $7 \frac{3}{4}$ inches long. The jacket should be lined with a wicking material and charged with 98 cu. in. of water for each 8 hours of operation. A pressure relief valve set at 9.46 psia should be provided to exhaust the water vapor.

COOLANT JACKET INSULATION:Assumptions:

1. Outer shell dimensions = 6 1/2 diameter x 7 3/4" long
2. Solar absorptance of outer shell $\alpha = .20$
3. Infra-red emittance of outer shell $\epsilon_s = .90$
4. Incident solar radiation $S = 443 \text{ Btu/hr. ft.}^2$
5. Lunar surface emittance $\epsilon_m = .95$
6. Heat flow through insulation = 1% of internal heat load
7. View factor to space from shell $F_{SO} = .5$
8. View factor lunar surface from shell $F_{SM} = .5$
9. Temperature of lunar surface $T_M = 700^\circ \text{ R}$
10. Use NRC-2 insulation: $k_i = 2.4 \times 10^{-5} \text{ Btu/hr. ft. } ^\circ \text{R}$

Computations:

$$\text{Projected area facing sun} = \frac{6.5 \times 7.75}{144} = .35 \text{ ft.}^2 = A_P$$

$$\text{Total shell surface area} = \left[\pi \times 6.5 \times 7.75 + \frac{\pi}{2} (6.5)^2 \right] \frac{1}{144} = 1.56 \text{ ft.}^2 = A_S$$

$$\text{Direct solar heat input} = \alpha S A_P = .20 \times 443 \times .35 = 31.0 \frac{\text{Btu}}{\text{hr}}$$

$$\begin{aligned} \text{Net infra-red heat input} &= A_S F_{SM} \epsilon_s \epsilon_m \sigma (T_M^4 - T_S^4) \\ &= 1.56 \times .5 \times .90 \times .95 \times .173 \left[\left(\frac{700}{100} \right)^4 - \left(\frac{T_S}{100} \right)^4 \right] \end{aligned}$$

$$= 276.4 - .115 (T_S/100)^4 \text{ Btu/hr}$$

$$\begin{aligned} \text{Heat output to space} &= A_S F_{SO} \epsilon_s \sigma T_S^4 = 1.56 \times .5 \times .9 \times .173 \left(\frac{T_S}{100} \right)^4 \\ &= .121 \left(\frac{T_S}{100} \right)^4 \text{ Btu/hr} \end{aligned}$$

$$\text{Heat flow through insulation} = 135 \times 3.41 \times .01 = 4.6 \text{ Btu/hr.}$$

(Continued)

Heat balance

$$31 + 276.4 - .115 \left(\frac{T_S}{100} \right)^4 = .121 \left(\frac{T_S}{100} \right)^4 + 4.6$$

 $T_S = 598^\circ \text{R}$ Temperature of external shell

$$4.6 = \frac{k_i}{x_i} A_S (T_S - T_{\text{vapor}}) = \frac{2.4 \times 10^{-5}}{x_i} \times 1.56 (598 - 537)$$

$$x_i = .00382 \text{ ft.} = .0046 \text{ inch required thickness of insulation}$$

Weight of insulation = .02 lbs. (from NRC chart)

Conclusion:

In order to maintain the coolant jacket at the required temperature of 77°F , it is necessary to surround it with a .005 inch thick layer of NRC-2 multi-layer insulation or equivalent. Also the outer layer should be coated with a solar reflector coating with solar absorptance of 0.2 and infra-red emittance of 0.95.

WEIGHT ESTIMATION:

1. Pressurization system:

Nitrogen storage tank	=	.34 lbs
Pressure transducer	=	.40
Pressure regulating valve	=	1.40
Piping and supports	=	<u>.30</u>

Sub total 2.44

2. Cooling system:

Water jacket	=	.83 lbs
Wicking	=	.34
Pressure relief valve	=	1.40
Piping and supports	=	.30
Insulation	=	<u>.02</u>

Sub total 2.89

3. Expendables: (For 8 hours operation)

Water	3.52
Nitrogen	<u>.01</u>

Sub total 3.53

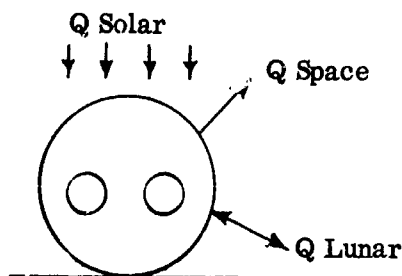
4. Grand Total 8.86 lbs.

APPENDIX H

CORING DEVICE CABLE TEMPERATURE

Assumptions:

1. Heat balance at subsolar point. Neglect conduction to or from lunar surface. Neglect lunar albedo since view factor from lunar surface to cable is zero. (See view factor calculations.) Calculations assume steady state. Temperature has been reached.

2. Lunar Properties.

- a. Temperature: Assume 130° C
- b. Emissivity: Assume 0.90

3. Cable Insulation Properties

0.50 inch diameter, 100 feet long, double conductor

	α	ϵ	α/ϵ	
Cable A	0.40	0.80	0.50	Note a.
Cable B	0.147	0.58	0.25	Note b.

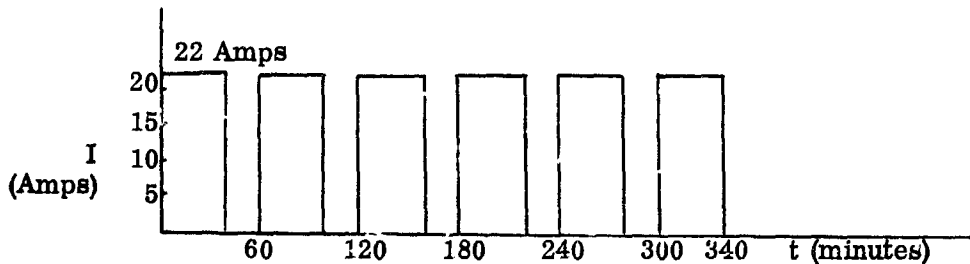
Notes

- a. Properties based on limited data available on white cloth (Ref. 2) since no data is available on cable coatings. Data must be verified by actual test on sample cables.
- b. Alternate cable assumed to be wrapped with 3M - #850 aluminized mylar tape.

4. Conductor Characteristics (#6 AWG Aluminum)

$$\begin{aligned}
 W &= 24.1 \text{ lb./1000 Ft.} \\
 R_{20^\circ \text{ C}} &= 0.648 \Omega / 1000 \text{ Ft. } (0.1296 \Omega / 100 \text{ Ft. Double Conductor}) \\
 \alpha &= 0.004 \text{ (Coefficient of Thermal Resistivity)} \\
 R_{100} &= R_{20} (1 + \alpha \Delta t) \\
 &= 0.1296 [1 + .004 (80)] = 0.171 \\
 R_{80} &= 0.161 \Omega \\
 R_{130} &= 0.187 \Omega
 \end{aligned}$$

ER 13952



TYPICAL CURRENT PROFILE FOR LUNAR DRILL

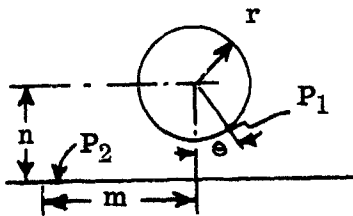
Assuming constant current:

$$\text{Average Power Dissipation @ } 80^{\circ} \text{ C} = \frac{2}{3} \times (22)^2 \times 0.161 = 51.3 \text{ watts}$$

$$\text{Average Power Dissipation @ } 100^{\circ} \text{ C} = \frac{2}{3} \times (22)^2 \times 0.171 = 55.1 \text{ watts}$$

$$\text{Average Power Dissipation @ } 130^{\circ} \text{ C} = \frac{2}{3} \times (22)^2 \times 0.187 = 60.4 \text{ watts}$$

5. View Factors (Ref. 3)



$$\begin{aligned} n &= r \\ m &= \infty \\ \Theta &= 90^{\circ} \\ \cos \Theta &= 0 \\ N &= n/r = r/r = 1 \\ M &= m/r = \infty \end{aligned}$$

Cable to Surface

$$P_1 \rightarrow P_2 = 1/2 (1 + \cos \Theta) = 1/2$$

Cable to Space, also 1/2

Lunar Surface to Cable

$$P_2 \rightarrow P_1 = \frac{N}{N^2 - M^2} = \frac{1}{1^2 - \infty^2} = 0$$

Solar Input

$$Q_{\text{Solar}} = \alpha S A_p$$

$$A_p = \text{Projected Areas} = \frac{.5 \times 100 \times 12}{144}$$

$$\text{Cable A} = .40 \times 443 \times 4.17$$

$$= 4.17 F_t^2$$

$$= 739 \text{ BTU/HR}$$

$$5 = 443 \text{ BTU/HR}/F_t^2$$

$$\text{Cable B} = .147 \times 443 \times 4.17$$

$$= 271 \text{ BTU/HR}$$

Electrical Heat Dissipation:

Cable Temperature - °C	80	100	130
Q Electrical - BTU/HR	176	186	205

Assuming cable temperature equals lunar surface temperature,
 $Q_{\text{Lunar}} = 0$ and $Q_{\text{Space}} = Q_{\text{Solar}} + Q_{\text{Electrical}}$

$$Q_{\text{Space}} @ T_{\text{Cable}} = 130^{\circ} \text{C} (266^{\circ}\text{F}, 726^{\circ}\text{R})$$

$$\text{Area} = \frac{.5 \times \pi \times 100 \times 12}{144} = 13.06 \text{ Ft}^2$$

$$Q_{\text{Space}} = A F_s \epsilon \delta (T_{\text{Cable}}/100)^4$$

$$\text{Cable A} = 13.06 \times .5 \times .8 \times .173 \times (7.26)^4 = 2515 \text{ BTU/HR}$$

$$\text{Cable B} = 13.06 \times .5 \times .58 \times .173 \times (7.26)^4 = 1828 \text{ BTU/HR}$$

Since heat loss capability (Q_{Space}) is greater than heat to be radiated ($Q_{\text{Solar}} + Q_{\text{Electrical}}$) cable temperature will be below and will receive heat from lunar surface. For example, at

$$T_{\text{Cable}} = 100^{\circ} \text{C} (212^{\circ}\text{F}, 672^{\circ}\text{R})$$

$$Q_{\text{Lunar}} = A F_l \epsilon_{\text{cab}} \epsilon_{\text{lun}} \left(\frac{T_{\text{Lunar}}^4}{100} - \frac{T_{\text{Cable}}^4}{100} \right)$$

$$\text{Cable A} = 13.06 \times .5 \times .8 \times .9 \times .173 (7.26^4 - 6.72^4) = 603 \text{ BTU/HR}$$

$$\text{Cable B} = 138 \text{ BTU/HR} (\epsilon = .58)$$

Summarizing Heat Balance

T Cable °C	80	100	130	Cable A
Q Electrical	176	186	205	
Q Solar	739	739	739	
Q Lunar	980	603	0	
Q Required	1895	1528	944	Cable A
Q Available (Q Space)	1425	1845	2515	
Q Electrical	176	186	205	
Q Solar	271	271	271	
Q Lunar	711	438	0	Cable B
Q Required	1158	895	476	
Q Available (Q Space)	1033	1340	1828	

Operating temperatures are shown on Fig. H.1 for the above heat balances.

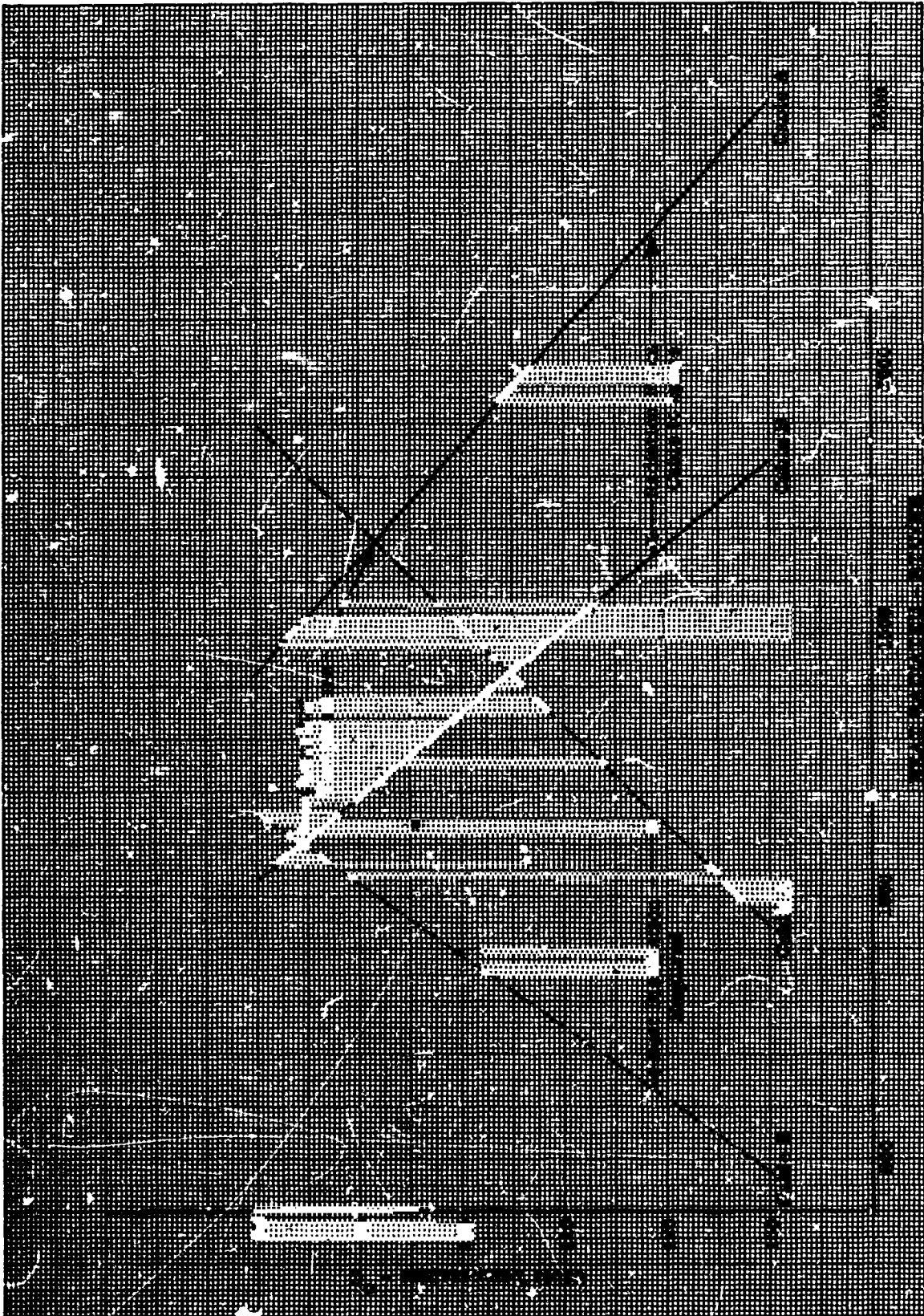


Figure H.1. Coring Device Cable Operating Temperature

ER 13952

References:

1. Lunar Flight Handbook. Prepared by Martin for NASA-MSFC, Contract NAS 3-5031.
2. G. G. Gubareff, J. E. Janssen, R. H. Torborg. Thermal Radiation Properties Survey, Second Edition, 1960. Minneapolis-Honeywell Regulator Company.
3. SAE Aero-Space Applied Thermodynamics Handbook.

APPENDIX I - LUNAR DRILL LOAD SIMULATOR

EQUIPMENT DESCRIPTION

Lunar Drill Motor

The preliminary prime mover selection for the Lunar Coring Device consists of a permanent magnet, DC, mechanically commutated electric motor. This selection was based on a system weight and power operating efficiency study.

The motor supplied with the Lunar Drill Load Simulator is similar to that employed in the breadboard model Lunar Coring Device. This particular model does not incorporate the environmental control system which will be required for extended operation in the high vacuum environment of the lunar surface. It is currently envisioned that the environmental control system for the final model coring device will consist of a nitrogen pressurized motor case with an evaporative water or glycol cooling jacket.

Performance characteristics of the lunar drill motor at 24 and 28 VDC input are illustrated in Figures I.1 and I.2. The efficiency of the motor ranges from 73 to 76 percent at the nominal operating loads of 20 to 25 amperes.

Electrodynamic Brake

The lunar drill motor is mechanically coupled to the electrodynamic brake armature (copper disk) on the Lunar Drill Load Simulator. The motor-driven armature rotates within the air gap between two pairs of field electromagnets. A controllable DC current is supplied to the coils of the electromagnets which, in turn, creates a variable magnetic flux within the air gap between the two pairs of magnets. As the copper armature rotates between the pole faces, eddy currents are induced which create a restraining magnetic flux proportional to the armature speed and flux density of the field magnets. Therefore, controlled loading of the lunar drill motor can be accomplished by varying the magnitude of the DC current supplied to the field magnets of the electrodynamic brake.

Electrodynamic Brake Control Box

The control box contains a DC power supply which is operated from a 115V, 60 cps power source. The power supply is a simple full-wave bridge rectifier employing eight 1N538 diodes and an 80 microfarad electrolytic filter capacitor. Control of the DC output voltage is accomplished by controlling the AC input power with a variable transformer. The variable DC voltage is supplied to the electrodynamic brake on the Lunar Drill Load Simulator by a control cable as illustrated in Figure I.3.

Power Cables

The Lunar Coring Device Design Study resulted in the preliminary selection of No. 6 AWG aluminum wire for the 28V power cable. Aluminum was selected because its resistance-to-weight ratio is less than copper. The study also showed that the cable operating temperature in the lunar environment would be within the limits allowable for aluminum.

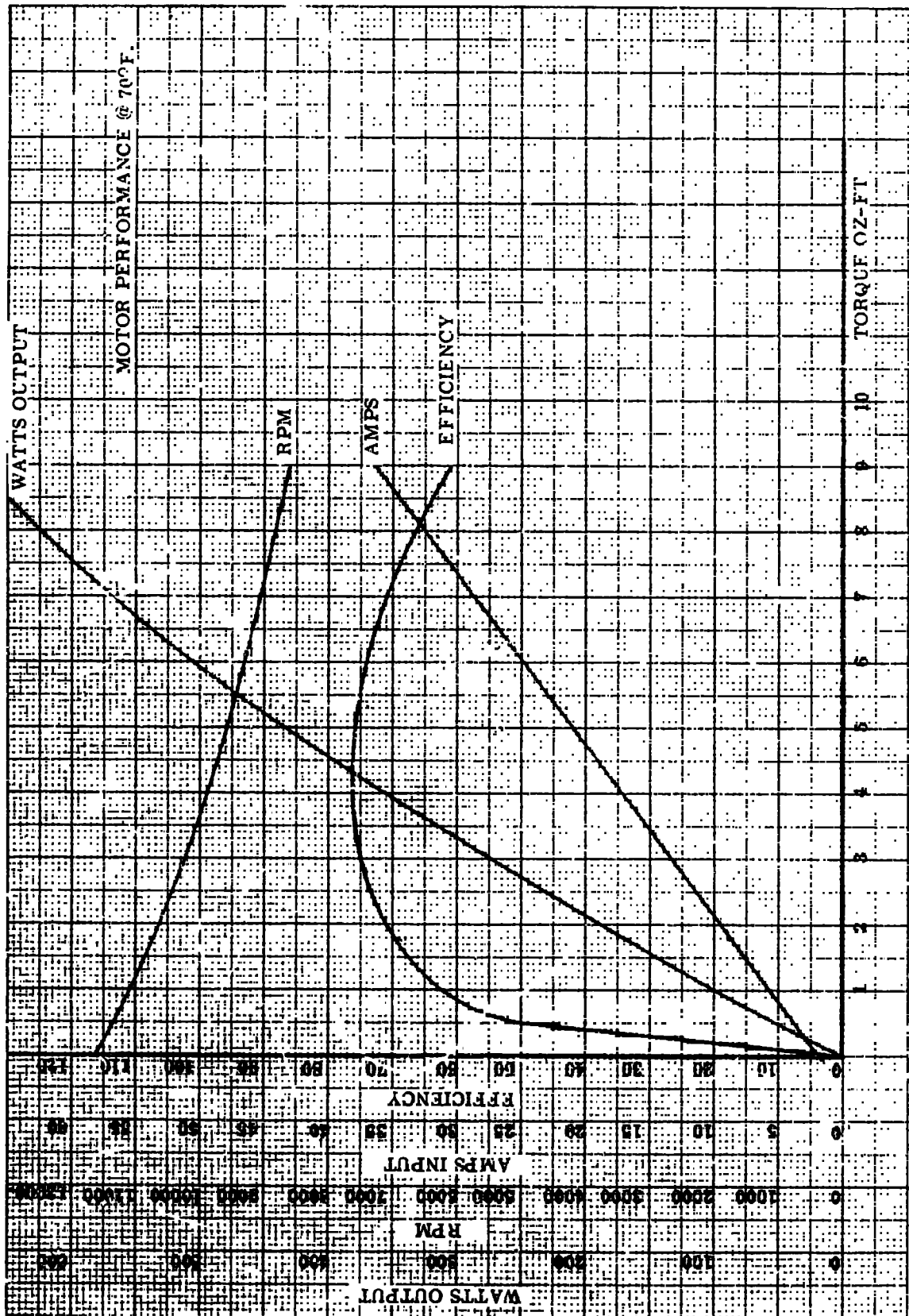


Figure I.1. Motor Performance Characteristics at 28.0 Volts

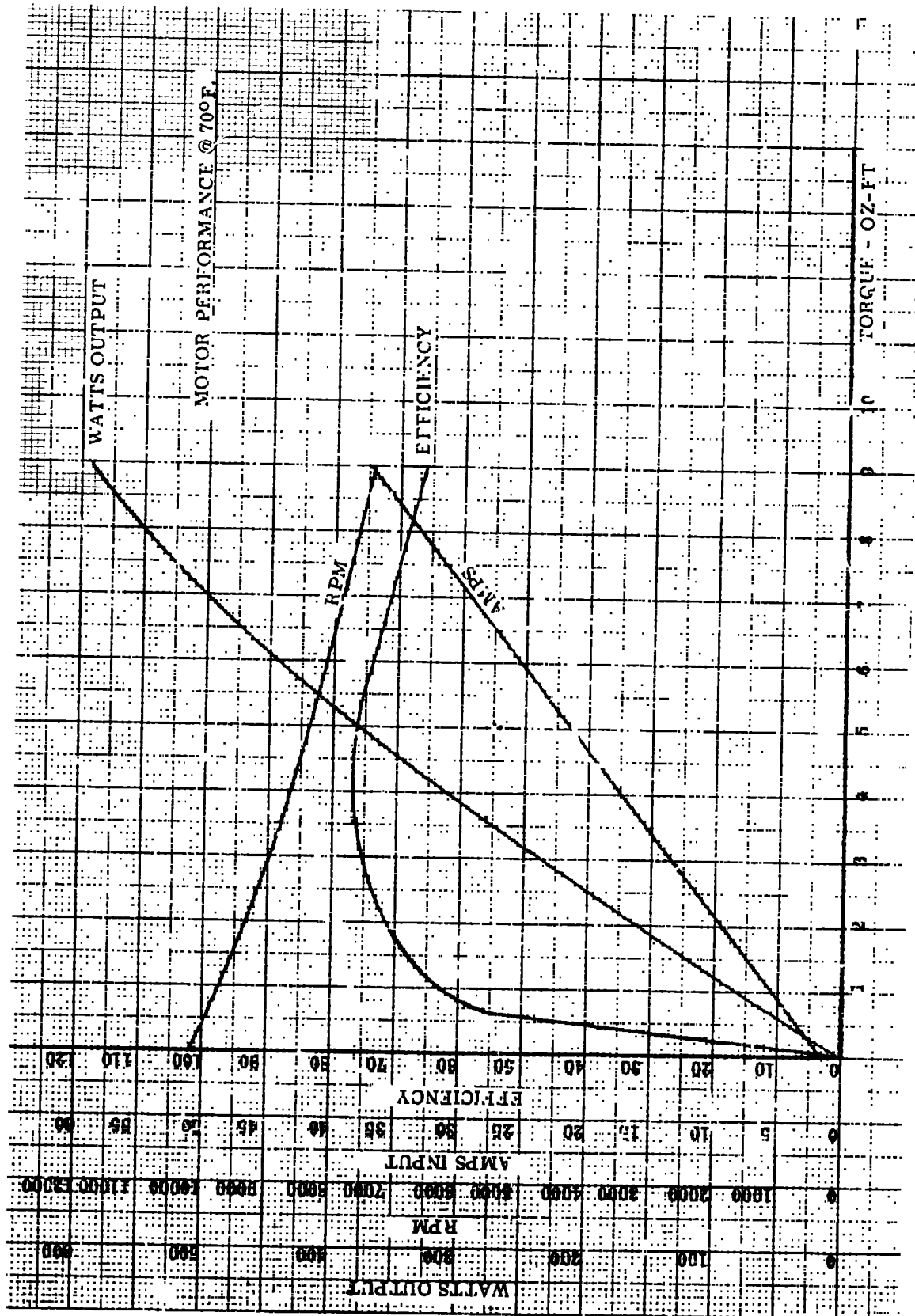


Figure I.2. Motor Performance Characteristics at 24.0 Volts

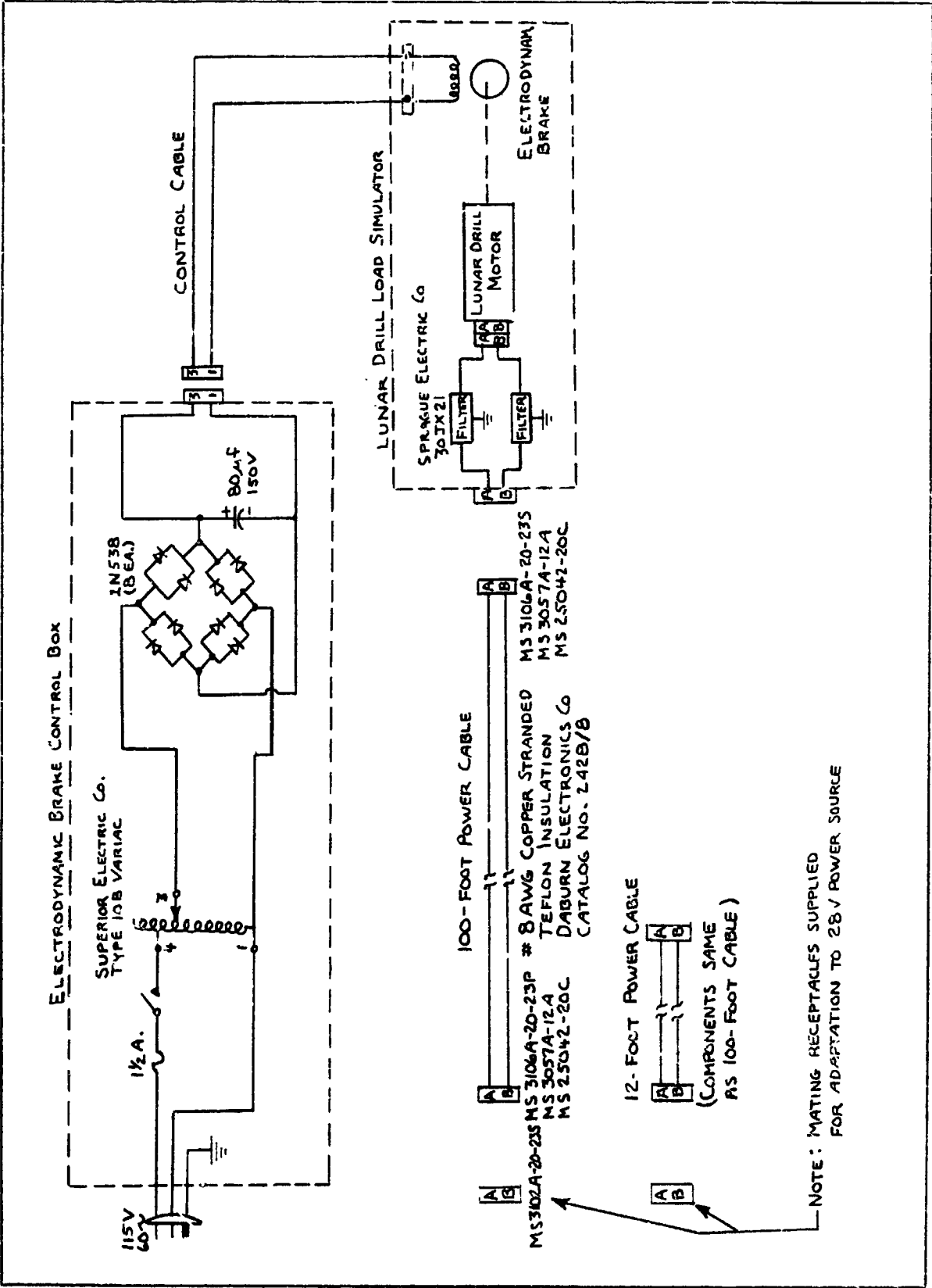


Figure I.3. Lunar Drill Load Simulator & Associated Equipment

In the interests of economy and expediency, a No. 8 AWG copper conductor cable was supplied for the Lunar Drill Load Simulator in lieu of a "special order" aluminum cable. The resistivity of the No. 8 AWG copper (0.628 ohms per 1000 feet @ 20° C) is sufficiently close for test purposes to the resistivity of No. 6 AWG aluminum (0.648 ohms per 1000 feet @ 20° C).

The schematic and hardware employed in the fabrication of the 12-foot and 100-foot power cables is shown in Figure I.3.

OPERATING PROCEDURES

Auxiliary Equipment Requirements

1. Ammeter - A 50-ampere ammeter should be employed in the 28 V power circuit in order to monitor proper current loading of the lunar drill motor by the electrodynamic brake and control adjust.
2. Cooling Fan - Relatively high quantities of heat are generated by the electrodynamic brake when the lunar drill motor is operated under load. The brake assembly is not encased to facilitate cooling. It is recommended that an auxiliary portable fan be used to cool the entire Lunar Drill Load Simulator when operating the motor under load.
3. Power Sources - A 115 V, 60 cps source is required for operation of the electrodynamic brake control box, and a DC source is required for the lunar drill motor. The motor can be operated in either a cw or ccw direction, but the majority of the drilling operation is accomplished with the positive voltage at Pin "A" of the power receptacle. The motor armature is currently optimized for 24 VDC operation, but can be operated in the 20 to 30 VDC range.

Operating Instructions

1. Connect power cable to Lunar Drill Load Simulator. (A standard laboratory 50-ampere ammeter should be employed in this circuit.)
2. Connect electrodynamic brake control cable to control box.
3. Ensure that control box power switch is off, and control transformer adjustment knob is fully ccw. Connect control box power cable to 115 V, 60 cps source.
4. Position auxiliary cooling fan so that the air stream is directed across the Lunar Drill Load Simulator.
5. Apply DC power to lunar drill motor. No load current should read approximately 1.5 amperes.
6. Turn control box power switch on, and adjust transformer control knob in a cw direction until the desired current load is attained in the drill motor power circuit. Return transformer control knob to the extreme ccw position to "unload" the lunar drill motor.

Note: It is recommended that "load" tests of the drill motor be kept to a minimum consistent with the LEM power system test requirements.

7. Remove DC and AC power at the conclusion of the test.

Operating Power Profile

As a result of the initial Lunar Rock Coring Device Design Study, a preliminary power profile has been established for the drill. This power profile may change somewhat as additional development of the lunar drill continues, but the basic Lunar Drill Load Simulator can still be employed for simulating these profiles.

The breadboard model coring device field tests have been conducted with a 24 VDC input voltage, at average current levels of 20 to 25 amperes during the coring process. It is anticipated that the final model drill will obtain the ten feet of rock core in 20-inch segments. Assuming the higher power level of 25 amperes the power profile will consist of six, 600-watt power cycles, each ranging in duration from 20 to 40 minutes. The duration of each 20-inch drilling cycle depends upon the hardness of the rock to be cored. In addition, a small power expenditure of approximately 120 watts for two minutes is required for reverse traversing of the drill string after each forward (coring) traverse.

The coring device automatically stops at the completion of each 20-inch coring segment. Astronaut attendance is required for reverse traversing, removal of the 20-inch core, and coupling of a core barrel extension tube in preparation for the next coring cycle. Therefore, the period of time between each 600-watt coring cycle is variable, depending upon the availability of the astronaut.

LUNAR DRILL LOAD SIMULATOR TESTS

In accordance with contractual requirements, several tests were performed on the Lunar Drill Load Simulator as outlined in Gruman Aircraft Interface Control Document LIS-360-22501. Although this document was not included as a requirement for the original Lunar Coring Device Design Study, the tests were performed and the results are included in this report.

A preliminary RF filter selection (Sprague Electric 30JX21) was made for the motor, and comparative tests with and without the filter were performed. However, the scope and time required for this ten-week program did not permit an exhaustive investigation of the filter problem.

Load Generated Ripple (LIS-360-22501, Para. 3.3.1.2)

A load generated ripple test was conducted on the Lunar Drill Load Simulator operating at a 20-ampere load. A maximum ripple voltage of 3.0 volts peak at 12 KC was measured with an oscilloscope. The ripple voltage amplitude was not improved by incorporation of the RF filters. A 17 KC low pass filter was employed to facilitate the ripple measurement. The measured amplitude of ripple voltage exceeds the specification limit by 2.5 volts.

Dielectric Strength (LIS-360-22501, para. 3.3.1.4)

A dielectric strength test was performed on the Lunar Drill Load Simulator. A 1500 VAC rms, 60 cps source was connected between the power input receptacle pins and case ground of the motor. The maximum leakage current measured during the 60-second test was 0.2 milliamperes, which was within the tolerance specification.

The 115 VAC rms, 400 cps test was not performed because the DC motor is not considered to be a coil type device. If the test were performed, the relatively low AC impedance (approximately 1.25 ohms) of the motor armature would result in excessive current and subsequent damage to the armature wire.

Electromagnetic Interference (LSP-530-001)

Conducted and radiated electromagnetic interference tests were performed in an RF screen room as illustrated in Figure I.4. A NF-105 Noise and Field Intensity meter was employed for the tests using two line stabilization units wired in accordance with page 55 of LSP-530-001. Impedance curves for the line stabilization units are illustrated in Figures I.8 and I.9.

Conducted Interference.—This test was performed in accordance with LSP-530-001 (paragraph 3.3.1 and Figure 2) using line stabilization units in both the positive and negative power leads as shown in Figure I.4. Conducted interference measurements were obtained for both the positive and negative input leads, with and without the filters. The results of this test are illustrated in Figures I.5 and I.6.

Radiated Interference.—This test was performed in accordance with LSP-530-001 (paragraph 3.3.2 and Figure 8). The results are illustrated in Figure I.7.

CONCLUSIONS AND RECOMMENDATIONS

As illustrated in Figures I.5 and I.6, incorporation of the Sprague Electric Company 30JX21 filters resulted in a significant decrease in the conducted noise amplitude. However, the specification limits were exceeded at frequencies above approximately 2 to 3 megacycles. Radiated interference levels were also improved by incorporation of the filters, but again, specification limits were exceeded above 4 megacycles.

The physical location of the filters on the Lunar Drill Load Simulator is not optimum for radiated noise suppression. The motor case on flight models should be designed so that the RF filters are completely encased. Also, time limitations prohibited the investigation and test of other types of filters which may have been more effective for this particular application.

The following recommendations are submitted for consideration by NASA:

1. The Lunar Drill Load Simulator should be employed for the LEM electromagnetic interference tests in order to evaluate system-level effects.

ER 13952

2. An extensive electromagnetic interference investigation should be included during development of the prototype model coring device. Consideration should also be given to the use of a brushless type DC motor if noise levels cannot be attenuated sufficiently to meet LEM specifications. The additional weight and other tradeoff characteristics of the brushless motor would require further investigation.

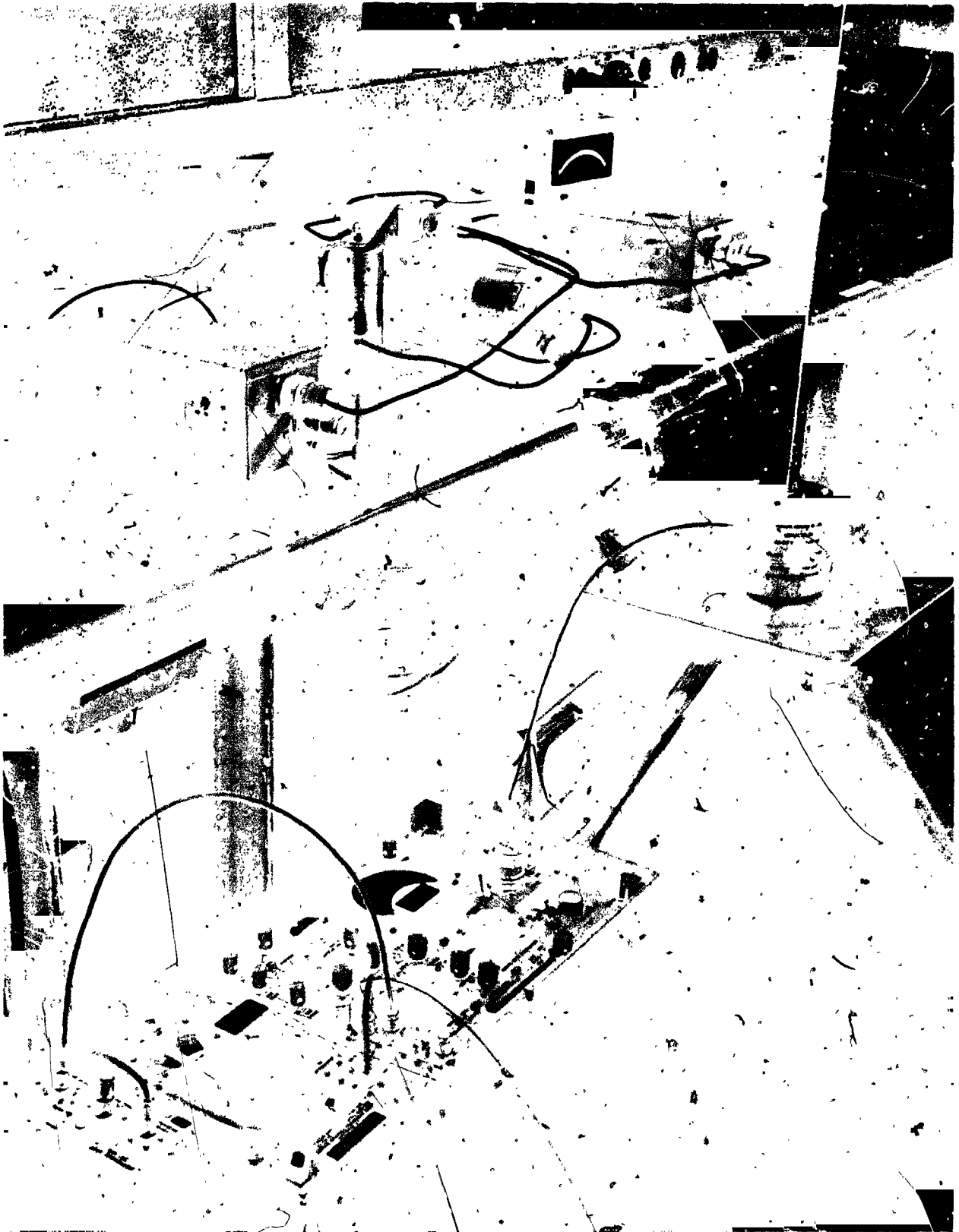


Figure I.4. Electromagnetic Interference Tests

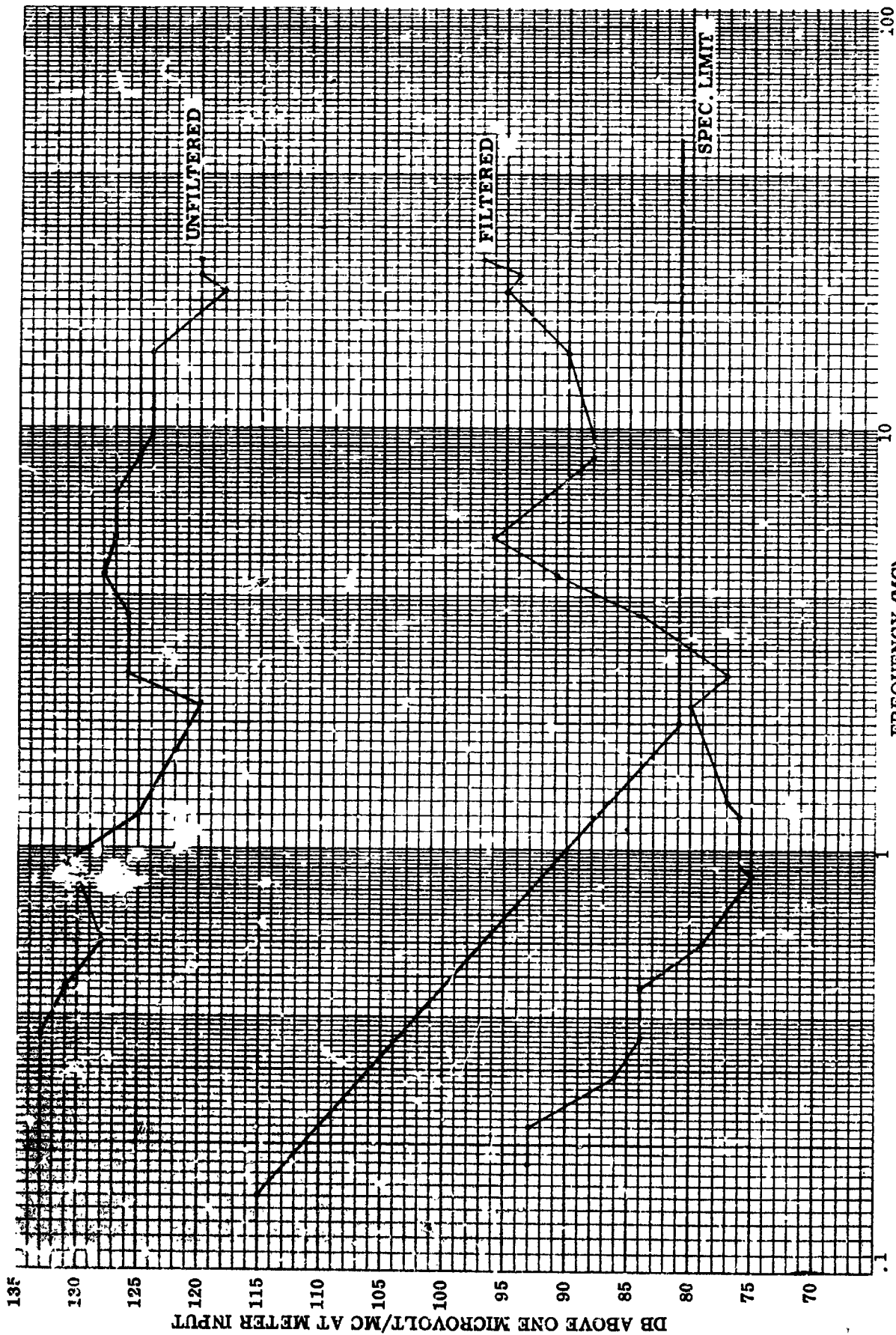


Figure 1.5. Conducted Interference (Positive Lead)

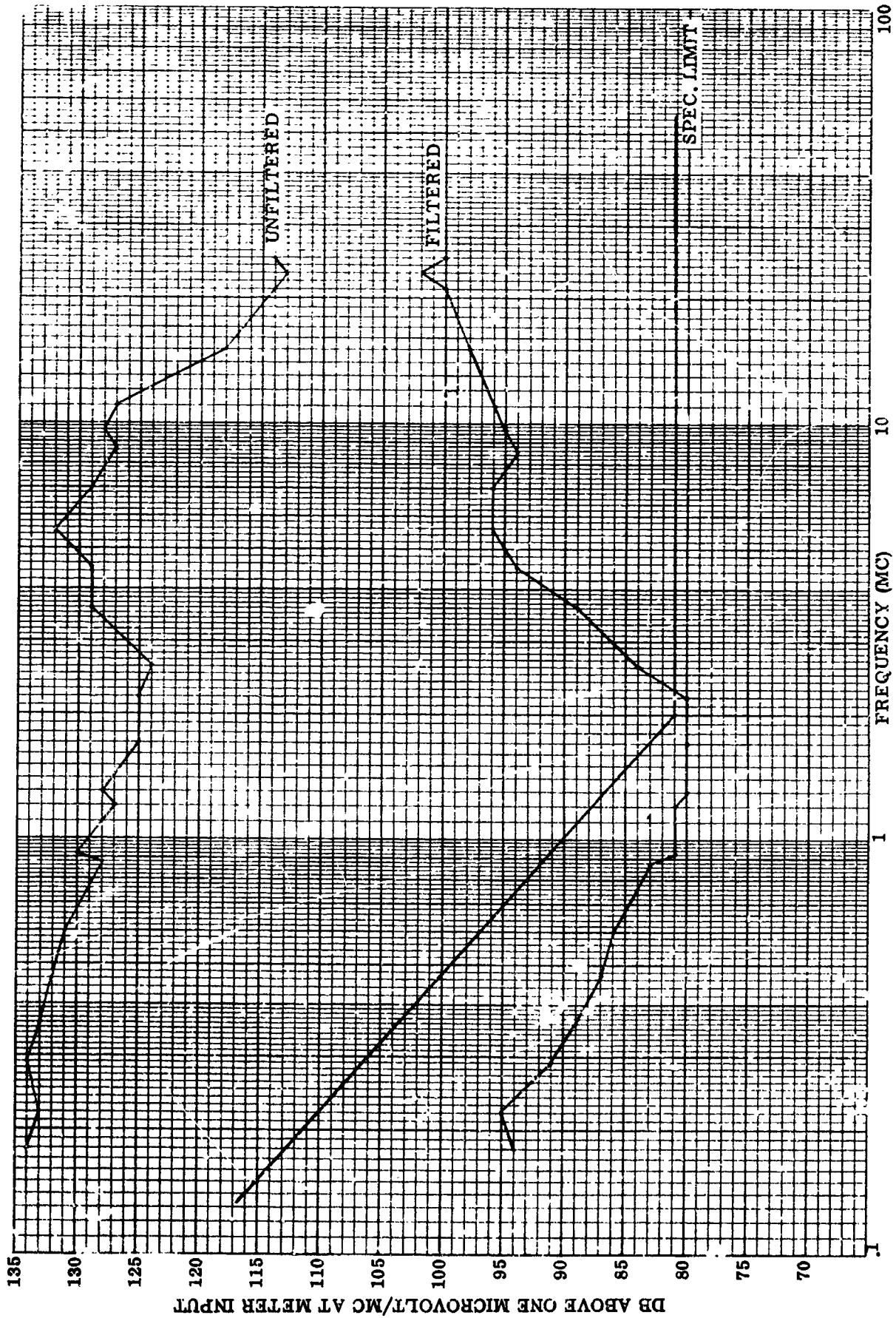


Figure I.6. Conducted Interference (Negative Lead)

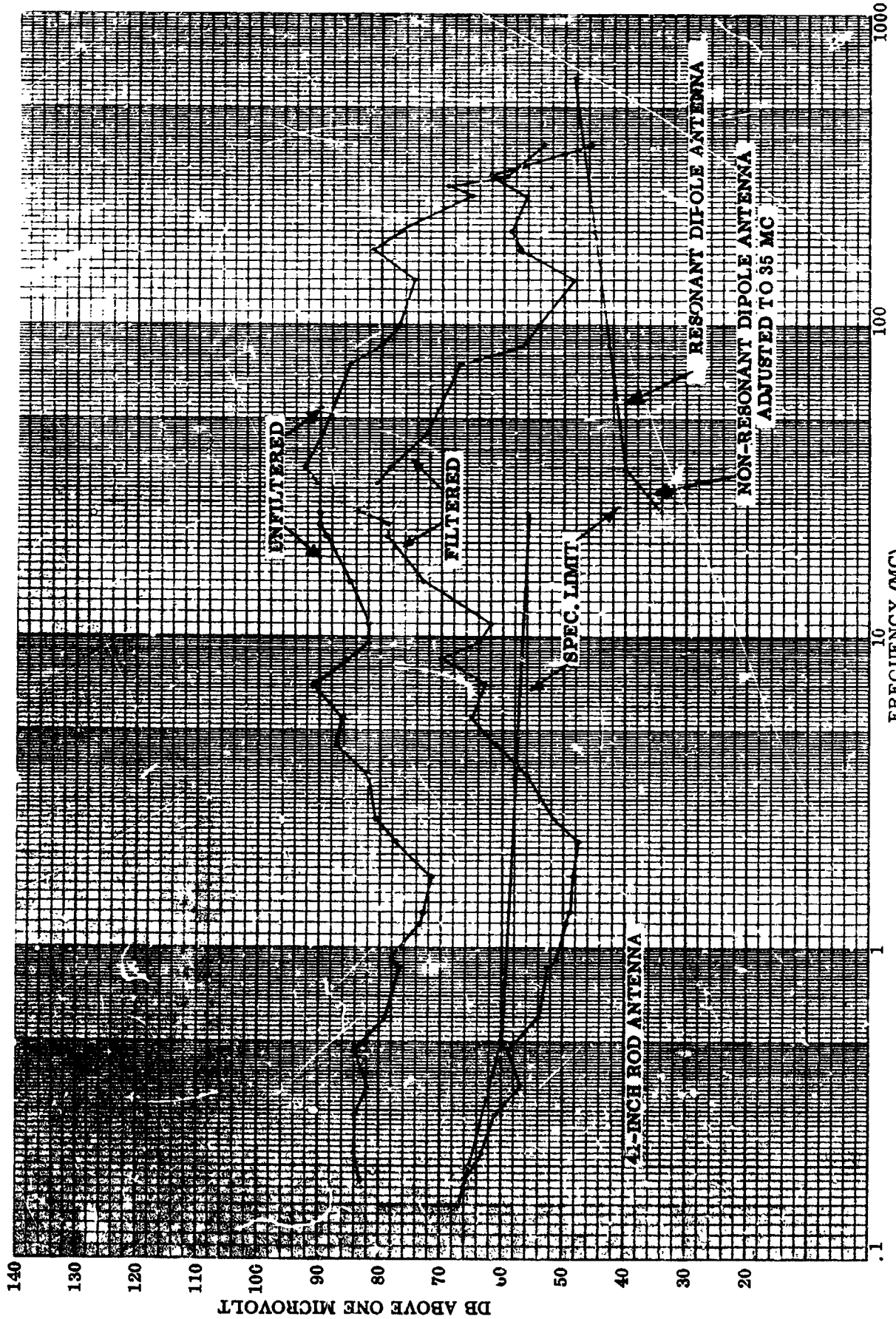


Figure I.7. Radiated Interference

ER 13952

CONDUCTED AND RADIATED ELECTROMAGNETIC TEST DATA

Test Equipment

Type of Test	Equipment	Serial No.
Radiated and Conducted Inter- ference	NF-105 Noise & Field Intensity Meter	1361
	(Filtron) Line Stabilization Unit Positive Lead	ME42143
	(Filtron) Line Stabilization Unit Negative Lead	ME42138
Ripple Test	Tektronix Scope Model 561	010251
	Dytronics Low-Pass Filter Model 723	650207
Dielectric Test	Standard Hi-Pot Tester	8321
	AC Voltmeter - Weston Model 433	78869
All Tests	DC Ammeter - Weston Model 901	2-29

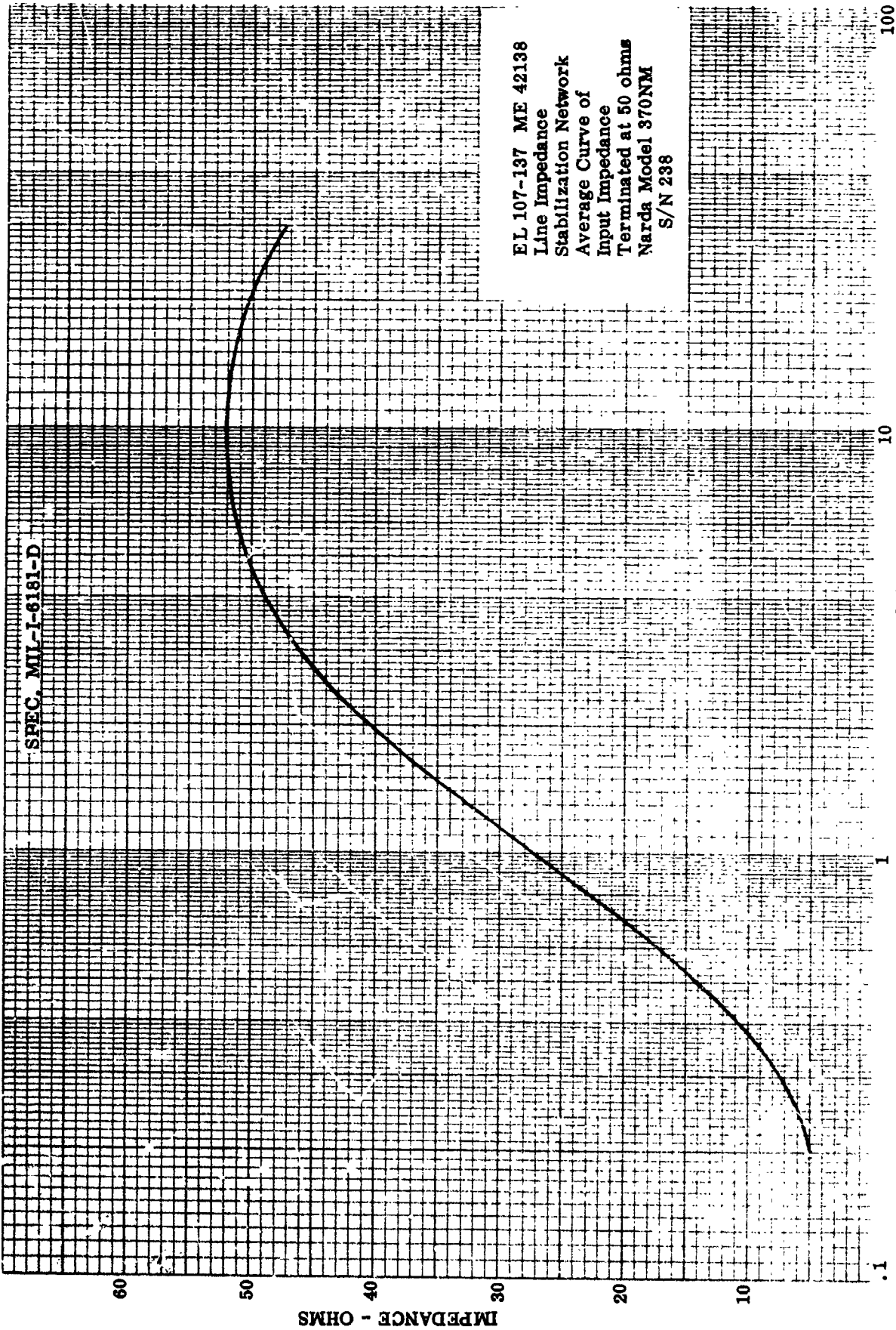


Figure I. 8. - Line Stabilization Unit Impedance

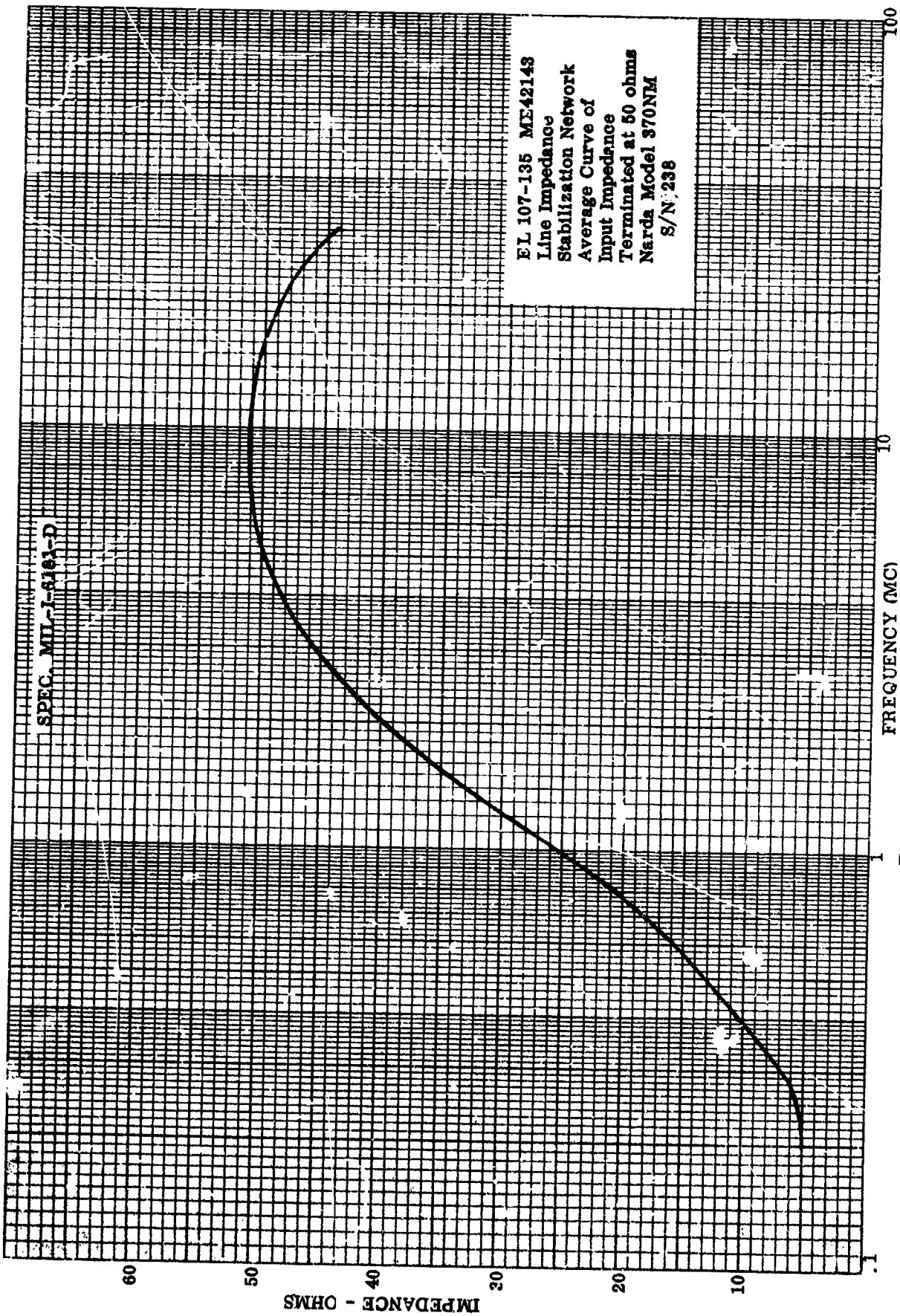


Figure I.9 - Line Stabilization Unit Impedance